Development, Applicability, and Comparison of Bioassays for Metabolism of (New) Psychoactive Substances

Dissertation

zur Erlangung des Grades

des Doktors der Naturwissenschaften

der Naturwissenschaftlich-Technischen Fakultät

der Universität des Saarlandes

von

Lilian Helga Johanne Richter

Saarbrücken

2018

Tag des Kolloquiums:	14.12.2018
Dekan:	Univ.-Prof. Dr. rer. nat. Guido Kickelbick
Berichterstatter:	Univ.-Prof. Dr. rer. nat. Dr. h.c. Hans H. Maurer
	Univ.-Prof. Dr. rer. nat. Thorsten Lehr
Vorsitz:	Univ.-Prof. Dr. med. Veit Flockerzi
Akad. Mitarbeiter:	Dr. rer. nat. Jessica Hoppstädter

VORWORT

Die nachfolgende Arbeit entstand unter der Anleitung von Herrn Univ.-Prof. Dr. Dr. h.c. Hans H. Maurer in der Abteilung für Experimentelle und Klinische Toxikologie der Fachrichtung Experimentelle und Klinische Pharmakologie und Toxikologie der Universität des Saarlandes in Homburg (Saar) von November 2014 bis Juni 2018.

DANKSAGUNG

Mein besonderer Dank gilt:

Herrn Professor Hans H. Maurer für die herzliche Aufnahme in seinen Arbeitskreis, die Vergabe dieses interessanten, innovativen und herausfordernden Dissertationsthemas, die Möglichkeit des selbstständigen Arbeitens und der aktiven Teilnahme und Präsentation auf nationalen und internationalen Fachkongressen, für seine stetige Diskussionsbereitschaft mit kritischen, aber berechtigten fachlich kompetenten Fragen, die vertrauensvoll von ihm übertragene Labor- und Personalverantwortung, sowie den Ansporn, immer das Bestmöglichste zu leisten,

Herrn Professor Thorsten Lehr für die Übernahme des Koreferats,

Herrn Professor Markus R. Meyer für seine fachliche Unterstützung, stetige Diskussionsbereitschaft um neue Sichtweisen und Lösungsansätze aufzuzeigen (auch als er nicht persönlich vor Ort war), sein Vertrauen in meine fachlichen Fähigkeiten, den reibungslosen Institutsleiterwechsel ohne Nachteile für die Mitarbeiter, sowie nicht zuletzt ein freundschaftliches und angenehmes Arbeitsklima,

Herrn Professor Veit Flockerzi für die Ermöglichung der Zellkulturversuche,

meinen Kolleginnen und Kollegen oder auch „Leidensgenossen“ für das geteilte Leid nach langen Dienstnächten, dem wissenschaftlichen Austausch, die freundschaftliche Zusammenarbeit und natürlich das Feierabendbier,

Herrn Armin A. Weber für seine bedingungslose Einsatzbereitschaft, sowie Rat und Hilfe bei technischen Fragestellungen und der Lösung jedweder Probleme,

Frau Heidi Löhr für die tatkräftige Unterstützung im Bereich der Zellkultur und die produktive, organisierte und sehr angenehme Zusammenarbeit,

Frau Gabriele Ulrich und Herrn Carsten Schröder für gewissenhaft ausgeführte Laborarbeiten,

den Auszubildenden für ihre fleißige Mitwirkung,

meiner Familie, vor allem meinem Schwesterherz für ihren Rückhalt und die Unterstützung auch in schwierigen Zeiten,

meinem Partner, der alle Höhen und Tiefen und die dadurch bedingten Launen der Promotionszeit am nächsten miterlebt und ausgehalten hat, für die stetige Unterstützung auf fachlicher und vor allem auf nicht fachlicher Seite, für erneute Motivation und Kraft, sowie immer ein offenes Ohr,

meiner besten Freundin, die trotz großer Entfernung, wenig Zeit und Leben, die nicht unterschiedlicher sein könnten immer für mich da war, an mich glaubte, und mich bei allem unterstützte, was ich tat,

und allen Menschen die sonst auf irgendeine Art und Weise mein Leben bereichern.

“Die Zukunft ist morgen und heute ist hier”

Dritte Wahl (Runde um Runde)

TABLE OF CONTENTS

TABLE OF CONTENTS

1. GENERAL PART

1.1. (NEW) PSYCHOACTIVE SUBSTANCES (NPS)

Since human recollection, psychoactive substances were consumed e.g. during religious rituals to extend the spirit. However, since the 80's, psychoactive substances such as amphetamine, methamphetamine, and MDMA were often misused in the "rave and dance club scene".[1,2] Therefore, the "classic" psychoactive substances are nowadays scheduled in most countries[3,4] and known as drugs of abuse (DOA) or their chemical derivatives as designer drugs.[1,2] To overcome legislation issues, new psychoactive substances (NPS) emerged on the market derived from DOA with often only slight structural modifications. Thus, they are not scheduled although having similar pharmacological properties. They continuously appear on the illicit DOA market worldwide.[5-8] When a compound gets controlled by national or international laws, usually a new variety arises that then gets controlled again with certain time offset, making it a "never ending story". In most cases, NPS are produced by chemical and pharmaceutical companies e.g. in China or by clandestine laboratories all over the world.[7] Afterwards, they are sold as "legal highs" in "head shops" or in online shops via the internet under terms such as "research chemical", "bath salts", "plant food", or "spice".[1,9] To get an overview of upcoming NPS, there are monitoring systems such as those by the European Monitoring Centre for Drugs and Drug Addiction (EMCDDA) or by the United Nation Organization on Drugs and Crime (UNODC), who regularly publish documents with data of appearance.[6,7] According to them, more than 620 compounds appeared only in Europe in the last years and the total number of NPS is increasing.[6,7] They are

released on the DOA market without any testing of their pharmacodynamic or pharmacokinetic properties. Hence, consumers, voluntarily or not, are the first test persons for NPS. Their intake can be of high risk and can lead to severe or fatal intoxications even without overdosing.[7] To dame the flood of compounds, many countries introduced blanket bans or generic and analogue-based legislation in recent years. In Germany, the “Neue psychoaktive Stoffe Gesetz” was taking effect in 2016. This law covers whole chemical groups of amphetamine-type stimulants and indoles as well as imidazole-type synthetic cannabinoids.[10] This law was a huge advance, but not all groups of NPS were covered by far such as synthetic benzodiazepines, lysergic acid diethylamide (LSD) derivatives, synthetic opioids, phenethylamines, piperazines, *N*-2-methoxybenzyl phenethylamine (NBOMe) derivatives, or tryptamine derivatives. For their analysis in human urine, metabolites are the usual targets for urine screening approaches to confirm NPS consumption.[11,12]

1.2. TOXICOLOGICAL URINE SCREENING PROCEDURES

Metabolite-based urine screening by low or high resolution (HR) mass spectrometry (MS) techniques coupled to gas or liquid chromatography (GC, LC) are usually the first choice for drug testing due to the fact that the risk of false positive or negative results is minimized in contrast to immunoassays.[13,14] Nowadays, LC-MS approaches, which do not necessarily need cleavage of conjugates prior to analysis become more and more important, especially in clinical and emergency toxicology due to time-saving sample preparation.[13,15] Comprehensive screening procedures are characterized by full scan data in combinations with data-dependent or better -

independent acquisition and library-based compound identification.[13-15] A big advantage is the possibility of retrospective data analysis after updating the reference library[16] because, as already mentioned, the NPS drug market is continuously changing. The most suitable matrix for screening procedures is urine due to the longer detection window, higher analyte concentrations, and thanks to metabolites higher target numbers. Especially for compounds, which are extensively metabolized and excreted exclusively as metabolites, false negative results can be prevented by including metabolites as targets.[12,17,18] Furthermore, the body passage could be confirmed, which might be a task in forensic toxicology.[14,15] In contrast to “classic” psychoactive substances, where targets for toxicological urine screening are well known, for NPS they are unknown as data of biotransformation are often unavailable or lacks of information.[11,12] Therefore, urinary targets of NPS must be investigated first by fast, simple, cost-efficient, and reliable metabolism studies.

1.3. MODELS FOR METABOLISM STUDIES

Metabolism studies can be performed using in vivo and/or in vitro models. Controlled human studies would of course be best suited for elucidating the human metabolism of NPS, but due to ethical reasons and lack of preclinical safety data, they are usually not possible. Authentic human samples are often not (yet) available.[8,12] Animal experiments using e.g. rats or other rodents are well established as surrogate, but still with the risk of species differences.[17,19,20] They should also be minimized due to ethical reasons and according to the 3R principle. Thus, in recent years more human in vitro models were developed to mimic the human in vivo hepatic metabolism. The different in vitro models are introduced in detail in part 1.3.1-3.

1.3.1. HUMAN LIVER PREPARATIONS

Homogenization of liver tissue with break-up of cells followed by centrifugation at 9,000*g* lead to a supernatant that consists of microsomes and cytosol and is called S9 fraction or S9 mix.[21,22] It contains microsomal and cytosolic enzymes that are responsible for catalyzing phase I and II metabolic steps.[21,22] By means of a two-stepped centrifugation at 10,000*g* and 100,000*g* microsomes and cytosol can be separated.[21,22] Here, in contrast to S9 fraction, enzymes are enriched in microsomes which can result in a higher metabolite formation rate.[22] Moreover, some enzymes mainly responsible for the phase I metabolism of xenobiotics are exclusively localized in the microsomes such as cytochrome P450 monooxygenases (CYPs) and flavin-containing monooxygenases (FMOs). Uridine diphosphate glucuronyltransferases (UGTs) are localized in microsomes, too.[21,23] In contrast, *N*-acetyltransferases (NATs) and sulfotransferases (SULTs) are soluble enzymes of the cytosol.[21,24] For catechol-*O*-methyltransferases (COMTs) and glutathione-*S*-transferases (GSTs), soluble and membrane bound forms exist.[21,22,25] By working with human liver preparations, it is important to add co-substrates for the corresponding metabolic reaction e.g. nicotinamide adenine dinucleotide phosphate (NADPH) for oxidation, uridine diphosphate glucuronic acid (UDPGA) for glucuronidation, 3′-phosphoadenosine-5′-phosphosulfate (PAPS) for sulfation, S-(5′-adenosyl)-L-methionine (SAM) for catechol *O*-methylation, acetylcarnitine (AC) for *N*-acetylation, and reduced glutathione (GSH) for glutathione conjugation.[11,12,22] To prevent the influence of different enzyme expressions or activity of single donors, such as CYP2D6 rapid metabolizer, nowadays pooled S9 fraction (pS9), pooled human liver

microsomes (pHLM), and pooled human liver cytosol (pHLC) from up to 100 donors are used for in vitro studies to obtain reproducible results.[11]

1.3.2. PRIMARY HUMAN HEPATOCYTES

Primary human hepatocytes (PHH) are isolated under sterile conditions from freshly resected liver tissue of donors that should be younger than 50 years and have a single pathological finding (e.g. single metastasis or liver tumor) or trauma.[26] They are considered as gold standard for in vitro metabolism studies due to natural enzyme clusters, co-substrates, and drug transporters and thus should provide the most authentic human metabolite pattern.[12,27-31] However, they have some disadvantages such as high costs, limited availability, differences in cell viability, and variability in the expression and activity of metabolizing enzymes.[20,21,31,32] Minimization of variability can be achieved by using pooled PHH. Despite the fact that cryopreserved pooled PHH from a maximum of ten donors are commercially available[11], there is still a high variability of cryopreserved pooled PHH between producers and even from batch to batch. [31]

1.3.3. HUMAN HEPATIC CELL LINES

Human hepatic cell lines are immortalized cells originated from hepatic tumors.[26,33,34] They also contain co-substrates and drug transporters, but have the advantage of unlimited growth and availability as well as a stable phenotype in contrast to PHH leading to higher reproducibility of the results.[26,31] HepG2 is the oldest, but also best known and most frequently used human hepatic cell line.[33] During the immortalization process, cell lines can loose their hepatic-specific properties.[26,33] For example, HepG2 cells have a low gene expression for phase I metabolizing enzymes,

especially CYP enzymes,[26,31,33] but for most phase II metabolizing enzymes, except for single UGTs, the gene expression level is comparable to PHH.[33,35] Thus, their applicability for metabolism studies is limited.[26,31] In the last years, a new cell line called HepaRG became more and more popular. Proliferating HepaRG cells can be maintained in culture for several weeks and at confluence, or after addition of differentiation inducing culture medium, cells differentiate into biliary epithelial cells and hepatocytes.[33,36] The extraordinary property of differentiated HepaRG cells is the stable gene expression level for all metabolizing enzymes comparable to PHH except for CYP2D6.[33,36] Differentiated HepaRG cells have all advantages of cell lines combined with the enzyme features of PHH, making them a promising alternative in vitro model for metabolism studies of NPS. But in contrast to HepG2, HepaRG cells need sophisticated handling e.g. special culture media or collagen coated well plates are needed. [11]

2. AIMS AND SCOPES

The aims of this dissertation were to develop, apply, and compare bioassays for metabolism studies of NPS from different drug classes using human liver preparations, PHH, and human hepatic cell lines. The best suited model for identifying main urinary excretion products as targets for developing toxicological urine screening procedures should be ascertained. For comparison and applicability testing, psychoactive substances and NPS with known metabolic pathways were included in the studies as well as NPS with unknown metabolic pathway (Figure 1).

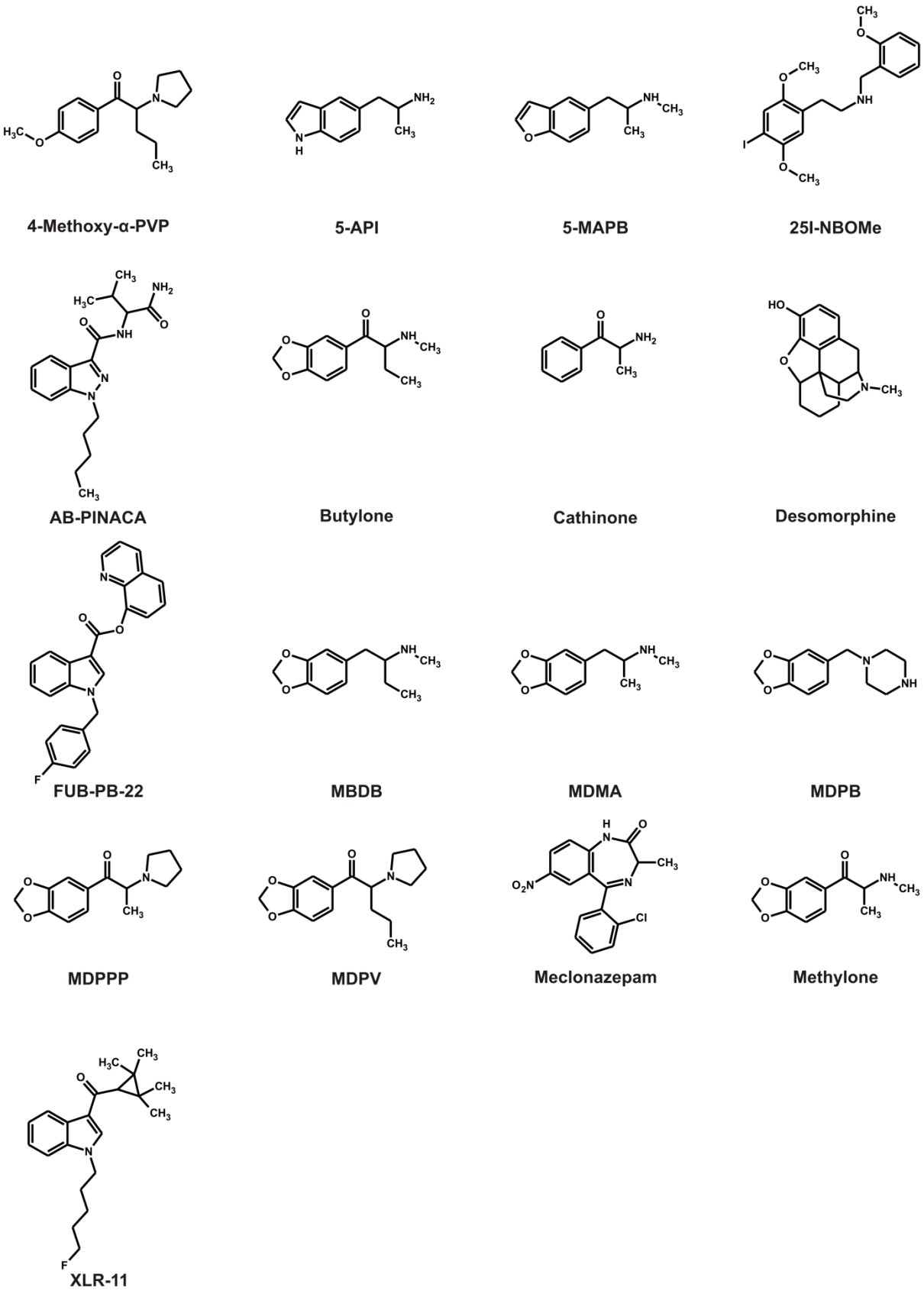

Figure 1. Chemical structures of all investigated compounds arranged according to alphabetic order.

The following investigations should be performed:

- Implementation of a conventional metabolism study by LC-HR-MS/MS and comparison with results obtained using new in vitro models (HepG2 and HepaRG) and desomorphine as model drug
- Investigation of general involvement of human CYP and human UGT isoenzymes in the main metabolic steps of desomorphine
- Detectability of desomorphine in rat urine by standard urine screening approaches (SUSAs) using GC-MS,[37,38] LC-multi stage mass spectrometry (MS^n),[14,39] and LC-HR-MS/MS[15,40] approaches
- Development of an incubation assay using human liver preparations covering all main phase I and II metabolic steps and monitoring the applicability using model compounds for the corresponding metabolic steps
- Identification of the best suited in vitro model for metabolism studies in order to develop toxicological urine screening procedures, exemplified for methylenedioxy derivatives and bioisosteric analogues by LC-HR-MS/MS
- Comparison of the best suited in vitro model (human liver preparations) with primary human hepatocytes as current gold standard

3. PUBLICATIONS OF THE RESULTS

The results of the studies were published in the following papers:

3.1. METABOLIC FATE OF DESOMORPHINE ELUCIDATED USING RAT URINE, POOLED HUMAN LIVER PREPARATIONS, AND HUMAN HEPATOCYTE CULTURES AS WELL AS ITS DETECTABILITY USING STANDARD URINE SCREENING APPROACHES[41] (DOI: 10.1007/S00216-016-9740-4)

Anal Bioanal Chem
DOI 10.1007/s00216-016-9740-4

RESEARCH PAPER

Metabolic fate of desomorphine elucidated using rat urine, pooled human liver preparations, and human hepatocyte cultures as well as its detectability using standard urine screening approaches

Lilian H. J. Richter[1] · **Yeda Rumi Kaminski**[2] · **Fozia Noor**[2] · **Markus R. Meyer**[1,3] · **Hans H. Maurer**[1]

Received: 18 April 2016 / Revised: 14 June 2016 / Accepted: 22 June 2016

Abstract Desomorphine is an opioid misused as "crocodile", a cheaper alternative to heroin. It is a crude synthesis product homemade from codeine with toxic byproducts. The aim of the present work was to investigate the metabolic fate of desomorphine in vivo using rat urine and in vitro using pooled human liver microsomes and cytosol as well as human liver cell lines (HepG2 and HepaRG) by Orbitrap-based liquid chromatography-high resolution-tandem mass spectrometry or hydrophilic interaction liquid chromatography. According to the identified metabolites, the following metabolic steps could be proposed: *N*-demethylation, hydroxylation at various positions, *N*-oxidation, glucuronidation, and sulfation. The cytochrome P450 (CYP) initial activity screening revealed CYP3A4 to be the only CYP involved in all phase I steps. UDP-glucuronyltransferase (UGT) initial activity screening showed that UGT1A1, UGT1A8, UGT1A9, UGT1A10, UGT2B4, UGT2B7, UGT2B15, and UGT2B17 formed desomorphine glucuronide. Among the tested in vitro models, HepaRG cells were identified to be the most suitable tool for prediction of human hepatic phase I and II metabolism of drugs of abuse. Finally, desomorphine (crocodile) consumption should be detectable by all standard urine screening approaches mainly via the parent compound and/or its glucuronide assuming similar kinetics in rats and humans.

Keywords Desomorphine · Crocodile · LC-HR-MS/MS · Metabolism · Human liver preparation · Hepatocyte cell cultures

Introduction

Desomorphine (structure given in Fig. 1) is an opioid first synthesized in the United States in 1932 as therapeutic drug and alternative to morphine. It has a higher pharmacological potency but a shorter duration of action than morphine [1]. It was in therapeutic use from 1940 to 1952 in Switzerland under the brand name Permoid [2]. Its ongoing misuse, especially in Russia, as "crocodile", "Krok", or "Russian Magic", a cheaper alternative to heroin, was first reported in 2002 and later on also in the United States [1, 3, 4]. Crocodile is a crude synthesis product homemade from codeine requiring easily obtainable chemicals and rudimentary laboratory needs. Besides desomorphine, the final product contains huge amounts of byproducts and residuals. These contaminants caused crocodile's characteristic side effects such as damage of vasculature, muscle, and bone, which may quickly progress to tissue necrosis and gangrene at the injection site [1, 5]. Crocodile is mainly injected, but also ingested orally (http://content.time.com/time/world/article/0,8599,2078355,00.html). Therefore, detection of desomorphine as potential marker of crocodile use or as cause of an opioid poisoning is needed. So far, gas chromatography–mass spectrometry (GC-MS) and liquid chromatographic analysis of desomorphine and codeine-derived byproducts in confiscated samples of suspected "crocodile" consumers was described [6]. They could also detect desomorphine itself in some urine samples of consumers.

✉ Hans H. Maurer
hans.maurer@uks.eu

[1] Department of Experimental and Clinical Toxicology, Institute of Experimental and Clinical Pharmacology and Toxicology, Saarland University, Kirrberger Strasse 100, 66421 Homburg (Saar), Germany

[2] Biochemical Engineering Institute, Saarland University, Campus A1 5, 66123 Saarbrücken, Germany

[3] Present address: Department of Pharmacology and Pharmacoepidemiology, Heidelberg University Hospital, Im Neuenheimer Feld 410, 69120 Heidelberg, Germany

Published online: 02 July 2016

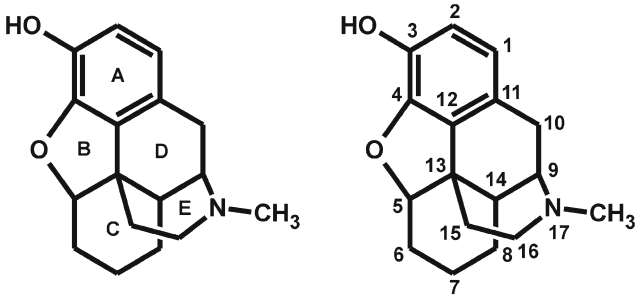

Fig. 1 Structure of desomorphine with marked rings (*left*) and carbon numbering (*right*)

To date, no data are available about the metabolic fate of desomorphine in the human body and about its detectability in common standard urine screening approaches (SUSAs). Metabolites could be important targets for SUSAs [7–9] commonly used in clinical and forensic toxicology. The aim of the present work was to investigate the metabolic fate of desomorphine in vivo using rat urine and in vitro using pooled human liver microsomes (pHLM) and pooled human liver cytosol (pHLC) as well as human liver cell lines (HepG2 and HepaRG) by Orbitrap (OT)-based liquid chromatography-high resolution-tandem mass spectrometry (LC-HR-MS/MS) or hydrophilic interaction liquid chromatography (HILIC)-HR-MS/MS. In addition, HepG2 and HepaRG cell lines should be tested as new tools for the prediction of human hepatic metabolism of drugs of abuse. Finally, the detectability of desomorphine and its metabolites by common SUSAs [9–12] should be investigated.

Experimental

Chemicals and reagents

Desomorphine and dihydromorphine were obtained from Lipomed (Weil am Rhein, Germany); codeine-d_6 from LGC Standards (Wesel, Germany); Isolute HCX cartridges (130 mg, 3 mL) from Biotage (Uppsala, Sweden); isocitrate, isocitrate dehydrogenase, 3′-phosphoadenosine-5′-phosphosulfate (PAPS), dimethyl sulfoxide (DMSO), *p*-nitrophenol, and epidermal growth factor from Sigma-Aldrich (Taufkirchen, Germany); $NADP^+$ from Biomol (Hamburg, Germany); acetonitrile (LC-MS grade), ammonium formate (analytical grade), formic acid (LC-MS grade), methanol (LC-MS grade), and mixture (100,000 Fishman units/mL) of glucuronidase (EC No. 3.2.1.31) and arylsulfatase (EC No. 3.1.6.1) from *Helix pomatia*; and all other chemicals and reagents (analytical grade) from VWR (Darmstadt, Germany). The baculovirus-infected insect cell microsomes (Supersomes) containing human cDNA-expressed cytochrome P450 (CYP) enzymes CYP1A2, CYP2A6, CYP2B6, CYP2C8, CYP2C9, CYP2C19, CYP2D6, CYP3A4 (1 nmol/mL, each), or CYP2E1, CYP3A5 (2 nmol/mL, each), UGT1A1, UGT1A4, UGT1A6, UGT1A7, UGT1A8, UGT1A9, UGT1A10, UGT2B4, UGT2B7, UGT2B15, UGT2B17 (5 mg protein/mL, each), pHLM (20 mg microsomal protein/mL, 330 pmol total CYP/mg protein), pHLC (20 mg cytosolic protein/mL), UGT reaction mix solution A (25 mM UDP-glucuronic acid), and UGT reaction mix solution B (250 mM Tris–HCl, 40 mM $MgCl_2$, and 0.125 mg/mL alamethicin) were obtained from Corning (Amsterdam, The Netherlands). After delivery, the enzyme preparations were thawed at 37 °C, aliquoted, snap-frozen in liquid nitrogen, and stored at −80 °C until use. HepG2 cells were obtained from the German collection of microorganism and cell cultures (DSMZ, Braunschweig, Germany), 96-well plates from Greiner Bio-One (Frickenhausen, Germany), Williams E Medium from Pan Biotec (Aidenbach, Germany), penicillin and streptomycin from c. c. pro (Oberdorla, Germany), and fetal bovine serum from PAA Laboratories (Pasching, Austria). Cryopreserved, differentiated HepaRG cells (HPR116), additive ADD650, and thaw, seed, and general purpose additive ADD670 were obtained from Biopredic International (Saint-Grégoire, France); 96-well plates coated with 50 μg/mL type I collagen from Roche Applied Sciences (Penzberg, Germany); and human hepatocyte growth factor from Humanzyme (Chicago, IL, USA).

In vivo drug metabolism studies using rat urine

As reported earlier [13], the investigations were performed using rat urine samples from male Wistar rats (Charles River, Sulzfeld, Germany) for toxicological diagnostic reasons according to the corresponding German law. The compound was administered in an aqueous suspension by gastric intubation of a single dose of 20 and 1 mg/kg body weight (BW) for the identification of the metabolites and for screening, respectively. The rats were housed in metabolism cages for 24 h, having water ad libitum. Urine was collected separately from the feces over a 24-h period. Blank urine samples were collected before drug administration to confirm the absence of interfering compounds. The samples were directly analyzed and the remains stored at −20 °C.

Sample preparation for the identification of phase I metabolites was done as described previously [13]. A volume of 2 mL of urine was adjusted to pH 5.2 with acetic acid (1 M, approximately 50 μL) and incubated at 56 °C for 2 h with 50 μL of a mixture of glucuronidase and arylsulfatase. The urine sample was loaded on an HCX cartridge previously conditioned with 1 mL of methanol and 1 mL of water. After passage of the sample, the cartridge was washed with 1 mL of water, 1 mL of 0.01 M hydrochloric acid, and again with 1 mL of water. The acidic and neutral compounds (eluate A) were eluted with 1 mL of methanol into a 1.5-mL reaction vial and the basic compounds (eluate B) with 1 mL of a freshly prepared mixture of methanol/aqueous ammonia 32 % (98:2, *v/v*). Only eluate B was evaporated to dryness under a stream of nitrogen and reconstituted with 50 μL of a mixture of eluent

A and B (1:1, *v*/*v*) for LC-HR-MS/MS or HILIC-HR-MS/MS analysis. A 10-μL aliquot was injected onto LC-HR-MS/MS or 1 μL onto HILIC-HR-MS/MS.

Sample preparation for the identification of the phase II metabolites was carried out according to a published method [12, 13]. A volume of 100 μL of urine was mixed with 500 μL of acetonitrile for precipitation. After shaking and centrifugation, the supernatant was gently evaporated to dryness and reconstituted in 50 μL of a mixture of eluent A and B (1:1, *v*/*v*), and again 10 μL was injected onto the LC-HR-MS/MS system.

In vitro drug metabolism studies using pHLM and pHLC

Combined pHLM and pHLC incubations (pHLM/pHLC) both at a final protein concentration of 1 mg/mL were performed after 10 min of preincubation at 37 °C with 20 μL UGT reaction mix solution B, 90 mM phosphate buffer (pH 7.4), 2.5 mM Mg^{2+}, 2.5 mM isocitrate, 0.6 mM $NADP^{+}$, 0.8 U/mL isocitrate dehydrogenase, and 100 U/mL superoxide dismutase. Thereafter, 10 μL UGT reaction mix solution A, 40 μM aqueous PAPS, and 25 μM desomorphine in phosphate buffer were added and the mixture (final volume, 100 μL) incubated for 30 min. All given concentrations mean final concentrations. Reactions were initiated by the addition of desomorphine and stopped with 50 μL of ice-cold acetonitrile. The solution was centrifuged for 2 min at 10,000×*g* and 100 μL of the supernatant was transferred into an autosampler vial and 10 μL injected onto the LC-HR-MS/MS system or 1 μL onto the HILIC-MS/MS system. In control sample, enzyme was replaced with buffer; in blank sample, substrate was replaced with buffer. Glucuronidation and sulfation of *p*-nitrophenol (25 μM) were used as positive control samples [14].

In vitro drug metabolism studies using HepG2 and HepaRG cell lines

All cell cultures were maintained in an incubator (Memmert Schwabach, Germany) at 37 °C with 95 % air humidity and 5 % CO_2 atmosphere. Cell handling was done under sterile conditions using a laminar flow bench class II (Luft- und Reinraumtechnik, Sonnenbühl, Germany). HepG2 cells were seeded in a density of 50,000 cells per well in 96-well plates. The cultures were maintained in Williams E Medium supplemented with 100 U/mL penicillin, 100 μg/mL streptomycin, and 10 % fetal bovine serum for 3 days prior to desomorphine exposure. Cryopreserved, differentiated HepaRG cells (HPR116) were cultivated according to the manufacturer's instructions. HepaRG cells were seeded (72,000 cells/well) in 96-well plates coated with 50 μg/mL type I collagen. Cell seeding was performed in Williams E medium supplemented with ADD670, 100 U/mL penicillin, 100 μg/mL streptomycin, and 0.5 % DMSO. HepaRG cells were maintained under these conditions for 6 days with medium renewal every 2 days before desomorphine exposure. Medium volume was always 100 μL.

The day before desomorphine exposure, medium was changed to Williams E Medium (serum-free) supplemented with additive ADD650, 100 U/mL penicillin, 100 μg/mL streptomycin, 0.5 % DMSO, 10 ng/mL human hepatocyte growth factor, and 2 ng/mL epidermal growth factor [15, 16]. HepG2 and HepaRG cells were exposed to desomorphine concentrations of 0.01, 0.1, or 1 mM for 3 or 24 h. All given concentrations are the final concentrations. Medium supernatants were collected for the analysis of the metabolites. A 50-μL aliquot of each sample was precipitated by 50 μL acetonitrile, containing 10 μM codeine-d_6 as internal standard, and 50 μL of 35 mg/mL zinc sulfate solution in methanol/water (30:70, *v*/*v*) [17] and subsequently cooled at −18 °C for 30 min. The solution was centrifuged for 2 min at 10,000×*g*, 100 μL of the supernatant transferred to an autosampler vial, and 10 μL injected onto the LC-HR-MS/MS or 1 μL onto the HILIC-MS/MS system. Blank cell cultures were prepared to confirm the absence of interfering compounds. Control samples without cells, but containing desomorphine at 0.01, 0.1, and 1 mM, were prepared to check for not metabolically originated compounds. Blank in vitro cell cultures were prepared to check whether the samples were free of interfering compounds.

CYP initial activity screening

As described previously [13, 18], microsomal incubations were performed for 30 min at 37 °C at concentrations of 25 μM desomorphine in phosphate buffer with the particular CYP isoenzyme (50 pmol/mL, each) CYP1A2, CYP2A6, CYP2B6, CYP2C8, CYP2C9, CYP2C19, CYP2D6, CYP2E1, CYP3A4, or CYP3A5 for the CYP initial activity screening. Besides enzymes and desomorphine, the incubation mixtures (final volume, 50 μL) contained 90 mM phosphate buffer (pH 7.4), 5 mM Mg^{2+}, 5 mM isocitrate, 1.2 mM $NADP^{+}$, 1.6 U/mL isocitrate dehydrogenase, and 200 U/mL superoxide dismutase. According to the Gentest manual, for incubations with CYP2A6 or CYP2C9, phosphate buffer was replaced with 45 and 90 mM Tris buffer (pH 7.4), respectively. All given concentrations mean final concentrations. Reactions were initiated by the addition of desomorphine and stopped with 50 μL of ice-cold acetonitrile containing 10 μM codeine-d_6 as internal standard. The solution was centrifuged for 2 min at 10,000×*g*, 70 μL of the supernatant transferred into an autosampler vial, and 10 μL injected onto the LC-HR-MS/MS system. In control sample, enzyme was replaced with buffer; in blank sample, substrate was replaced by phosphate buffer.

UGT initial activity screening

The UGT isoenzymes (0.25 mg protein/mL, each) UGT1A1, UGT1A4, UGT1A6, UGT1A7, UGT1A8, UGT1A9, UGT1A10, UGT2B4, UGT2B7, UGT2B15, and UGT2B17 were preincubated for 10 min at 37 °C with 20 μL UGT reaction mix solution B and 90 mM Tris buffer (pH 7.4). Thereafter, 10 μL UGT reaction mix solution A and 25 μM desomorphine in Tris buffer were added and the mixture (final volume, 100 μL) incubated for 30 min. All given concentrations mean final concentrations. Reactions were initiated by addition of desomorphine and stopped with 50 μL of ice-cold acetonitrile containing 10 μM codeine-d_6 as internal standard. The solution was centrifuged for 2 min at 10,000×*g*, 100 μL of the supernatant transferred into an autosampler vial, and 10 μL injected onto the LC-HR-MS/MS system. In control sample, enzyme was replaced with buffer; in blank sample, substrate was replaced by Tris buffer.

LC-HR-MS/MS for identification of phase I and II metabolites and initial activity screening with CYPs and UGTs

Based on published procedures [9, 19], the processed samples were analyzed using a ThermoFisher Scientific (TF, Dreieich, Germany) Accela LC system consisting of a degasser, a quaternary pump, and an HTC PAL Autosampler (CTC Analytics AG, Zwingen, Switzerland), coupled to a TF Q-Exactive system equipped with a heated electrospray ionization (HESI)-II source and Xcalibur 3.0.63 software. Mass calibration was done prior to analysis according to the manufacturer's recommendations using external mass calibration.

Gradient elution was performed on a TF Accucore PhenylHexyl column (100 × 2.1 mm, 2.6 μm). The mobile phases consisted of 2 mM aqueous ammonium formate containing formic acid (0.1 %, *v*/*v*) and acetonitrile (1 %, *v*/*v*) (pH 3, eluent A) and ammonium formate solution with acetonitrile/methanol (1:1, *v*/*v*) containing formic acid (0.1 %, *v*/*v*) and water (1 %, *v*/*v*; eluent B). The flow rate was set to 500 μL/min for 10 min and 800 μL/min from 10 to 13.5 min using the following gradient: 0–1.0 min 99 % A, 1–10 min to 1 % A, 10–11.5 min hold 1 % A, and 11.5–13.5 min hold 99 % A. Chromatography was performed at 35 °C maintained by an analytical column heater (HotDog 5090; Prolab, Reinach, Switzerland). The HESI-II source conditions were as follows: ionization mode, positive; sheath gas, 60 arbitrary units (AU); auxiliary gas, 10 AU; spray voltage, 3.00 kV; heater temperature, 320 °C; ion transfer capillary temperature, 320 °C; and S-lens RF level, 60.0. Mass spectrometry was performed using full scan (FS) data and a subsequent data-dependent acquisition (DDA) mode with an inclusion list of the masses of desomorphine and its potential metabolites. According to common metabolism routes, the following metabolites were included: nor, oxo, or hydroxy metabolites, combinations of them, sulfation and glucuronidation of the parent compound, and corresponding phase I metabolites.

The settings for FS data acquisition were as follows: resolution, 35,000; microscans, 1; automatic gain control (AGC) target, 1e6; maximum injection time, 120 ms; and scan range, *m*/*z* 70–750. The settings for the DDA mode with an inclusion list ("do pick others" mode) for desomorphine and the expected metabolites were as follows: protonated precursor ions (PPI), transferred to an exclusion list for 1 s (dynamic exclusion); resolution, 17,500; microscans, 1; loop count 5; AGC target, 2e5; maximum injection time, 250 ms; isolation window, *m*/*z* 1.0; high collision dissociation (HCD) cell normalized collision energy (NCE), 50 eV; spectrum data type, profile; and underfill ratio, 0.5 %. HCD 50 eV Xcalibur Qual Browser software version 3.0.63 was used for data handling.

HILIC-HR-MS/MS for separation of the hydroxy isomers and *N*-oxide

The processed samples were analyzed using a ThermoFisher Scientific (TF, Dreieich, Germany) Dionex UltiMate 3000 RS pump consisting of a degasser, a quaternary pump, and an UltiMate Autosampler, coupled to a TF Q-Exactive Plus system equipped with an HESI-II source. Mass calibration was done prior to analysis according to the manufacturer's recommendations using external mass calibration.

Gradient elution was performed on a Macherey Nagel (Düren, Germany) HILIC Nucleoshell column (100 × 2 mm, 2.7 μm). The mobile phases consisted of 2 mM aqueous ammonium formate containing formic acid (0.1 %, *v*/*v*) and acetonitrile (1 %, *v*/*v*) (pH 3, eluent A) and acetonitrile containing formic acid (0.1 %, *v*/*v*) (eluent B). The gradient and flow rate were programmed as follows: 0–1 min hold 98 % B, curve 5; 1–6 min 40 % B, curve 8; 6–7 min 40 % B, curve 9; 7–8.5 min 40 % B, curve 8; 8.5–9 min 98 % B, curve 5; and 9–12.1 min 98 % B at 500 μL/min. Chromatography was performed at 40 °C maintained by an analytical column heater (Dionex UltiMate 3000). The HESI-II source conditions were as follows: ionization mode, positive; sheath gas, 53 AU; auxiliary gas, 14 AU; sweep gas, 3 AU; spray voltage, 4.00 kV; heater temperature, 438 °C; ion transfer capillary temperature, 269 °C; and S-lens RF level, 60.0. Mass spectrometry was performed using FS data and a subsequent DDA mode with an inclusion list ("do pick others" mode) on the masses of desomorphine and its potential metabolites as described above. MS settings were as described above, with the exception of the pseudo-MS^3 settings, which were as follows: mode, parallel reaction monitoring for ion of *m*/*z* 260.1645; in-source collision-induced dissociation, 75 eV; NCE, 60 eV; maximum injection time, 100 ms; and isolation window, *m*/*z* 1.0. Xcalibur Qual Browser software version 3.0.63 was used for data handling.

Standard urine screening approaches

The SUSAs were performed as described previously. Briefly, for GC-MS, acid hydrolysis, liquid-liquid extraction, and acetylation were performed before FS GC-MS, AMDIS data evaluation, and library search [10, 11, 20]. Urine was precipitated for both liquid chromatography-mass spectrometry (LC-MS) approaches [8, 9, 12]. The data of LC-MS^n were evaluated using TF ToxID and library search [8, 12, 21] and of LC-HR-MS/MS using TF TraceFinder [9] and library search (Maurer HH, Helfer AG, Meyer MR, Weber AA (2016) Maurer/Helfer/Meyer/Weber MHMW LC-HR-MS/MS library of drugs, poisons, and their metabolites. Wiley-VCH, Weinheim (Germany), in preparation).

Results and discussion

HR-MS/MS fragmentation for identification of desomorphine phase I metabolites

In previous optimization experiments for the MS settings, no increase of the scan rate was observed by lowering the maximum IT. The reason for that might be the given AGC target as second criterion, what resulted in lower IT for most compounds. However, some low abundant metabolites benefited from the relatively high max IT.

The selection of potential metabolites was performed by using an inclusion list covering the common metabolic changes. In the following, the corresponding calculated exact masses are used. The MS^2 spectrum of desomorphine (**1** in Fig. 2) showed besides the PPI of *m/z* 272.1645, the most abundant FI of *m/z* 215.1066, which was a result of a cleavage between nitrogen and carbon 9 and a cleavage between carbon 13 and 15 (elimination of ring E; structure given in Fig. 1). Elimination of hydrogen resulted in the FI of *m/z* 213.0910. By elimination of water from the FI of *m/z* 215.1066 or 213.0910, the FI of *m/z* 197.0960 or 195.0804 was formed. Subsequent elimination of carbon monoxide led to the FI of *m/z* 169.1011 or 167.0855.

The nor metabolite (**2**, PPI of *m/z* 258.1488) showed a fragmentation pattern similar to desomorphine. The MS^2 spectrum contained FIs of *m/z* 215.1066, 213.0910, 197.0960, 195.0804, 169.1011, and 167.0855 as described above. The fragmentation pattern of desomorphine *N*-oxide (**3**, PPI of *m/z* 288.1594) was different from that of desomorphine. The most abundant FI of *m/z* 271.1566 originated from elimination of a hydroxy group, the FI of *m/z* 270.1488 from elimination of water. Subsequent elimination of the methyl group at the nitrogen led to FI of *m/z* 256.1332. Elimination of water, the *N*-methyl group, and the ethyl bridge (carbon 15 + 16) led to the FI of *m/z* 228.1019. The FI of *m/z* 215.1066, 213.0910, 197.0960, 195.0804, 169.1011, and 167.0855 were identical to those described above.

In the different models, several hydroxy metabolites were detected. In order to detect all isomers in one run, a mixture was analyzed of processed samples of diluted rat urine, incubations with pHLM/pHLC, HepG2, and HepaRG (Fig. 3) as the isomers were not present in one single sample (cf. Table 1). However, as can be seen in the lower part, only HILIC provided sufficient separation. This was particularly necessary for identifying isomer 1 as 6-hydroxy metabolite (**4**, PPI of *m/z* 288.1594) being dihydromorphine, a therapeutically applied opioid, an intake of which should be differentiated from a desomorphine/crocodile use. This was confirmed by co-chromatography and fragmentation pattern compared to the reference compound. The most abundant FI of *m/z* 185.0597, already described for morphine [22], was a result of the elimination of ring E and ethanol from ring C after cleavages between carbon 5 and 6 and between carbon 7 and 8, and as a consequence, the aromatic ring system is extended. Elimination of water led to the FI of *m/z* 270.1488, typical for aliphatic hydroxy groups [23]. The FI of *m/z* 231.1015 was a result of a cleavage between nitrogen and carbon 9 and a cleavage between carbon 13 and 15 in analogy to the FI of *m/z* of 215.1066 in the desomorphine spectra. Elimination of hydrogen led to the FI of *m/z* 229.0859. The FI of *m/z* 211.0753 resulted from the FI of *m/z* 213.0910 also by hydrogen elimination.

The MS^2 spectrum of hydroxy desomorphine isomer 2 (**5**, PPI of *m/z* 288.1594) showed FIs of *m/z* 270.1488, 231.1015, 229.0859, 213.0910, 195.0804, and 167.0855 as already described above. Due to the FI of *m/z* 270.1488 (loss of water), it is likely that the hydroxy group was located at an aliphatic position, and due to the FIs of *m/z* 231.1015 and 229.0859, hydroxylation in position 15 or 16 could be excluded. Based on the fragmentation patterns of the other hydroxy isomers, only position 8 remained as position for the hydroxy group as explained below. Hydroxy desomorphine isomer 3 (**6**, PPI of *m/z* 288.1594) showed a fragmentation pattern comparable to the hydroxy desomorphine isomer 1 but a different retention time. Hence, it is likely that the hydroxy group was located at ring C because at other positions, the FI of *m/z* 185.0597 was unlikely to be formed. Position 6 could be excluded due to the analytically confirmed hydroxy isomer 1. If the hydroxy group was located at position 8, elimination of ring E and ethanol from ring C after cleavages between carbon 6 and 7 and between carbon 8 and 14 should be needed to form FI of *m/z* 185.0597. In that case, no extend of the aromatic ring system was possible in contrast to the fragmentation described above. That might indicate the hydroxy group to be located at position 7.

Hydroxy desomorphine isomer 4 (**7**, PPI of *m/z* 288.1594) showed no FI of *m/z* 270.1488 (loss of water). Hence, it was likely that the hydroxy group was located at the aromatic ring

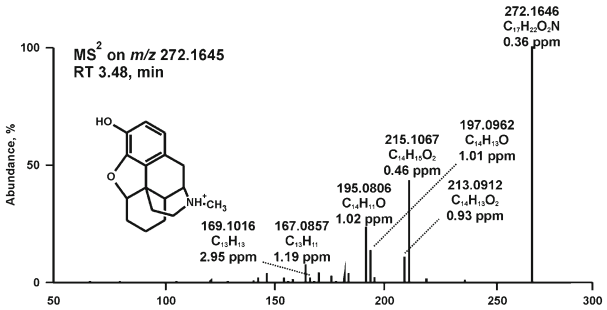

(1) Desomorphine

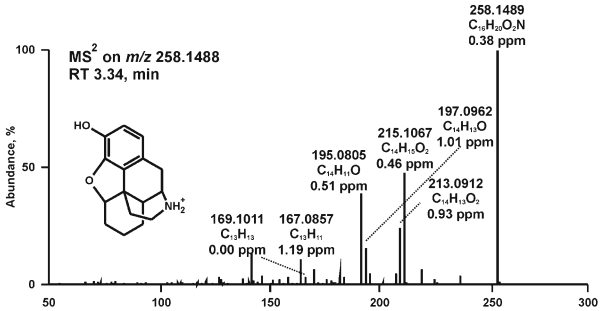

(2) Nor desomorphine

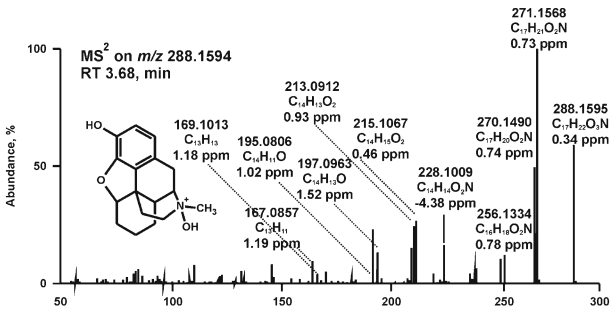

(3) Desomorphine -*N*-oxide

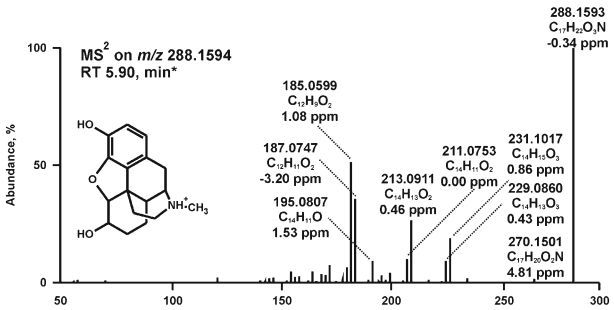

(4) Hydroxy desomorphine isomer 1

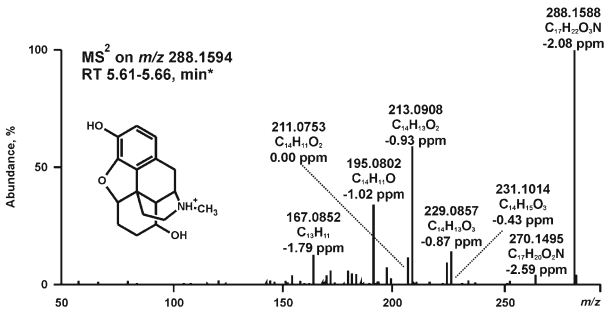

(5) Hydroxy desomorphine isomer 2

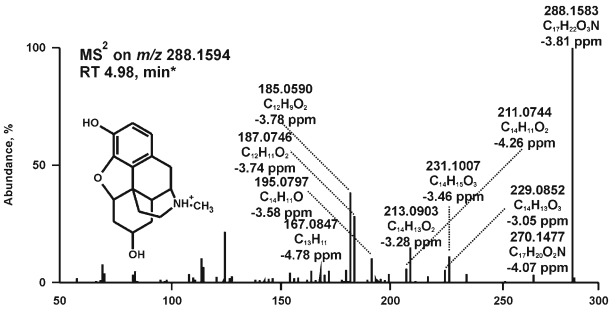

(6) Hydroxy desomorphine isomer 3

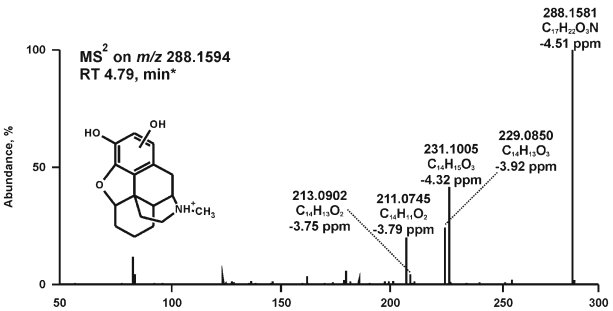

(7) Hydroxy desomorphine isomer 4

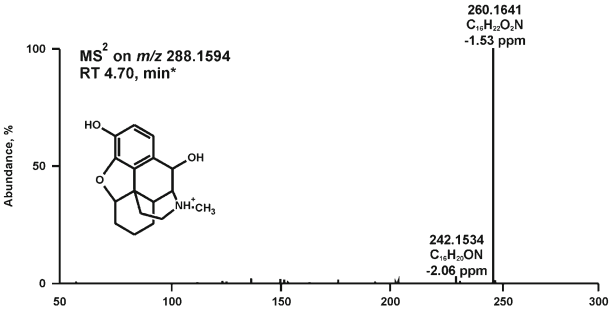

(8) Hydroxy desomorphine isomer 5

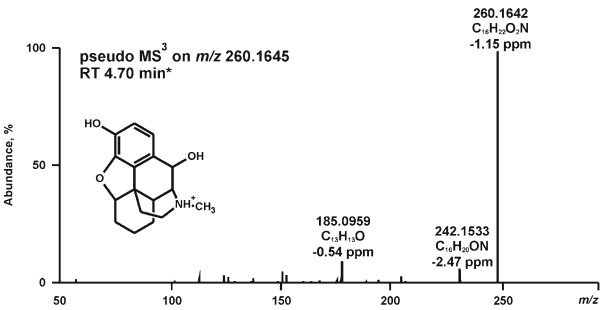

(9) Hydroxy desomorphine isomer 5

◀ **Fig. 2** HR-MS/MS spectra, proposed structures, and retention times (RT) of desomorphine and its phase I metabolites arranged according to increasing precursor ion intensity and hydroxy isomers according to their increasing retention times. The protonated precursor ions and fragment ions (FI) are given with the measured accurate masses and mass deviations (RT marked with an *asterisk* were determined by HILIC, cf. Fig. 3)

A. In addition, the FIs of *m/z* 231.0910, 229.0859, and 211.0753 are formed as described above.

Hydroxy desomorphine isomer 5 (**8**, PPI of *m/z* 288.1594) showed a fragmentation pattern different from the other hydroxy isomers. The most abundant FI of *m/z* 260.1645 was formed by elimination of carbon monoxide. All other FIs had a very low abundance, probably caused by stabilization via a hydrogen bridge between nitrogen and the hydroxy group if located in position 10. That would explain why isomer 5 showed a different fragmentation. The FI of *m/z* 242.1539 resulted by elimination of water from the FI of *m/z* 260.1645. For confirmation, a pseudo MS^3 experiment (**9**) was done [24]. The pseudo MS^3 spectrum showed FIs of *m/z* 260.1645 and 242.1539 as described above. In addition, the FI of *m/z* 185.0960 ($C_{13}H_{13}O$) was formed by subsequent elimination of ring E. It should be mentioned that the structure of this FI differed from that of *m/z* 185.0597 ($C_{12}H_9O_2$) described above.

HR-MS/MS fragmentation for identification of desomorphine phase II metabolites

Figure 4 shows the MS^2 spectra of the phase II metabolites. The glucuronidated metabolites (**12**, PPI of *m/z* 448.1965; **11**, PPI of *m/z* 434.1809; **13**, PPI of *m/z* 464.1915) eliminated glucuronic acid (−176.0321 u) and the sulfate (**10**, PPI of *m/z* 352.1213) sulfuric acid (−79.9568 u) leading to the known spectra of desomorphine or the corresponding phase I metabolites.

CYP initial activity screening

For identification of the CYPs catalyzing the initial metabolic steps, the ten most abundant human hepatic CYPs were incubated under conditions allowing a statement on the general involvement of a particular CYP enzyme. Only CYP3A4 was involved in the initial metabolic steps *N*-demethylation, hydroxylation, and *N*-oxidation, but the hydroxy isomers 1 and 3 were not detected.

UGT initial activity screening

As the desomorphine glucuronide was observed as relatively most abundant metabolite in vivo, 11 human hepatic UGTs were incubated under conditions allowing a statement on the general involvement of a particular UGT enzyme. UGT1A1, UGT1A8, UGT1A9, UGT1A10, UGT2B4, UGT2B7, UGT2B15, and UGT2B17 were identified as catalyzing enzymes. UGT2B7 is known to be the main catalyzing enzyme for glucuronidation of morphine too [25, 26].

Comparisons of the metabolites detected in the investigated models

To date, there are only two publications available on HepaRG cells used in studies of drugs of abuse. Dias-da-Silva et al. [27] compared HepG2, HepaRG cells, and primary rat hepatocytes as in vitro tool for hepatotoxicity studies of piperazine designer drugs without focus on the metabolites. Kanamori et al. [28]

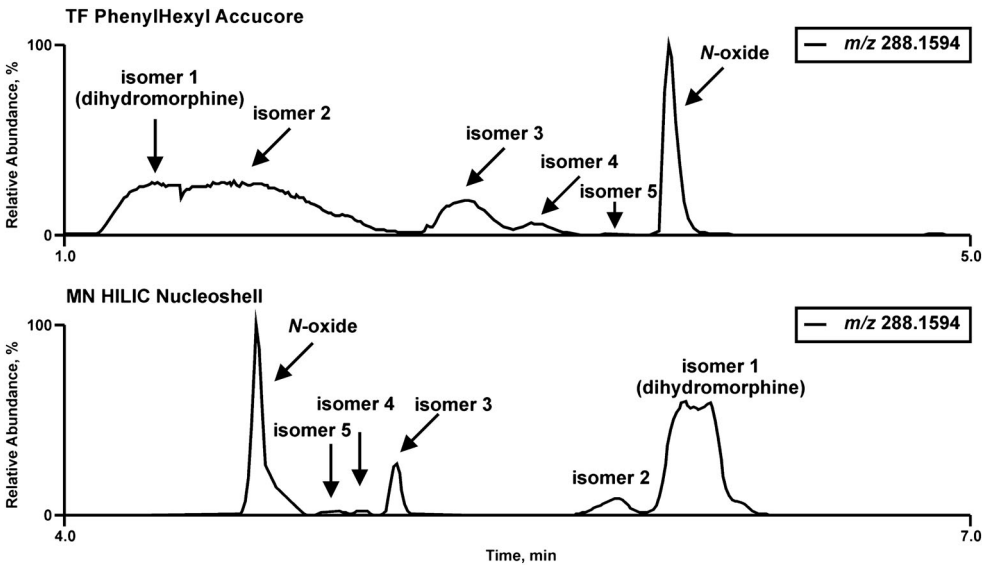

Fig. 3 Reconstructed LC-HR-MS chromatograms of ion of *m/z* 288.1594 indicating hydroxy desomorphine isomers and desomorphine *N*-oxide after reversed phase separation (upper part) or HILIC separation (lower part) in pooled processed samples of rat urine and incubations with pHLM/pHLC, HepG2, or HepaRG

Table 1 Overview of the detected desomorphine metabolites in the investigated models (+ detected, − not detected)

Metabolite		Rat urine	pHLM/pHLC	HepG2	HepaRG
Phase I	Nor	+	+	+	+
	Hydroxy isomer 1 (dihydromorphine)	+	−	−	−
	Hydroxy isomer 2	+	+	+	+
	Hydroxy isomer 3	+	−	+	+
	Hydroxy isomer 4	+	+	−	+
	Hydroxy isomer 5	−	+	−	−
	N-Oxide	+	+	+	+
Phase II	Glucuronide	+	+	+	+
	Sulfate	+		+	+
	Nor glucuronide	+	−	−	+
	N-Oxide glucuronide	+	−	−	+

investigated the metabolism of XLR-11, a synthetic cannabinoid, in HepaRG cells and human urine, but in contrast to the present study, they focused on phase I metabolites after cleavage of conjugates. They compared their results with those of Wohlfarth et al. [29], who studied the XLR-11 metabolism with primary human hepatocytes and found HepaRG cells to be a promising alternative to mimic human in vivo metabolism with the limitations of an in vitro system. In the present study, the metabolism of desomorphine in HepG2 and HepaRG cells was compared to established models using rat urine after high drug dose [30] and pHLM/pHLC with standard conditions [31, 32]. In order to assess the influence of substrate concentration and incubation time on the relative extend of metabolite formation, both cell lines were incubated with 0.01, 0.1, or 1 mM desomorphine for 3 or 24 h, respectively. As an example, Fig. 5 shows the peak area ratio of the desomorphine glucuronide versus codeine-d_6 with the highest amount in HepaRG cells incubated with 1 mM desomorphine for 24 h.

A list of the detected metabolites in the investigated models is given in Table 1. Desomorphine and its phase I metabolites, namely nor desomorphine and desomorphine *N*-oxide, were detected in all investigated models. In sum, five hydroxy metabolites could be detected in the different models. However, hydroxy desomorphine isomer 1 (dihydromorphine) was detected only in

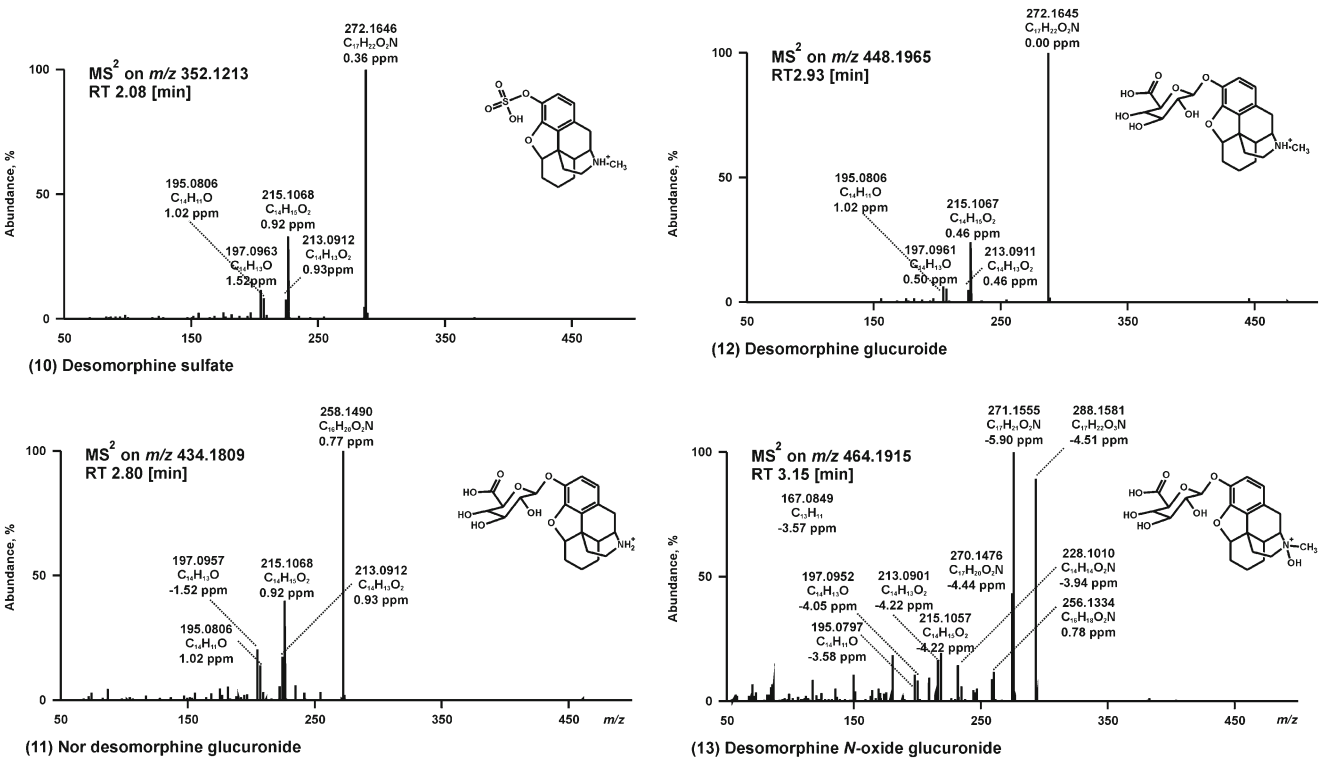

Fig. 4 HR-MS/MS spectra, proposed structures, and RTs of desomorphine phase II metabolites arranged according to increasing *m/z* intensity. The protonated precursor ions and fragment ions (FI) are given with the measured accurate masses and mass deviations

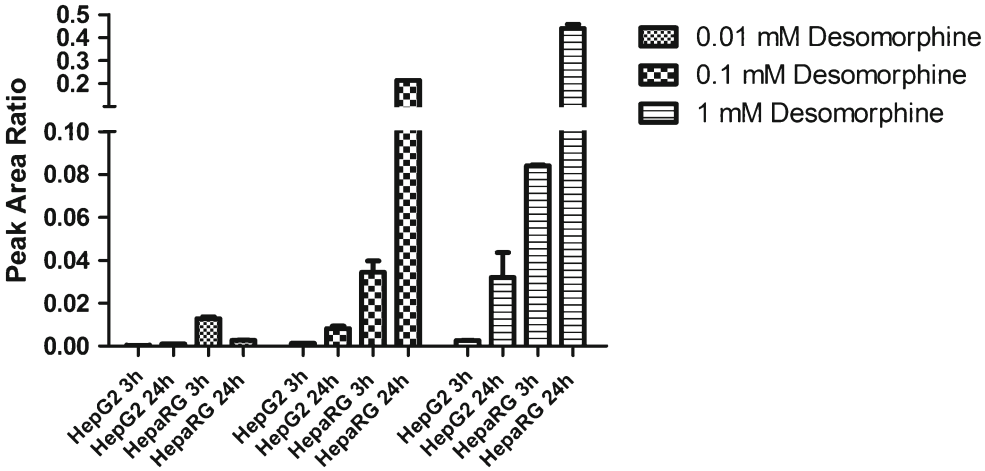

Fig. 5 Peak area ratios of desomorphine glucuronide versus codeine-d_6 in HepG2 and HepaRG cell lines, incubated with 0.01, 0.1, or 1 mM desomorphine for 3 or 24 h ($n = 3$)

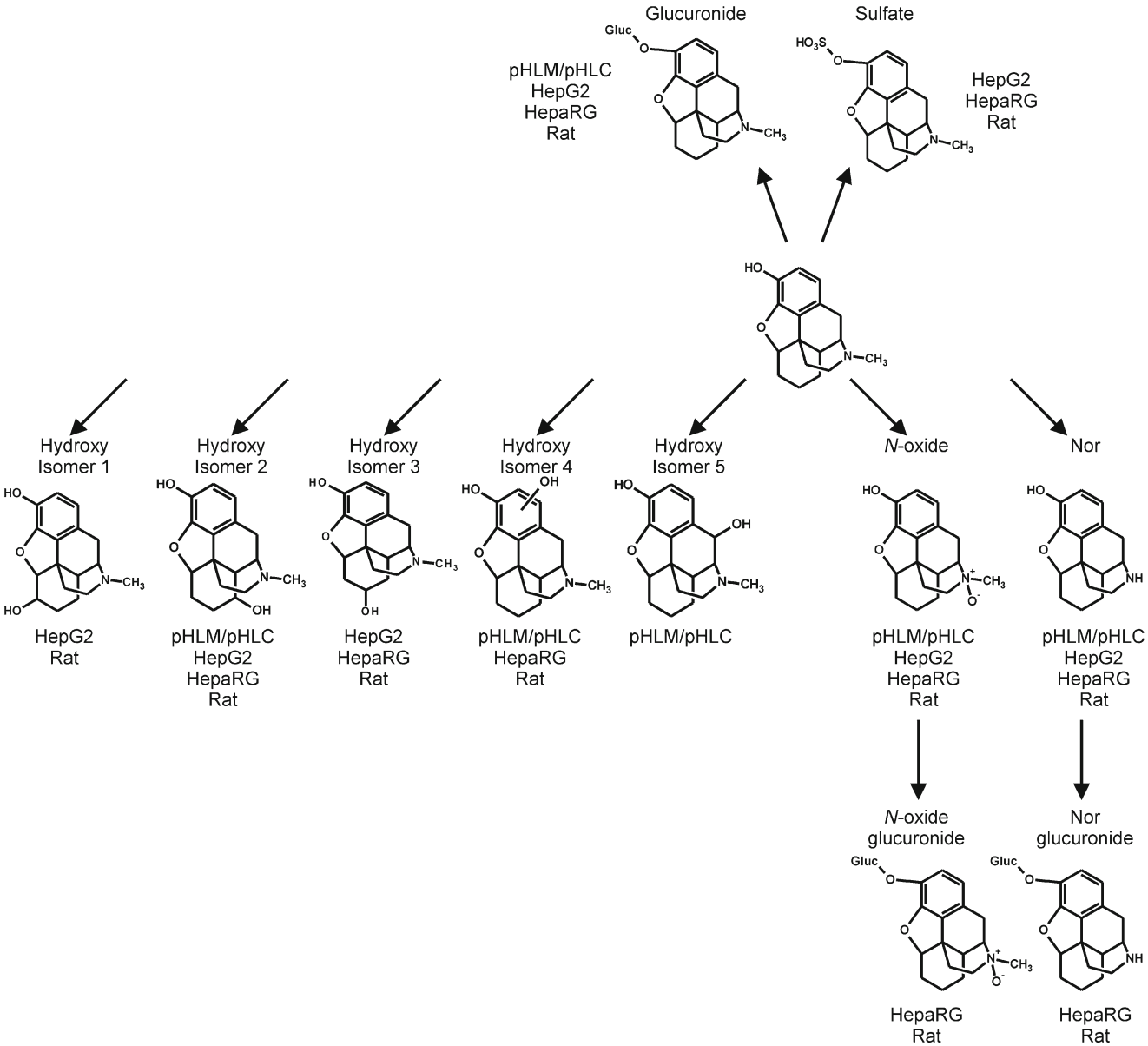

Fig. 6 Proposed metabolic pathways of desomorphine according to the metabolites detected in rat urine, pHLM/pHLC, HepG2, or HepaRG cells

Table 2 Targets for GC-MS SUSA monitoring desomorphine with molecular masses, five most abundant fragment ions, their relative abundances, and retention indices according to Kovats [42] (*AC* acetyl)

Compound	Molecular mass (u)	GC-MS fragment ions (*m/z*) and their relative abundance (%)	Retention index
Desomorphine	271	148 (18), 214 (30), 228 (18), 256 (15), 271 (100)	2300
Desomorphine AC	313	148 (13), 214 (27), 228 (14), 271 (63), 313 (100)	2370
Desomorphine-M (nor-) 2AC	341	87 (65), 213 (100), 255 (25), 299 (48), 341 (35)	2700

rat urine, which could be explained by species differences [33–35]. Isomer 2 was detected in all investigated models, but isomer 3 was not detected in pHLM/pHLC incubations. A possible explanation could be that isomer 3 has a low metabolite formation rate so it was not present after 30 min of incubation. Isomer 4 was not detected in HepG2 incubations. A reason for this might be that HepG2 cells are known to have a low gene expression level for CYP enzymes [36, 37]. In contrast, the gene expression level for CYPs in HepaRG cells was comparable to cryopreserved human hepatocytes [37, 38], which were also used for metabolism studies of drugs of abuse [29] as described above [34, 35].

Isomer 5 was detected only in pHLM/pHLC incubations (Table 1) most probably due to instability during the long urine collection time and the much longer incubation times in cells. In processed samples of pHLM/pHLC incubations measured after storage for 1 week at 4 °C, isomer 5 was not detected anymore. Another reason might be the difference of enzyme concentrations, cofactors, and general conditions between microsome incubations and hepatocyte cell cultures or different matrix effects.

Desomorphine glucuronide was detected in all investigated models with highest relative signal intensity of all metabolites. Nor desomorphine glucuronide and desomorphine *N*-oxide glucuronide were detected only in rat urine and HepaRG incubations. In contrast to the lower CYP gene expression in HepG2, gene expression of phase II enzymes (UDP-glucuronyltransferases, sulfotransferases, glutathione *S*-transferases, *N*-acetyl-transferases) should be comparable in HepG2 and HepaRG [37] with the exception of UGT1A, UGT2B4, UGT2B15, and UGT2B17 (UGT2B7 not evaluated) [37, 39]. The probable reason why no glucuronides were formed in pHLM/pHLC and HepG2 was the low formation of phase I metabolites or formation of these metabolites in concentrations below the detection limit because desomorphine was the main substrate. Desomorphine sulfate was detected in rat urine and both cell lines, but not in the pHLM/pHLC incubation. This might indicate sulfation to be a minor metabolic step in humans.

In summary, the most abundant peak in rat urine samples represented desomorphine glucuronide and the second abundant peak desomorphine. Peak areas of the metabolites in relation to that of desomorphine were lower in the in vitro models, most probably due to the static nature. The formed metabolites were not eliminated from the equilibrium and thus accumulated in the wells or reaction tubes reducing their further formation. Of course, also post-metabolism processes, such as reabsorption, enterohepatic circulation, and the renal elimination, limit the in vitro models. However, besides the in vivo model, all in vitro models were able to identify the relatively most abundant metabolite of desomorphine, its glucuronide. The peak area ratios of phase I and II metabolites were higher in HepaRG than in HepG2 cells. In HepaRG cells, the number of different metabolites was higher than in HepG2 cells and pHLM/pHLC incubations. HepaRG cells might be the most suitable in vitro tool for the prediction of human phase I and II hepatic metabolism of drugs of abuse among the tested models, but further studies are needed with compounds more extensively metabolized. Finally, a comparison of the in vitro data with human in vivo data, e.g., of clinical or forensic case work, would further confirm the suitability of the model.

Table 3 Targets for LC-MS^n SUSA monitoring desomorphine with protonated precursor ions, characteristic MS^2 and MS^3 fragment ions, and retention time (RT)

Target for SUSA	Precursor ion (*m/z*)	MS^2 fragment ions (*m/z*) and relative intensities (%)	MS^3 fragment ions (*m/z*) on the selected ion and relative intensities (%)	RT (min)
Desomorphine	272	195 (15), 197 (27), 213 (12), 215 (100), 272 (13)	215: 149 (37), 169 (52), 173 (51), 179 (90), 187 (100)	4.6
Desomorphine-M (glucuronide)	448	195 (1), 197 (1), 213 (1), 215 (5), 272 (100)	272: 187 (7), 195 (14), 197 (27), 213 (13), 215 (100)	1.7

Proposed metabolic pathways

According to the metabolites identified in vivo and in vitro, the following metabolic pathways, depicted in Fig. 6, could be proposed: *N*-demethylation, *N*-oxidation, and hydroxylation at various positions as well as glucuronidation and sulfation of the parent compound and glucuronidation of nor desomorphine and desomorphine *N*-oxide. The main metabolic step was the glucuronidation of the parent compound.

Toxicological detection of desomorphine by GC-MS, LC-MS^n, and LC-HR-MS/MS SUSAs

The GC-MS approach was able to detect desomorphine and its nor metabolite (mass lists given in Table 2, full spectra are given in Ref. [10]), the LC-MS^n approach to detect desomorphine and its glucuronide (mass list given in Table 3, full spectra will be given in the 2016 version of Ref. [21]), and the LC-HR-MS/MS screening approach to detect desomorphine, its glucuronide, and the nor metabolite (spectra given in Figs. 2 and 3) in rat urine after administration of 1 mg/kg BW dose. After scaling by the dose-by-factor approach from rat to man according to Sharma and McNeill [40], this dose would correspond to a human dose of 0.2 mg/kg. As the common therapeutic dose of desomorphine was up to 60 mg absolute corresponding to about 1 mg/kg BW [40, 41], a misuse should be monitored by the SUSAs assuming comparable kinetics in rats and humans.

Conclusion

Various metabolites were identified in the investigated models. All phase I metabolic steps were catalyzed by CYP3A4. Glucuronidation was catalyzed by UGT1A1, UGT1A8, UGT1A9, UGT1A10, UGT2B4, UGT2B7, UGT2B15, and UGT2B17. In vitro liver cell culture using HepaRG cells might be a suitable tool for the prediction of human phase I and II hepatic metabolism of drugs of abuse. A desomorphine intake should be detectable by all SUSAs mainly via the parent compound and its glucuronide.

Acknowledgments The authors thank Achim T. Caspar, Julia Dinger, Andreas G. Helfer, Julian A. Michely, Carsten Schröder, Gabriele Ulrich, Lea Wagmann, and Armin A. Weber for support and/or helpful discussion. The research leading to these results partly received funding from the European Community's Seventh Framework Programme (FP7/2007-2013) under grant agreement no. 267038 and Cosmetics Europe within the framework of the NOTOX project of the SEURAT-1 (safety evaluation ultimately replacing animal testing) initiative.

Compliance with ethical standards

Conflict of interest The authors declare that there are no conflicts of interest and that they followed the national guidelines for animal ethical care.

References

1. Katselou M, Papoutsis I, Nikolaou P, Spiliopoulou C, Athanaselis S. A "krokodil" emerges from the murky waters of addiction. Abuse trends of an old drug. Life Sci. 2014;102:81–7.
2. Gahr M, Freudenmann RW, Hiemke C, Gunst IM, Connemann BJ, Schonfeldt-Lecuona C. Desomorphine goes "crocodile". J Addict Dis. 2012;31:407–12.
3. Rech MA, Donahey E, Cappiello Dziedzic JM, Oh L, Greenhalgh E. New drugs of abuse. Pharmacotherapy. 2015;35:189–97.
4. United Nations Office on Drugs and Crime (UNODC) (2015) World Drug Report 2015. https://www.unodc.org/documents/wdr2015/World_Drug_Report_2015.pdf.
5. Grund JP, Latypov A, Harris M. Breaking worse: the emergence of krokodil and excessive injuries among people who inject drugs in Eurasia. Int J Drug Policy. 2013;24:265–74.
6. Savchuk SA, Barsegyan SS, Barsegyan IB, Kolosov GM. Chromatographic study of expert and biological samples containing desomorphine. J Anal Chem. 2008;63:361–70.
7. Meyer MR, Lindauer C, Maurer HH. Dimethocaine, a synthetic cocaine derivative: studies on its in vitro metabolism catalyzed by P450s and NAT2. Toxicol Lett. 2014;225:139–46.
8. Wissenbach DK, Meyer MR, Remane D, Philipp AA, Weber AA, Maurer HH. Drugs of abuse screening in urine as part of a metabolite-based LC-MS(n) screening concept. Anal Bioanal Chem. 2011;400:3481–9.
9. Helfer AG, Michely JA, Weber AA, Meyer MR, Maurer HH. Orbitrap technology for comprehensive metabolite-based liquid chromatographic-high resolution-tandem mass spectrometric urine drug screening—exemplified for cardiovascular drugs. Anal Chim Acta. 2015;891:221–33.
10. Maurer HH, Pfleger K, Weber AA. Mass spectral library of drugs, poisons, pesticides, pollutants and their metabolites. Weinheim: Wiley-VCH; 2016.
11. Meyer MR, Lindauer C, Welter J, Maurer HH. Dimethocaine, a synthetic cocaine derivative: studies on its in vivo metabolism and its detectability in urine by LC-HR-MS^n and GC-MS using a rat model. Anal Bioanal Chem. 2014;406:1845–54.
12. Wissenbach DK, Meyer MR, Remane D, Weber AA, Maurer HH. Development of the first metabolite-based LC-MSn urine drug screening procedure—exemplified for antidepressants. Anal Bioanal Chem. 2011;400:79–88.
13. Welter J, Kavanagh P, Meyer MR, Maurer HH. Benzofuran analogues of amphetamine and methamphetamine: studies on the metabolism and toxicological analysis of 5-APB and 5-MAPB in urine and plasma using GC-MS and LC-(HR)-MS^n techniques. Anal Bioanal Chem. 2015;407:1371–88.
14. Schwaninger AE, Meyer MR, Zapp J, Maurer HH. Sulfation of the 3,4-methylenedioxymethamphetamine (MDMA) metabolites 3,4-dihydroxymethamphetamine (DHMA) and 4-hydroxy-3-methoxymethamphetamine (HMMA) and their capability to inhibit human sulfotransferases. Toxicol Lett. 2011;202:120–8.
15. Mueller D, Kramer L, Hoffmann E, Klein S, Noor F. 3D organotypic HepaRG cultures as in vitro model for acute and repeated dose toxicity studies. Toxicol In Vitro. 2014;28:104–12.
16. Klein S, Mueller D, Schevchenko V, Noor F. Long-term maintenance of HepaRG cells in serum-free conditions and application in a repeated dose study. J Appl Toxicol. 2014;34:1078–86.
17. Sauvage FL, Saint-Marcous F, Duretz B, Deporte D, Lachatre G, Marquet P. Screening of drugs and toxic compounds with liquid chromatography-linear ion trap tandem mass spectrometry. Clin Chem. 2006;52:1735–42.
18. Wink CSD, Meyer GMJ, Wissenbach DK, Jacobsen-Bauer A, Meyer MR, Maurer HH. Lefetamine-derived designer drugs *N*-

ethyl-1,2-diphenylethylamine (NEDPA) and *N-iso*-propyl-1,2-diphenylethylamine (NPDPA): metabolism and detectability in rat urine using GC-MS, LC-MS^n and LC-high resolution (HR)-MS/MS. Drug Test Anal. 2014;6:1038–48.

19. Caspar AT, Helfer AG, Michely JA, Auwaerter V, Brandt SD, Meyer MR, et al. Studies on the metabolism and toxicological detection of the new psychoactive designer drug 2-(4-iodo-2,5-dimethoxyphenyl)-N-[(2-methoxyphenyl)methyl]ethanamine (25I-NBOMe) in human and rat urine using GC-MS, LC-MSn, and LC-HR-MS/MS. Anal Bioanal Chem. 2015;407:6697–719.
20. Meyer MR, Peters FT, Maurer HH. Automated mass spectral deconvolution and identification system for GC-MS screening for drugs, poisons, and metabolites in urine. Clin Chem. 2010;56:575–84.
21. Maurer HH, Wissenbach DK, Weber AA. Maurer/Wissenbach/Weber MWW LC-MSn library of drugs, poisons, and their metabolites. Weinheim (Germany): Wiley-VCH; 2014.
22. Poeaknapo C, Fisinger U, Zenk MH, Schmidt J. Evaluation of the mass spectrometric fragmentation of codeine and morphine after 13C-isotope biosynthetic labeling. Phytochemistry. 2004;65:1413–20.
23. Fenselau C. Applications of mass spectrometry. In: Kuwana T, editor. Physical methods in modern chemical analysis. New York: Academic Press; 1978. p. 110–1.
24. Mardal M, Gracia-Lor E, Leibnitz S, Castiglioni S, Meyer MR. Toxicokinetics of new psychoactive substances: plasma protein binding, metabolic stability, and human phase I metabolism of the synthetic cannabinoid WIN 55,212-2 studied using in vitro tools and LC-HR-MS/MS. Drug Test Anal. 2016. doi:10.1002/dta.1938.
25. Maurer HH, Sauer C, Theobald DS. Toxicokinetics of drugs of abuse: current knowledge of the isoenzymes involved in the human metabolism of tetrahydrocannabinol, cocaine, heroin, morphine, and codeine [review]. Ther Drug Monit. 2006;28:447–53.
26. Stone AN, Mackenzie PI, Galetin A, Houston JB, Miners JO. Isoform selectivity and kinetics of morphine 3- and 6-glucuronidation by human udp-glucuronosyltransferases: evidence for atypical glucuronidation kinetics by UGT2B7. Drug Metab Dispos. 2003;31:1086–9.
27. Dias-da-Silva D, Arbo MD, Valente MJ, Bastos ML, Carmo H. Hepatotoxicity of piperazine designer drugs: comparison of different in vitro models. Toxicol In Vitro. 2015;29:987–96.
28. Kanamori T, Kanda K, Yamamuro T, Kuwayama K, Tsujikawa K, Iwata YT, et al. Detection of main metabolites of XLR-11 and its thermal degradation product in human hepatoma HepaRG cells and human urine. Drug Test Anal. 2015;7:341–5.
29. Wohlfarth A, Pang S, Zhu M, Gandhi AS, Scheidweiler KB, Liu HF, et al. First metabolic profile of XLR-11, a novel synthetic cannabinoid, obtained by using human hepatocytes and high-resolution mass spectrometry. Clin Chem. 2013;59:1638–48.
30. Welter J, Meyer MR, Wolf E, Weinmann W, Kavanagh P, Maurer HH. 2-Methiopropamine, a thiophene analogue of methamphetamine: studies on its metabolism and detectability in the rat and human using GC-MS and LC-(HR)-MS techniques. Anal Bioanal Chem. 2013;405:3125–35.
31. Vollmer PA, Harty DC, Erickson NB, Balhon AC, Dean RA. Serum ethylene glycol by high-performance liquid chromatography. J Chromatogr B. 1996;685:370–4.
32. Wink CSD, Meyer GMJ, Zapp J, Maurer HH. Lefetamine, a controlled drug and pharmaceutical lead of new designer drugs: synthesis, metabolism, and detectability in urine and human liver preparations using GC-MS, LC-MS^n, and LC-high resolution-MS/MS. Anal Bioanal Chem. 2015;407:1545–57.
33. Yamazaki H. Fifty years of cytochrome P450 research. Tokyo: Springer; 2014. p. 293–306.
34. Carmo H, Hengstler JG, de Boer D, Ringel M, Carvalho F, Fernandes E, et al. Comparative metabolism of the designer drug 4-methylthioamphetamine by hepatocytes from man, monkey, dog, rabbit, rat and mouse. Naunyn Schmiedebergs Arch Pharmacol. 2004;369:198–205.
35. Carmo H, Hengstler JG, de Boer D, Ringel M, Remiao F, Carvalho F, et al. Metabolic pathways of 4-bromo-2,5-dimethoxyphenethylamine (2C-B): analysis of phase I metabolism with hepatocytes of six species including human. Toxicology. 2005;206:75–89.
36. Gerets HH, Tilmant K, Gerin B, Chanteux H, Depelchin BO, Dhalluin S, et al. Characterization of primary human hepatocytes, HepG2 cells, and HepaRG cells at the mRNA level and CYP activity in response to inducers and their predictivity for the detection of human hepatotoxins. Cell Biol Toxicol. 2012;28:69–87.
37. Hart SN, Li Y, Nakamoto K, Subileau EA, Steen D, Zhong XB. A comparison of whole genome gene expression profiles of HepaRG cells and HepG2 cells to primary human hepatocytes and human liver tissues. Drug Metab Dispos. 2010;38:988–94.
38. Kanebratt KP, Andersson TB. HepaRG cells as an in vitro model for evaluation of cytochrome P450 induction in humans. Drug Metab Dispos. 2008;36:137–45.
39. Westerink WM, Schoonen WG. Phase II enzyme levels in HepG2 cells and cryopreserved primary human hepatocytes and their induction in HepG2 cells. Toxicol In Vitro. 2007;21:1592–602.
40. Sharma V, McNeill JH. To scale or not to scale: the principles of dose extrapolation. Br J Pharmacol. 2009;157:907–21.
41. Eddy NB, Halbach H, Braenden OJ. Synthetic substances with morphine-like effect: clinical experience; potency, side-effects, addiction liability. Bull World Health Organ. 1957;17:569–863.
42. Kovats E. Gaschromatographische Charakterisierung organischer Verbindungen. Teil 1. Retentionsindices aliphatischer Halogenide, Alkohole, Aldehyde und Ketone. Helv Chim Acta. 1958;41:1915–32.

3.2. Pooled Human Liver Preparations, HepaRG, or HepG2 Cell Lines For Metabolism Studies of New Psychoactive Substances? A Study Using MDMA, MDBD, Butylone, MDPPP, MDPV, MDPB, 5-MAPB, and 5-API as Examples[11] (DOI: DOI: 10.1016/j.jpba.2017.05.028)

Journal of Pharmaceutical and Biomedical Analysis 143 (2017) 32–42

Contents lists available at ScienceDirect

Journal of Pharmaceutical and Biomedical Analysis

journal homepage: www.elsevier.com/locate/jpba

Pooled human liver preparations, HepaRG, or HepG2 cell lines for metabolism studies of new psychoactive substances? A study using MDMA, MDBD, butylone, MDPPP, MDPV, MDPB, 5-MAPB, and 5-API as examples

Lilian H.J. Richter[a], Veit Flockerzi[b], Hans H. Maurer[a], Markus R. Meyer[a,*]

[a] Department of Experimental and Clinical Toxicology, Institute of Experimental and Clinical Pharmacology and Toxicology, Center for Molecular Signaling (PZMS), Saarland University, 66421 Homburg, Germany
[b] Department of Experimental and Clinical Pharmacology, Institute of Experimental and Clinical Pharmacology and Toxicology, Center for Molecular Signaling (PZMS), Saarland University, 66421 Homburg, Germany

ARTICLE INFO

Article history:
Received 20 February 2017
Received in revised form 5 May 2017
Accepted 12 May 2017
Available online 18 May 2017

Keywords:
LC-HR-MS/MS
Metabolism
Human liver preparation
HepaRG
HepG2
Methylenedioxy NPS

ABSTRACT

Metabolism studies play an important role in clinical and forensic toxicology. Because of potential species differences in metabolism, human samples are best suitable for elucidating metabolism. However, in the case of new psychoactive substances (NPS), human samples of controlled studies are not available. Primary human hepatocytes have been described as gold standard for in vitro metabolism studies, but there are some disadvantages such as high costs, limited availability, and variability of metabolic enzymes. Therefore, the aim of our study was to investigate and compare the metabolism of six methylenedioxy derivatives (MDMA, MDBD, butylone, MDPPP, MDPV, MDPB) and two bioisosteric analogues (5-MAPB, 5-API) using pooled human liver microsomes (pHLM) combined with cytosol (pHLC) or pooled human liver S9 fraction (pS9) all after addition of co-substrates for six phase I and II reactions. In addition, HepaRG and HepG2 cell lines were used. Results of the different in vitro tools were compared to each other, to corresponding published data, and to metabolites identified in human urine after consumption of MDMA, MDPV, or 5-MAPB. Incubations with pHLM plus pHLC showed similar results as pS9. A more cost efficient model for prediction of targets for toxicological screening procedures in human urine should be identified. As expected, the incubations with HepaRG provided better results than those with HepG2 concerning number and signal abundance of the metabolites. Due to easy handling without special equipment, incubations with pooled liver preparations should be the most suitable alternative to find targets for toxicological screening procedures for methylenedioxy derivatives and bioisosteric analogues.

1. Introduction

Metabolism studies play an important role in clinical and forensic toxicology as metabolites can be the active component [1], reveal potential toxicity [2,3], and can represent targets for toxicological urine screening approaches [4–6]. Such assays should cover all important metabolic steps including phase II reactions as nowadays LC–MS approaches are often used for screening, which do not necessarily need cleavage of conjugates [5,7,8]. Because of potential species differences in metabolism [9,10], human samples would be best suitable for metabolism studies. However, particularly in the case of drugs of abuse (DOAs) and new psychoactive substances (NPS), human samples are often not available and controlled studies cannot be performed due to lack of preclinical safety data and thus ethical reasons.

In recent years, the phenomenon of the so-called NPS has emerged and numerous compounds have appeared on the DOAs market [11,12]. As no data are available on their metabolism, toxicity, and analytical targets in body fluids, their metabolism should be studied systematically using in vitro or in vivo models similar to human metabolism. Cell-free in vitro systems such as microsomes or S9 fraction were frequently used [10] for identifying either phase I [13–15] or, phase II metabolites [16,17] or, both [18,19]. The limitation of such studies was that not all co-substrates of the metabolizing enzymes were added losing the formation of the corresponding, maybe main metabolite, e.g. the demethylenyl

* Corresponding author.
E-mail address: markus.meyer@uks.eu (M.R. Meyer).

http://dx.doi.org/10.1016/j.jpba.2017.05.028
0731-7085/

methyl metabolite of MDPV [18]. As an attractive alternative, primary human hepatocytes were recommended [2,20–22], providing the natural enzyme clusters and drug transporters. However, they have some disadvantages such as high costs, limited availability, and variability in the expression of metabolic enzymes [3,10,23]. To minimize the variability, primary human hepatocytes are pooled to a maximum of ten donors. Further limits can be overcome by use of pooled human liver preparations or human hepatic cell lines such as HepaRG or HepG2 [20,24]. Cell lines can be cultivated to show constant gene expression over several passages [20], but there is still the risk of lacking enzymatic activity. HepaRG cells can differentiate into two cell types, biliary epithelial cells and hepatocytes [20], and differentiated HepaRG cells show gene expression levels for metabolizing enzymes comparable to primary human hepatocytes with the exception of cytochrome P450 (CYP) 2D6 [24]. HepG2 cells are easy to handle and the most frequently used human liver cell line [24]. One disadvantage is their low gene expression level for phase I drug metabolizing enzymes such as alcohol dehydrogenases, aldehyde dehydrogenases, CYP enzymes, and flavin containing monooxygenases [24]. Gene expression for phase II drug metabolizing enzymes (glutathione-*S*-transferases, GSTs; *N*-acetyltransferases, NATs; sulfotransferases, SULTs; and uridine diphosphate glucuronyltransferases, UGTs), and membrane transporter (ABCBs, ABCCs, ABCGs, and SLOCs) are comparable to HepaRG with exception of some down regulated UGTs [10,20,24]. All of the above mentioned in vitro systems have advantages and disadvantages. For toxicological screening procedures, it is important to identify the main excretion products in human fast, simple, cost effective, and reliable. Some studies were published comparing HepG2, HepaRG, and primary human hepatocytes [25–27] with focus on gene expression of CYP enzymes or phase I metabolism. No comparison with human liver preparation was done so far, particularly not with regard to phase II metabolism and with the focus on identification of targets for urine screening procedures for NPS.

Therefore, the aim of the presented study was to identify a more cost efficient alternative to primary human hepatocytes to allow the identification of targets for toxicological screening procedures in human urine. The metabolism of six methylenedioxy derivatives and two bioisosteric analogues (Fig. 1; MDMA, MDBD, butylone, MDPPP, MDPV, MDPB, 5-MAPB, and 5-API) was therefore exemplarily compared using pooled human liver microsomes combined with cytosol (pHLM/pHLC), pooled human liver S9 fraction (pS9), both after addition of co-substrates for six phase I and II reactions, HepaRG, and HepG2 cell cultures. Results of the different in vitro tools were then compared to each other, to corresponding published data, and to metabolites identified in human urine after drug intake. Finally, the fastest, simplest, most cost effective, and most reliable model for identification of the main excretion products in human urine in context of toxicological screening procedures should be identified.

2. Materials and methods

2.1. Chemicals, reagents, and materials

Clozapine was obtained from Sandoz (Basel, Switzerland), *p*-aminosalicylic acid from Kabi Pharma (Bad Homburg, Germany), 5-(2-aminopropyl)indole HCl (5-API also known as 5-IT), 1-(benzofuran-5-yl)-*N*-methylpropan-2-amine HCl (5-MAPB), *R,S*-butylone HCl, *R,S*-methylenedioxypyrovalerone HCl (MDPV), and *R,S*-3′,4′-methylenedioxy-α-pyrrolidinopropiophenone HCl (MDPPP) from LGC Standards (Wesel, Germany), *R,S*-2-methylamino-1-(3,4-methyledioxyphenyl)butane HCl (MBDB) from Lipomed AG (Arlesheim, Switzerland), *R,S-N*-methyl-3,4-dihydroxyamphetamine (DHMA) from Reseachem (Burgdorf, Switzerland), 1-(3,4-methylenedioxybenzyl)piperazine (MDBP) from Lancaster Synthesis (Frankfurt, Germany), and 1-phenyl-2-(pyrrolidin-1-yl)pentan-1-one HNO_3 (α-PVP) from LKA Wiesbaden (Wiesbaden, Germany) before it was scheduled in Germany, *R,S*-3,4-ethylendioxy-*N*-methylamphetamine HCl (MDMA), kynuramine, paracetamol, sulfamethazine, *p*-nitrophenol isocitrate, isocitrate dehydrogenase, superoxide dismutase, 3′-phosphoadenosine-5′-phosphosulfate (PAPS), dimethyl sulfoxide (DMSO), *p*-nitrophenol, S-(5′-Adenosyl)-L-methionine (SAM), dithiothreitol (DTT), reduced glutathione (GSH), acetylcarnitine transferase (AcT), acetylcarnitine, acetyl coenzyme A (AcCoA), carnitine, penicillin, streptomycin, and epidermal growth factor were purchased from Sigma-Aldrich (Taufkirchen, Germany), $NADP^+$ from Biomol (Hamburg, Germany), acetonitrile (LC–MS grade), ammonium formate (analytical grade), formic acid (LC–MS grade), methanol (LC–MS grade), and all other chemicals and reagents (analytical grade) from VWR (Darmstadt, Germany). Pooled human liver microsomes (pHLM, 20 mg microsomal protein/mL, 330 pmol total CYP/mg protein, from 34 individual donors), ultra pooled human liver cytosol (pHLC, 20 mg cytosolic protein/mL, from 150 individual donors), pS9 (20 mg protein/mL, from 30 individual donors), UGT reaction mix solution A (25 mM UDP-glucuronic acid), and UGT reaction mix solution B (250 mM Tris–HCl, 40 mM $MgCl_2$, and 0.125 mg/mL alamethicin) were obtained from Corning (Amsterdam, The Netherlands). After delivery, the enzyme preparations were thawed at 37 °C, aliquoted, snap-frozen in liquid nitrogen, and stored at −80 °C until use. Cryopreserved, differentiated HepaRG cells, 96-well plates coated with type I collagen, and fetal bovine serum were obtained from Life Invitrogen (Darmstadt, Germany), Williams E Medium, (HPR116), additive ADD650, and thaw, seed, and general purpose additive ADD670 from Biopredic International (Saint-Grégoire, France), HepG2 cells from the German collection of microorganism and cell cultures (DSMZ, Braunschweig, Germany), and human hepatocyte growth factor from Humanzyme (Chicago, IL, USA).

2.2. In vitro drug metabolism studies using pHLM plus pHLC or pS9

The final volume of the incubation mixture was 150 μL. Incubations using pHLM/pHLC, both at a final protein concentration of 1 mg/mL or pS9 at a final protein concentration of 2 mg/mL were performed after 10 min preincubation at 37 °C with 25 μg/mL alamethicin (UGT reaction mix solution B), 90 mM phosphate buffer (pH 7.4), 2.5 mM Mg^{2+}, 2.5 mM isocitrate, 0.6 mM $NADP^+$, 0.8 U/mL isocitrate dehydrogenase, 100 U/mL superoxide dismutase, 0.1 mM AcCoA, 2.3 mM acetyl carnitine, and 8 U/mL carnitine acetyltransferase. Thereafter, 2.5 mM UDP-glucuronic acid (UGT reaction mix solution A), 40 μM aqueous PAPS, 1.2 mM SAM, 1 mM DTT, 10 mM GSH, and 25 μM substrate in phosphate buffer were added. All given concentrations are final concentrations.

Reactions were initiated by addition of substrate and the mixture was incubated for a maximum of 480 min. After 60 min, 60 μL of the mixture was transferred into a reaction tube and reactions were terminated by addition of 20 μL ice-cold acetonitrile containing α-PVP as internal standard. The remaining mixture was incubated for additional 7 h and thereafter stopped by addition of 30 μL ice-cold acetonitrile containing α-PVP. The solutions were cooled for 30 min at −18 °C, centrifuged for 2 min at 10,000 × *g*, and 60 μL of the supernatants were transferred into an autosampler vial and 1 μL injected onto the Orbitrap (OT)-based liquid chromatography-high resolution-tandem mass spectrometry (LC-HR-MS/MS) system as described below. Blank incubations without substrate and control samples without pHLM/pHLC or pS9, were prepared to confirm the absence of interfering compounds and to identify not metabolically originated compounds.

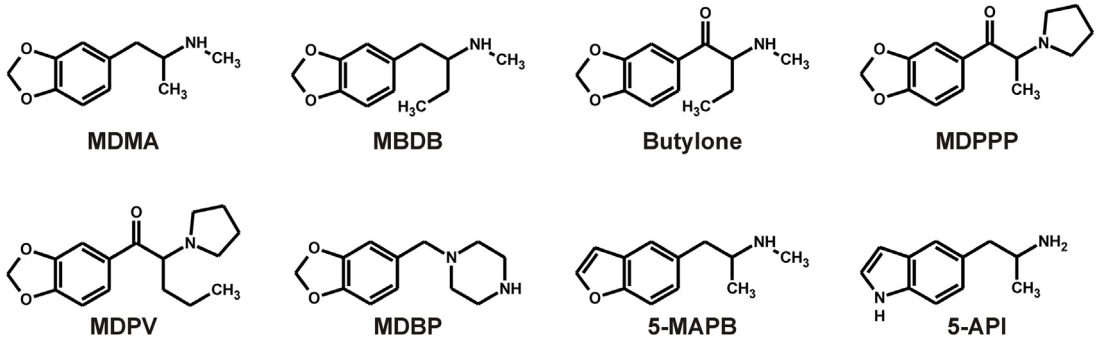

Fig. 1. Chemical structures of investigated methylenedioxy derivatives and the respective bioisosteric analogues.

For assessing the corresponding formation potential, *p*-nitrophenol was incubated for glucuronidation and sulfation [28], *p*-aminosalicylic acid for acetylation by NAT1 [29], sulfamethazine for acetylation by NAT2 [30], DHMA for *O*-methylation [16], kynuramine for deamination by monoamine oxidases A and B [31], or paracetamol or clozapine for GSH conjugation [32]. These positive control samples were incubated for 60 min at a substrate concentration of 25 μM. For assessing time-dependent metabolite formation, out of a final volume of 300 μL, 30-μL aliquots were taken after 0, 5, 10, 15, 30, 60, 120, 240, and 480 min, transferred into reaction tubes, and stopped by addition of 10 μL ice-cold acetonitrile containing α-PVP. MDPV was used as model substrate for studying time dependency. All incubations were done in duplicates.

2.3. In vitro drug metabolism studies using HepaRG or HepG2 cell lines

According to previous studies [33], all cell cultures were maintained in an incubator (Binder, Tuttlingen, Germany) at 37 °C with 95% air humidity and 5% CO_2 atmosphere. Cell handling was done under sterile conditions using a laminar flow bench class II (Thermo Scientific Schwerte, Germany). All given concentrations are final concentrations. Cryopreserved, differentiated HepaRG cells were cultivated according to the manufacturer's instructions, seeded in a density of 72,000 cells/well in collagen-coated 96-well plates using Williams E medium supplemented with ADD670, 100 U/mL penicillin, 100 μg/mL streptomycin, and 0.5% DMSO and maintained under these conditions for six days with medium renewal every two days before substrate exposure. HepG2 (passage 2) cells were seeded in a density of 50,000 cells/well in 96-well plates. The cultures were maintained in Williams E Medium supplemented with 100 U/mL penicillin, 100 μg/mL streptomycin, and 10% fetal bovine serum for three days. One day before substrate exposure, medium was changed to Williams E Medium (serum-free) supplemented with additive ADD650, 100 U/mL penicillin, 100 μg/mL streptomycin, 0.5% DMSO, 10 ng/mL human hepatocyte growth factor, and 2 ng/mL epidermal growth factor [34,35].

Afterwards, HepaRG and HepG2 cells were incubated with substrate concentrations of 0.01, 0.1, and 1 mM for 24 h and medium supernatants were collected for the analysis of the metabolites. A 50-μL aliquot each was precipitated using 50 μL acetonitrile containing 10 μM α-PVP as internal standard and 50 μL of a 35 mg/mL zinc sulfate solution in methanol:water (30:70, *v*/*v*) [36] and subsequently cooled at −18 °C for 30 min. The solution was centrifuged for 2 min at 10,000 × *g*, 100 μL of the supernatant transferred to an autosampler vial, and 1 μL injected onto the LC-HR-MS/MS system as described below. Blank cell cultures without substrate were prepared to confirm the absence of interfering compounds and control samples without cells were done to identify not metabolically formed compounds. All incubations were done in triplicates.

2.4. Detection of metabolites in human urine samples

Human urine samples after intake of MDMA, MDPV, or 5-MAPB were submitted for clinical toxicological analysis to the authors' laboratory, whereby dosage and time point of intake were unknown. According to published procedures [37], 100 μL of urine was mixed with 500 μL of acetonitrile, shaken, centrifuged, the supernatant gently evaporated to dryness, reconstituted in 50 μL of methanol, and 1 μL injected onto the LC-HR-MS/MS system as described below. Pure methanol was the best choice for reconstitution of polar and nonpolar compounds and considering the injection volume of 1 μL at a flow rate of 500 μL/min, the influence of methanol on the chromatographic separation should be negligible.

2.5. Apparatus for analysis of metabolites

Based on published procedures [5,15,33], the processed samples were analyzed using a ThermoFisher Scientific (TF, Dreieich, Germany) Dionex UltiMate 3000 RS pump consisting of a degasser, a quaternary pump and an UltiMate Autosampler, coupled to a TF Q-Exactive Plus system equipped with an heated electrospray ionization (HESI)-II source. Mass calibration was done prior to analysis according to the manufacturer's recommendations using external mass calibration.

Gradient elution was performed on a TF Accucore PhenylHexyl column (100 mm × 2.1 mm, 2.6 μm). The mobile phases consisted of 2 mM aqueous ammonium formate containing acetonitrile (1%, *v*/*v*) and formic acid (0.1%, *v*/*v*, pH 3, eluent A) and ammonium formate solution with acetonitrile:methanol (1:1, *v*/*v*) containing water (1%, *v*/*v*) and formic acid (0.1%, *v*/*v*, eluent B). The flow rate was set to 500 μL/min using the following gradient: 0–1.0 min 99% A, 1–10 min to 50% A, 10–11.5 min hold 1% A, 11.5–13.5 min hold 99% A. The HESI-II source conditions were as follows: ionization mode, positive; sheath gas, 53 AU; auxiliary gas, 14 AU; sweep gas, 3 AU; spray voltage, 3.50 kV; heater temperature, 438 °C; ion transfer capillary temperature, 320 °C; and S-lens RF level, 60.0. Mass spectrometry was performed using full scan data and a subsequent data-dependent acquisition (DDA) with priority to masses of substrates and its expected metabolites in an inclusion list.

The settings for FS data acquisition were as follows: resolution, 35,000; microscans, 1; automatic gain control (AGC) target, 1e6; maximum injection time, 120 ms; and scan range, *m*/*z* 50–750. The settings for the DDA mode with an inclusion list ("do not pick others" mode) for substrates and the expected metabolites were as follows: option "do not pick others", enabled, dynamic exclusion, 0.1 s; resolution, 17,500; microscans, 1; loop count, 5; AGC target, 2e4; maximum injection time, 250 ms; isolation window, *m*/*z* 1.0; high collision dissociation (HCD) with stepped normalized collision energy (NCE), 17.5, 35, and 52.5%; spectrum data type,

profile; and underfill ratio, 1%. The inclusion list contained *m/z* values of metabolites, which were already described in the literature and metabolites, which were likely to be formed such as hydroxy, oxo, carboxy, dihydro, dealkyl, demethylenyl, demethylenylmethyl metabolites (phase I) and sulfates, glucuronides, *N*-acetyl, GSH-conjugated metabolites (phase II) and combinations of these. Xcalibur Qual Browser software version 3.0.63 was used for data handling. The obtained MS^2 spectra were compared to published LC-HR-MS/MS spectra [37–39]. The kynuramine incubations were analyzed according to Wagmann L. et al. [31].

3. Results and discussion

As already mentioned controlled clinical trials would provide ideal samples to identify targets for toxicological urine screening procedures of NPS, but such studies cannot be performed due to ethical reasons [4,5] and potential species differences in metabolism limit animal studies. Therefore, it should be figured out, which human in vitro systems can be used for mimicking human metabolism for elucidating the main analytical target for urine screening. Such assays should allow performing almost all metabolic steps including phase II reactions as nowadays LC–MS approaches are often used for screening, which do not necessarily need cleavage of conjugates [5,7,8] in contrast to GC–MS approaches [8]. Preliminary testing with positive/negative switching mode showed that, as expected, no additional metabolites could be detected and no benefit of the negative mode was observed for detection of sulfates or glucuronides. Therefore, positive mode only was used for further studies. Furthermore, only metabolites measured with a mass tolerance lower than 5 ppm were included in the study.

The S9 fraction typically contains cytosol and microsomes but with enzyme activities, which are usually lower than those in isolated microsomes or cytosol [40,41]. Therefore, pHLM/pHLC, a slightly more expensive alternative, was tested besides pS9. The tested methylenedioxy derivatives and their analogues were selected for several reasons. First, they are known to be extensively metabolized by several enzymes including phase II reaction such as glucuronidation, sulfation, *O*-methylation, and GSH conjugation [18,28,38,42–49]. Second, the initial step in metabolism of methylenedioxy derivatives is the *O*-demethylenation via CYP2D6 [50], which is the CYP enzyme with low gene expression level in HepaRG [24], but important in metabolism of various DOAs [3]. Third, for some compounds such as MDMA detailed data about excretion in human urine were available [51], on the other hand, compounds such as 5-API for which no data were available should be included to elucidate if the investigated models are suitable for NPS, too.

3.1. In vitro drug metabolism studies using pHLM/pHLC or pS9

In vitro systems such as pHLM, pHLC, or pS9 were already frequently used [10] for identifying especially phase I [13–15], but also phase II metabolites [16,17] or both [18,19]. Therefore, pHLM plus pHLC or pS9 should be used and the co-substrates of almost all metabolizing enzymes have to be added. Thus, the risk of losing metabolites formed by several steps can be minimized, e.g. conjugates of the demethylenyl methyl metabolite of MDMA [49]. The functionality of such assays for the common steps is well documented [3], but the activity of additional phase II enzymes should be tested by incubation of the corresponding substrates in the so-called positive control samples. The *p*-nitrophenol glucuronidation and sulfation, *p*-aminosalicylic acid or sulfamethazine acetylation, DHMA *O*-methylation, and kynuramine deamination were used as additional qualitative control reactions. For GSH conjugation of paracetamol or clozapine, substrate concentration had to be increased to 250 μM for reliable detection of the product. This could be explained by the physiological function of this step, what is the detoxification of high xenobiotic concentrations. For GSH conjugation studies, incubations according to Meyer et al. [32] are recommended. Optimal incubation time was studied using the extensively metabolized MDPV with sampling points ranging from 5 to 480 min after start of the reaction. Initial metabolites were detected within the first 30 min and the total number of metabolites after 60 min (Fig. 2). Longer incubation times did not result in higher numbers but in change of the peak area ratios of particular metabolites. Especially those of initial metabolites decreased. Therefore, 60 and 480 min were chosen as sampling points for identification of the metabolic pattern as well as late reaction products most probably representing urinary excretion products.

Fig. 3 shows the ratio of response between the metabolites of MDMA, MBDB, butylone, MDPPP, MDPV, MDBP, 5-MAPB, and 5-API over that of the internal standard α-PVP detected in pHLM/pHLC (above baseline) or pS9 samples (below baseline) incubated for 60 or 480 min. Metabolite numbering is according to Table 1a,b.

3.2. In vitro drug metabolism studies using HepaRG or HepG2 cell lines

Human liver cell lines have the advantage that there is no need for addition of co-substrates. HepaRG cells have in general a gene expression level for metabolizing enzymes comparable to primary human hepatocytes [2,20], except of CYP2D6 [24], which is however involved in the metabolism of various DOAs [3], e.g. the demethylenation of methylenedioxy derivatives [38,52,53]. HepG2 cell line is easy to handle and the most frequently used human liver cell line [24]. Again, the gene expression level for phase I metabolizing enzymes such as alcohol dehydrogenases, aldehyde dehydrogenases, CYP enzymes, and flavin-containing monooxygenases is rather low [24], while that of phase II enzymes are comparable to HepaRG except for some UGTs [10,20,24].

Only few publications on the metabolism of DOAs in HepaRG and HepG2 cells were available. Dias-da-Silva et al. [9] compared HepaRG cells, HepG2 cells, and primary rat hepatocytes as in vitro tools for hepatotoxicity studies of piperazine designer drugs without focusing on metabolites. Kanamori et al. [54] investigated the metabolism of XLR-11, a synthetic cannabinoid, in HepaRG cells and human urine and compared their results with these of Wohlfarth et al. [55] who studied the XLR-11 metabolism with primary human hepatocytes. In conclusion, they found that HepaRG cells might be a promising alternative to mimic human in vivo metabolism with limitations of an in vitro system. However, in their study a cleavage of conjugates was conducted and therefore only phase I metabolites were identified in contrast to the present study. Richter et al. [33] investigated the metabolism of desomorphine in HepaRG and HepG2, but no human data were presented due to lack of authentic samples.

Fig. 4 shows the ratio of response between the metabolites of MDMA, MBDB, butylone, MDPPP, MDPV, MDBP, 5-MAPB, and 5-API over that of the internal standard α-PVP detected in HepaRG (above baseline) or HepG2 samples (below baseline) after incubation of 1 mM substrate for 24 h. The numbering of the metabolites is given in Table 1a,b.

3.3. In vivo drug metabolism studies using human urine

Metabolites detected in authentic human urine samples after intake of unknown amounts of MDMA, MDPV, or 5-MAPB are listed in Table 2. In every case, the sample preparation was a simple precipitation for analysis by LC-HR-MS/MS. Results were compared between the four in vitro incubations as well as with those already

Table 1a
Retention times (RT), formula, and exact masses of the metabolites detected in different models or reported in literature of MDMA, MBDB, butylone, and MDPPP (—: formation not possible due to chemical structure, N.A.: no retention time available, due to no detection in any investigated model, blank line: not detected in any sample, but formation theoretically possible).

		MDMA			MBDB			Butylone			MDPPP		
		RT [min]	Formula	*m/z*	RT [min]	Formula	*m/z*	RT [min]	Formula	*m/z*	RT [min]	Formula	*m/z*
	Parent compound	4.0	$C_{11}H_{16}NO_2$	194.1175	5	$C_{12}H_{18}NO_2$	208.1332	4.5	$C_{12}H_{16}NO_3$	222.1124	4.4	$C_{14}H_{18}NO_3$	248.1281
Phase I	**M1** *N*-Dealkyl	3.7	$C_{10}H_{14}NO_2$	180.1019	N.A.	$C_{11}H_{16}NO_2$	194.1175	4.1	$C_{11}H_{14}NO_3$	208.0968			
	M2 Demethylenyl	1.1	$C_{10}H_{16}NO_2$	182.1175	2.5	$C_{11}H_{18}NO_2$	196.1332	2	$C_{11}H_{16}NO_3$	210.1124	2.5	$C_{13}H_{18}NO_3$	236.1281
	M3 Dihydro	—			—			N.A.	$C_{12}H_{18}NO_3$	244.1281	4.1	$C_{14}H_{20}NO_3$	250.1437
	M4 Hydroxy	N.A.	$C_{11}H_{16}NO_3$	210.1124	N.A.	$C_{12}H_{18}NO_3$	224.1281	N.A.	$C_{12}H_{16}NO_4$	238.1073	3.7	$C_{14}H_{18}NO_4$	264.123
	M5 *N*-Oxide	N.A.	$C_{11}H_{16}NO_3$	210.1124	N.A.	$C_{12}H_{18}NO_3$	224.1281	N.A.	$C_{12}H_{16}NO_4$	238.1073	5.1	$C_{14}H_{18}NO_4$	264.123
	M6 Dihydro-hydroxy isomer 1	—			—			N.A.	$C_{12}H_{18}NO_4$	240.1230	N.A.	$C_{14}H_{20}NO_4$	266.1386
	M7 Dihydro-hydroxy isomer 2	—			—			N.A.	$C_{12}H_{18}NO_4$	240.1230	N.A.	$C_{14}H_{20}NO_4$	266.1386
	M8 Oxo	—			—			—			8.3	$C_{14}H_{16}NO_4$	262.1073
	M9 Dihydroxy	N.A.	$C_{11}H_{16}NO_4$	226.1073	N.A.	$C_{12}H_{18}NO_4$	240.123	N.A.	$C_{12}H_{16}NO_5$	254.1022	N.A.	$C_{14}H_{18}NO_5$	280.1179
Phase I	**M12** Demethylenyl methyl isomer 1	2.7	$C_{11}H_{18}NO_2$	196.1332	3.7	$C_{12}H_{20}NO_2$	210.1488	3.4	$C_{12}H_{18}NO_3$	224.1281	3.2	$C_{14}H_{20}NO_5$	250.3129
	M13 Demethylenyl methyl isomer 2	3.1	$C_{11}H_{18}NO_2$	196.1332	N.A.	$C_{12}H_{20}NO_2$	210.1488	N.A.	$C_{12}H_{18}NO_3$	224.1281	3.6	$C_{14}H_{20}NO_5$	250.3129
	M15 Demethylenyl sulfate isomer 1	1.8	$C_{10}H_{16}NO_5S$	262.0743	3.2	$C_{11}H_{18}NO_5S$	276.0900	2.3	$C_{11}H_{16}NO_6S$	290.0692	2.6	$C_{13}H_{18}NO_6S$	316.0849
	M16 Demethylenyl sulfate isomer 2	2	$C_{10}H_{16}NO_5S$	262.0743	N.A.	$C_{11}H_{18}NO_5S$	276.0900	N.A.	$C_{11}H_{16}NO_6S$	290.0692	2.9	$C_{13}H_{18}NO_6S$	316.0849
	M17 Demethylenyl glucuronide isomer 1	1.7	$C_{16}H_{24}NO_8$	358.1496	N.A.	$C_{17}H_{26}NO_8$	372.1652	1.5	$C_{17}H_{24}NO_9$	386.1445	2.2	$C_{19}H_{26}NO_9$	412.1602
	M18 Demethylenyl glucuronide isomer 2	1.8	$C_{16}H_{24}NO_8$	358.1496	N.A.	$C_{17}H_{26}NO_8$	372.1652	N.A.	$C_{17}H_{24}NO_9$	386.1445	2.3	$C_{19}H_{26}NO_9$	412.1602
	M19 Demethylenyl methyl sulfate isomer 1	2.5	$C_{11}H_{18}NO_5S$	276.09	3.6	$C_{12}H_{20}NO_5S$	290.3553	2.9	$C_{12}H_{18}NO_6S$	304.0849	3.3	$C_{14}H_{20}NO_6S$	330.1005
	M20 Demethylenyl methyl sulfate isomer 2	N.A.	$C_{11}H_{18}NO_5S$	276.09	N.A.	$C_{12}H_{20}NO_5S$	290.3553	N.A.	$C_{12}H_{18}NO_6S$	304.0849	N.A.	$C_{14}H_{20}NO_6S$	330.1005
	M21 Demethylenyl methyl glucuronide isomer 1	1.9	$C_{17}H_{26}NO_8$	372.1652		$C_{18}H_{28}NO_8$	386.1809	2.6	$C_{18}H_{26}NO_9$	400.1602	2.3	$C_{20}H_{28}NO_9$	426.4370
	M22 Demethylenyl methyl glucuronide isomer 2	2.1	$C_{17}H_{26}NO_8$	372.1652	N.A.	$C_{18}H_{28}NO_8$	386.1809	2.9	$C_{18}H_{26}NO_9$	400.1602	2.9	$C_{20}H_{28}NO_9$	426.4370
	M21 Demethylenyl methyl glucuronide isomer 1	3.7	$C_{22}H_{32}NO_9$	454.2071	N.A.	$C_{18}H_{27}N_2O_8$	399.1761	—			—		
	M22 Demethylenyl methyl glucuronide isomer 2	4.8	$C_{22}H_{32}NO_9$	454.2071	N.A.	$C_{18}H_{27}N_2O_8$	399.1761	—			—		

Table 1b
Retention times (RT), formula, and exact masses of the metabolites detected in different models or reported in literature of MDPV, MDBP, 5-MAPB, and 5-API (—: formation not possible due to chemical structure, N.A.: no retention time available, due to no detection in any investigated model, blank line: not detected in any sample, but formation theoretically possible).

		MDPV			MDBP			5-MAPB			5-API		
		RT [min]	Formula	*m/z*	RT [min]	Formula	*m/z*	RT [min]	Formula	*m/z*	RT [min]	Formula	*m/z*
	Parent compound	6.1	$C_{16}H_{22}NO_3$	276.1594	1.3	$C_{12}H_{17}N_2O_2$	221.1284	5.2	$C_{12}H_{16}NO$	190.1226	3.7	$C_{11}H_{15}N_2$	175.1229
Phase I	**M1** *N*-Dealkyl	N.A.			0.4	$C_{10}H_{15}N_2O_2$	195.1128	4.8	$C_{11}H_{14}NO$	176.1069	—		
	M2 Demethylenyl	4.0	$C_{15}H_{22}NO_3$	264.1594	N.A.	$C_{11}H_{17}N_2O_2$	209.1284	—			—		
	M3 Dihydro	5.3	$C_{15}H_{24}NO_3$	278.1750	—			N.A.	$C_{12}H_{18}NO$	192.1382	N.A.	$C_{11}H_{17}N_2$	177.1386
	M4 Hydroxy	5.5	$C_{16}H_{22}NO_4$	292.1543	0.8	$C_{12}H_{17}N_2O_3$	237.1233	N.A.	$C_{12}H_{16}NO_2$	206.2039	2.4	$C_{11}H_{15}N_2O$	191.1178
	M5 *N*-Oxide	N.A.	$C_{16}H_{22}NO_4$	292.1543	2.6	$C_{12}H_{17}N_2O_3$	237.1233	6.2	$C_{12}H_{16}NO_2$	206.2039	N.A.	$C_{11}H_{15}N_2O$	191.1178
	M6 Dihydro-hydroxy isomer 1	N.A.	$C_{16}H_{24}NO_4$	294.1699	—			2.7	$C_{12}H_{18}NO_2$	208.1332	N.A.	$C_{11}H_{17}N_2O$	193.1335
	M7 Dihydro-hydroxy isomer 2	N.A.	$C_{16}H_{24}NO_4$	294.1699	—			4.9	$C_{12}H_{18}NO_2$	208.1332	N.A.	$C_{11}H_{17}N_2O$	193.1335
	M8 Oxo	10.4	$C_{16}H_{20}NO_4$	290.1386	N.A.	$C_{12}H_{15}N_2O_3$	235.1077	—			—		
	M9 Dihydroxy	N.A.	$C_{16}H_{24}NO_5$	310.1648	N.A.	$C_{12}H_{17}N_2O_4$	253.1182	N.A.	$C_{12}H_{16}NO_3$	222.1124	1.2	$C_{11}H_{15}N_2O_2$	207.1128
	M10 3-Hydroxyethyl-4-hydroxy methamphetamine	—			—			2.6	$C_{12}H_{20}NO_2$	210.2921	—		
	M11 3-Carboxymethyl-4-hydroxy methamphetamine	—			—			2.7	$C_{12}H_{18}NO_3$	224.1281	—		
Phase II	**M12** Demethylenyl methyl isomer 1	4.7	$C_{16}H_{24}NO_3$	278.1750	0.5	$C_{12}H_{19}N_2O_2$	223.1441	—			—		
	M13 Demethylenyl methyl isomer 2	5.1	$C_{16}H_{24}NO_3$	278.1750	N.A.	$C_{12}H_{19}N_2O_2$	223.1441	—			—		
	M14 *N*-Acetyl	—			—			—			7.2	$C_{11}H_{17}N_2O$	217.1335
	M15 Demethylenyl sulfate isomer 1	3.9	$C_{15}H_{22}NO_6S$	344.1162	N.A.	$C_{11}H_{17}N_2O_5S$	289.0852	—			—		
	M16 Demethylenyl sulfate isomer 2	3.3	$C_{15}H_{22}NO_6S$	344.1162	N.A.	$C_{11}H_{17}N_2O_5S$	289.0852	—			—		
	M17 Demethylenyl glucuronide isomer 1	2.9	$C_{21}H_{30}NO_9$	440.1915	N.A.	$C_{17}H_{25}N_2O_8$	385.1605	—			—		
	M18 Demethylenyl glucuronide isomer 2	3.6	$C_{21}H_{30}NO_9$	440.1915	N.A.	$C_{17}H_{25}N_2O_8$	385.1605	—			—		
	M19 Demethylenyl methyl sulfate isomer 1	4.6	$C_{16}H_{24}NO_7S$	374.1267	N.A.	$C_{12}H_{19}N_2O_5S$	303.1009	—			—		
	M20 Demethylenyl methyl sulfate isomer 2	N.A.	$C_{16}H_{24}NO_7S$	374.1267	N.A.	$C_{12}H_{19}N_2O_5S$	303.1009	—			—		
	M21 Demethylenyl methyl glucuronide isomer 1	3.7	$C_{22}H_{32}NO_9$	454.2071	N.A.	$C_{18}H_{27}N_2O_8$	399.1761	—			—		
	M22 Demethylenyl methyl glucuronide isomer 2	4.8	$C_{22}H_{32}NO_9$	454.2071	N.A.	$C_{18}H_{27}N_2O_8$	399.1761	—			—		

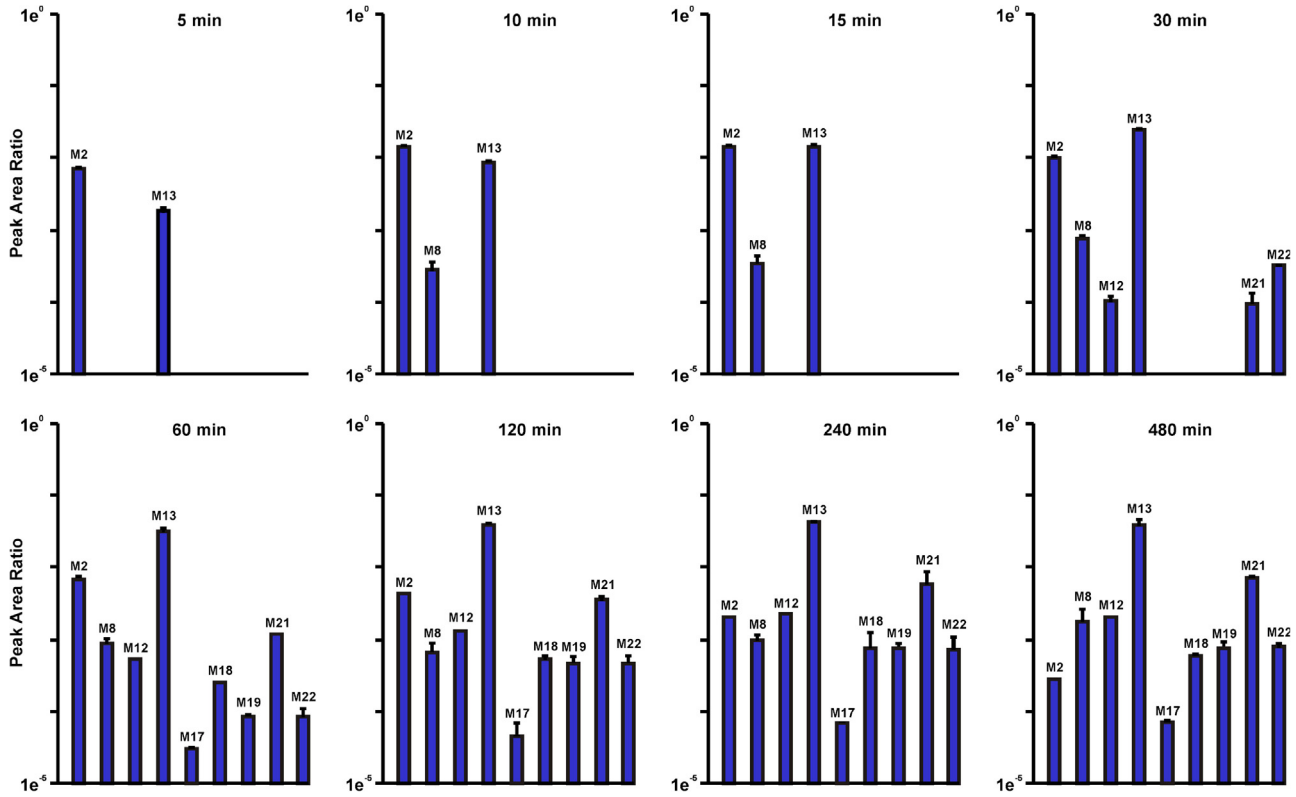

Fig. 2. Ratio of response between the metabolites of MDPV metabolites and the internal standard α-PVP measured in pHLM/pHLC samples incubated for 5, 10, 15, 30, 60, 120, 240, and 480 min. Data points represent means and ranges (error bars) of duplicate measurement. Metabolite numbering is according to Tables 1a,b.

published. Comparing the results to published data, it should be kept in mind that different sample preparations (e.g. enzymatic, acidic, or no conjugate cleavage, liquid-liquid or solid-phase extraction) and/or instrumentations (GC–MS, LC–MS^n, and/or LC-HR-MS/MS) may influence the findings.

3.4. Comparison of the metabolites detected in the different samples and their comparison to literature

A list of retention times, formula, and exact masses of the detected and in literature reported metabolites is given in Tables 1a,b. In the present study, the metabolites of six methylenedioxy derivatives and two bioisosteric analogues were elucidated in pHLM/pHLC, pS9, HepaRG, and HepG2 cell lines. They were compared to those detected in human urine and/or reported in literature to see whether the in vitro assays allow assessing the possible targets for urine drug testing. For this purpose, the limitations of such in vitro models concerning e.g. lack of reabsorption, enterohepatic circulation, or renal elimination are of minor relevance. As expected and already described [18,28,38,42–49], all methylenedioxy derivatives showed similar metabolic patterns. The initial step was the *O*-demethylenation followed by an *O*-methylation via catechol-*O*-methyltransferase (COMT) with preference for the position 3 [43,49]. Subsequent conjugation to sulfate or glucuronic acid was observed. Further reactions were the formation of dihydro, hydroxy, or oxo metabolites. A list of metabolites detected in the investigated samples and previously reported in literature is given in Table 2. However, direct comparison of the different models is difficult as cell culture incubations matrix is different to that of human liver preparation. This might influence the findings due to matrix effects, ion enhancement, or suppression.

3.4.1. MDMA

According to Schwaninger et al. [28,49], *O*-demethylenation followed by *O*-methylation mainly to demethylenyl-3-methyl-methamphetamine (4-hydroxy-3-methoxymethamphetamine, HMMA) and conjugation mainly via SULTs were the main metabolic pathways. Hence, human MDMA urinary metabolites are primarily sulfates and glucuronides, with sulfates usually in higher concentrations than glucuronides. As minor metabolic pathways, *N*-demethylation followed by *O*-demethylenation, *O*-methylation, and conjugation with sulfate or glucuronic acid were described. In the in vitro models tested here, all the above-mentioned metabolites were detected except for the glucuronides. Again, glucuronidation of the phase I metabolites of MDMA was described as minor metabolic pathway in humans [56]. The main urinary excretion product described in literature was detected in the investigated in vitro incubations and the authentic urine sample. In contrast, rats formed higher amounts of glucuronides than sulfates [57] showing the problem of species differences, but they have no relevance as long as cleavage of conjugates is performed for urinalysis. Meyer et al. [32] studied GSH conjugation of MDMA and its phase I metabolites in vitro using a much higher substrate concentration than in the present study, which was obviously essential for formation of GSH conjugates.

In pHLM/pHLC and pS9 incubations, all the above-mentioned metabolites were detected, except for glucuronides. In HepaRG, the same metabolites were detected except for the sulfates of the demethylenyl metabolite. This fact could be explained by the low gene expression levels by CYP2D6 in HepaRG what catalyzed the initial *O*-demethylation [24,50]. The resulting minor formation of the corresponding phase I metabolite led consequently also to minor formation of its conjugates. In HepG2, only the *N*-demethyl and one sulfate of the demethylenyl methyl metabolites could be detected. The most obvious reason for this was the already men-

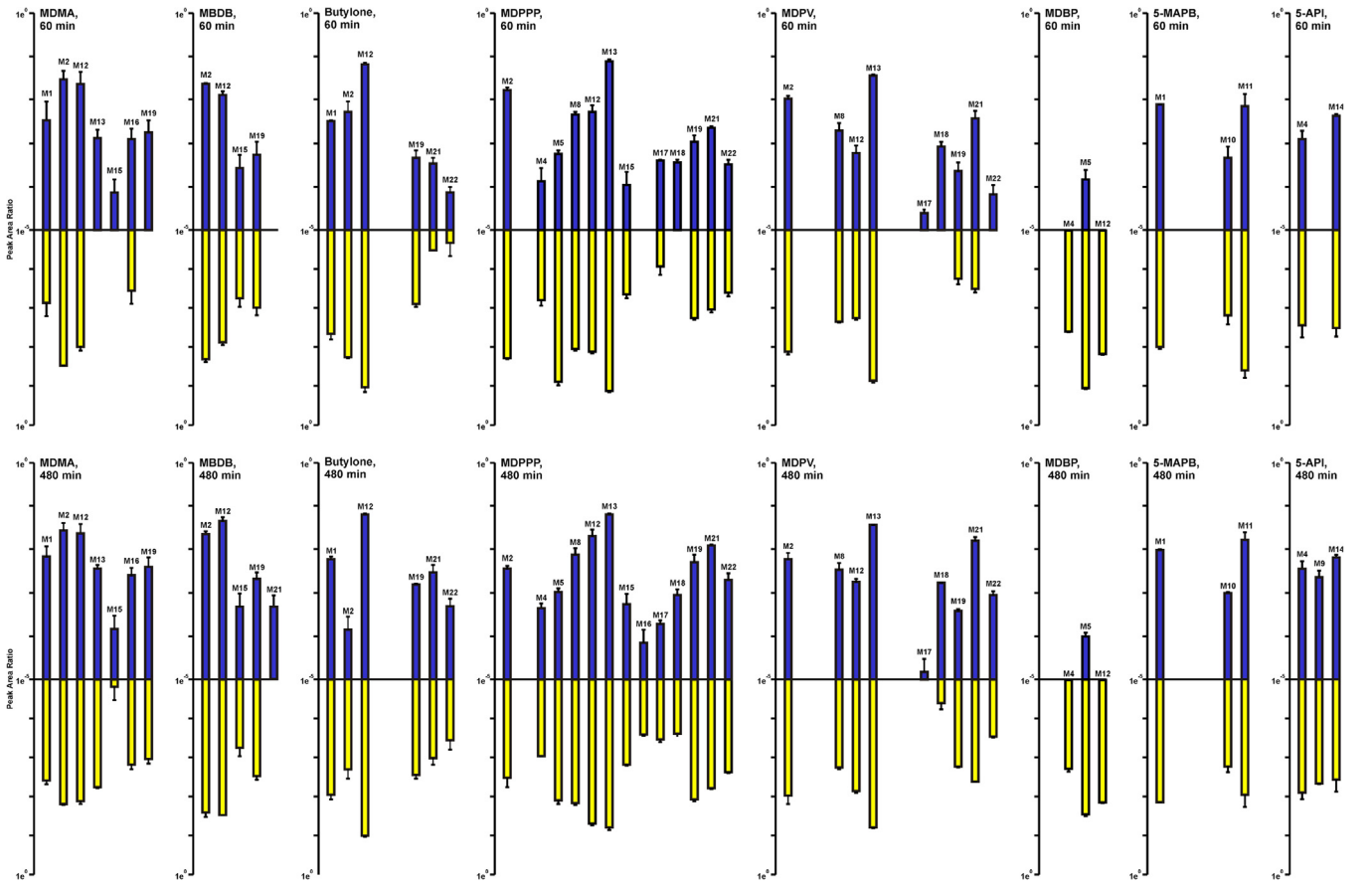

Fig. 3. Ratio of response between the metabolites of MDMA, MBDB, butylone, MDPPP, MDPV, MDBP, 5-MAPB, 5-API and the internal standard α-PVP measured in pHLM/pHLC (above baseline, blue) or pS9 samples (below baseline, yellow) incubated for 60 (upper part) or 480 (lower part) min with 25 μM substrate concentration. Data points represent means and ranges (error bars) of duplicate measurement. Metabolite numbering is according to Table 1a. (For interpretation of the references to colour in this figure legend, the reader is referred to the web version of this article.)

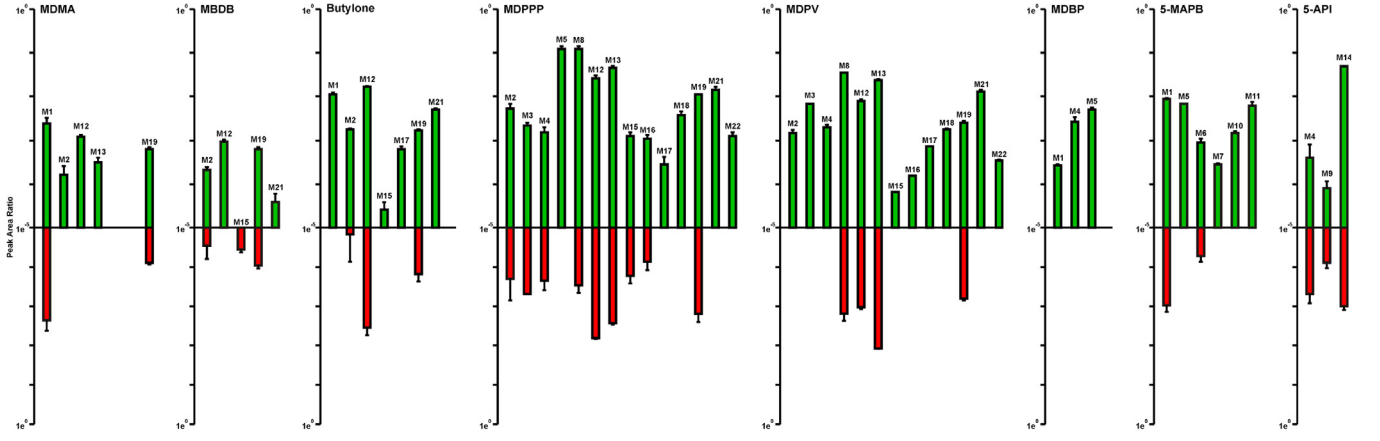

Fig. 4. Ratio of response between the metabolites of MDMA, MBDB, butylone, MDPPP, MDPV, MDBP, 5-MAPB, 5-API and the internal standard α-PVP measured in HepaRG (above baseline, green) or HepG2 samples (below baseline, red) incubated for 24 h with 1 mM substrate concentrations ($n = 3$). Metabolite numbering is according to Table 1a. (For interpretation of the references to colour in this figure legend, the reader is referred to the web version of this article.)

tioned low gene expression level for CYP enzymes [24]. Another reason, also true for pHLM/pHLC and pS9, might be the inhibition potential of MDMA towards CYP2D6 activity [58].

3.4.2. MBDB

The phase I metabolism of MBDB was described to be similar to that of MDMA [46,59] but the relative amounts of the excretion products in human urine were not described. All phase I metabolites were observed in the current study with exception of the *N*-demethyl metabolite, the demethylenyl methyl sulfate metabolites, and one demethylenyl methyl glucuronide. Metabolites detected in pHLM/pHLC, pS9, HepaRG, or HepG2 incubations were similar to those detected after incubation of MDMA. Additionally, a demethylenyl methyl glucuronide could be detected in the pHLM/pHLC and HepaRG incubations. In pS9 incubation,

Table 2
Metabolites detected in different models or reported in literature (α: pHLM/pHLC; β: pS9; γ: HepaRG; δ: HepG2; ε: human urine; κ: literature; •: no literature available; —: formation not possible due to chemical structure; blank line: not detected in any sample and not described in literature, but formation theoretically possible). Metabolites not detected in the investigated models, but described in literature are not listed in the Table, but discussed in the text.

		MDMA	MBDB	Butylone	MDPPP	MDPV	MDBP	5-MAPB	5-APB
Phase I	**M1** *N*-Dealkyl	α β γ δ ε κ	κ	α β γ κ			γ κ	α β γ δ ε κ	---
	M2 Demethylenyl	α β γ ε κ	α β γ δ κ	α β γ δ κ	α β γ δ κ	α β γ ε κ	κ	---	---
	M3 Dihydro	---	---	κ	γ δ	γ ε κ	---		
	M4 Hydroxy				α β γ δ	γ ε κ	β γ	κ	α β γ δ
	M5 *N*-Oxide				α β γ	γ	α β γ	γ	
	M6 Dihydro-hydroxy isomer 1	---	---				---	γ δ κ	
	M7 Dihydro-hydroxy isomer 2	---	---				---	γ	
	M8 Oxo	---	---	---	α β γ δ κ	α β γ δ κ			---
	M9 Dihydroxy							κ	α β γ δ
	M10 3-Hydroxyethyl-4-hydroxy methamphetamine	---	---	---	---	---	---	α β γ ε κ	---
	M11 3-Carboxymethyl-4-hydroxy methamphetamine	---	---	---	---	---	---	α β γ ε κ	---
Phase II	**M12** Demethylenyl methyl isomer 1	α β γ ε κ	α β γ κ	α β γ δ κ	α β γ δ κ	α β γ δ ε κ	β κ	---	---
	M13 Demethylenyl methyl isomer 2	α β γ ε κ	κ	κ	α β γ δ κ	α β γ δ ε κ		---	---
	M14 *N*-Acetyl	---	---	---	---	---	---	---	α β γ δ
	M15 Demethylenyl sulfate isomer 1	α β ε κ	α β δ κ	γ	α β γ δ κ	γ ε κ		---	---
	M16 Demethylenyl sulfate isomer 2	α β ε κ	κ		α β γ δ κ	γ ε κ		---	---
	M17 Demethylenyl glucuronide isomer 1	ε κ	κ	γ	α β γ κ	α γ ε κ		---	---
	M18 Demethylenyl glucuronide isomer 2	ε κ	κ		α β γ κ	α β γ ε κ		---	---
	M19 Demethylenyl methyl sulfate isomer 1	α β γ δ ε κ	α β γ δ κ	α β γ δ κ	α γ δ κ	α β γ δ ε κ	κ	---	---
	M20 Demethylenyl methyl sulfate isomer 2	κ	κ	κ	κ			---	---
	M21 Demethylenyl methyl glucuronide isomer 1	ε κ	α γ κ	α β γ κ	α β γ κ	α β γ ε κ	κ	---	---
	M22 Demethylenyl methyl glucuronide isomer 2	ε κ	κ	α β κ	α β γ κ	α β γ ε κ		---	---
References		[28,49]	[46,59]	[44,45]	[42]	[18,38]	[43]	[37]	

the demethylenyl methyl metabolite was detected, indicating that these models might be more suitable than the HepG2 model.

3.4.3. Butylone

There are two published studies dealing with the metabolism of butylone, one after analyzing human urine [44] and one after analyzing rat urine [45]. Postulated metabolic steps were *N*-demethylation, *O*-demethylenation followed by *O*-methylation, reduction of the β-keto group, and conjugation of the dihydro and demethylenyl methyl metabolites most probably to glucuronic acid or sulfate. Zaitsu et al. quantified the phase I metabolites before and after hydrolysis and identified the 4-hydroxy-3-methoxy metabolite to be the most abundant in hydrolyzed human urine after unknown dose [44]. This was also the case in the current in vitro incubations, although no conjugate cleavage was done. Further pathways included the reduction of the β-keto group, which was superior to the *N*-methylation. In contrast to these in vivo data, dihydro butylone metabolites could not be detected in any in vitro model, even if the dihydro metabolites of other β-keto compounds could be detected in the HepaRG and HepG2 incubations, but not in pHLM/pHLC or pS9.

3.4.4. MDPPP

There are no detailed data available about the MDPPP metabolism in humans but Springer et al. [42] investigated metabolism of MDPPP in rat urine. They also showed the involvements of human CYP2C19 and CYP2D6 in *O*-demethylenation [53]. The postulated metabolic pathways were similar to that of the other methylenedioxy derivatives. In addition to the steps already described above, hydroxylation in position 2 of the pyrrolidine ring followed by dehydrogenation to the corresponding lactam (oxo-metabolite) was found. In the current in vitro models, MDPPP was as extensively metabolized as described for rats. Some additional, but minor phase I metabolites could be detected in the in vitro models, probably due to better sensitivity of the used LC-HR-MS/MS device in contrast to GC–MS applied by Springer et al. [42]. The dihydro metabolite could only be detected in HepaRG and HepG2 incubations.

3.4.5. MDPV

Meyer et al. [38] identified the metabolites of MDPV in rat and human urine as well as in pHLM. *O*-Demethylenation via human CYP1A2, CYP2D6, and CYP2C19 followed by *O*-methylation was described besides the other metabolic steps already mentioned above. In addition, hydroxylation and ring opening with oxida-

tion was observed. In rat urine, glucuronides, but no sulfates were detected.

Not all above-mentioned metabolites could be detected in the current in vitro incubations, particularly metabolites formed after more than one phase I step. This might be a consequence of the different compound concentrations/amounts used for studying the metabolism. However, main excretion products were formed and identified. A previously published in vitro study using pHLM and pHLC to study phase I and II metabolism [18] of MDPV did not describe demethylenyl methyl MDPV to be formed due to the lack of SAM in their incubations. The dihydro metabolite was again not detected in pHLM/pHLC or pS9 incubations. In HepG2 only four metabolites were detected, most probably due to the already mentioned low gene expression level of CYP enzymes. In the present study, sulfates were also detected besides glucuronides in all in vitro models as well as in the human urine indicating that the used in vitro models might be more suitable for prediction of human phase II metabolism than the rat model.

3.4.6. MDBP

Metabolism of MDBP was investigated by Staack et al. [43] using rat urine samples. Again, the expected metabolic pathways for methylenedioxy derivatives were described as well as the *N*-dealkylation at the benzyl carbon and twice *N*-dealkylation at the piperazine moiety. In the current in vitro models, only four metabolites were detected. A possible explanation might be the cytotoxic effect of MDBP described after exposure to HepaRG (EC50 3.65 mM) and HepG2 (EC50 3.62 mM) [9]. No metabolites were detected in HepG2 incubations and solely phase I metabolites were detected in HepaRG and pHLM/pHLC incubations. In pS9 incubations, the demethylenyl methyl metabolite could be detected in addition, indicating to be the most suitable model for MDBP.

3.4.7. 5-MAPB

N-Demethylation was the predominant step in metabolism of 5-MAPB in rat besides various phase I and phase II reactions [37]. In human urine after ingestion of an unknown dose, *N*-demethyl-5-MAPB, hydroxy-5-MAPB, 3-hydroxyethyl-4-hydroxymethamphetamine, and 3-carboxymethyl-4-hydroxymethamphetamine were detected. The same metabolites were detected in the current in vitro models. The *N*-demethyl metabolite was the most abundant one in all investigated models, what is in accordance to the study of Welter et al. [37]. *N*-demethyl-3-hydroxyethyl-4-hydroxy methamphetamine and *N*-demethyl-3-carboxymethyl-4-hydroxy methamphetamine were detected in urine samples of the patient with highest plasma concentration of 5-MAPB [37]. In human urine sample investigated in this study, the same metabolites were detected as in pHLM/pHLC, pS9, and HepaRG except of the dihydro hydroxy *N*-oxide. Only two metabolites were detected in HepG2 because of the above-mentioned reason. Most metabolites were detected in HepaRG indicating to be the most suitable model for simulating in vivo 5-MAPB metabolism.

3.4.8. 5-API

So far, no data are available on the in vivo or in vitro metabolism of 5-API. Metabolic pathways similar to those of 5-MAPB were expected and all studied in vitro models provided the same metabolites. Mass spectra of the most abundant metabolites can be found in Supplementary Fig. 1. The most abundant product was the *N*-acetyl metabolite. This metabolite was confirmed by co-chromatography and comparison of the fragmentation pattern to those of the artificially acetylated parent compound using acetic acid anhydride and pyridine [37]. In addition, a hydroxy and a dihydroxy metabolite were detected. Beside 5-API, *N*-acetyl-5-API should be considered as target for toxicological screening procedures, but no human samples were available so far for confirmation.

3.5. Best model for prediction of urinary excretion products for toxicological screening procedures

This study was done to elucidate, which of the investigated in vitro models might be the most suitable to predict the main urinary excretion products in context of toxicological screening procedures. Therefore, there was no need to identify all possible metabolites as the information on the main urinary excretion products was sufficient. It is important particularly for small forensic and clinical laboratories to investigate the metabolism of NPS in a fast, simple, cost efficient, and reliable way. Due to the high cost and high variability [3,10,23] of primary human hepatocytes, they were not included in this study.

Comparing the two investigated cell lines, HepaRG provided better results than HepG2 concerning total number and abundance of metabolites, as expected. The HepG2 cell line were easier to handle and required less complicate cultivation media. The use of HepG2 was thus more cost efficient and they are in contrast to HepaRG not patent protected. Using HepG2, it was possible to detect the main urinary excretion products but there was no benefit when results were compared to human liver preparations. HepaRG formed slightly more metabolites than human liver preparations but all additional metabolites were identified to be minor in vivo metabolites. In general, working with cell lines have some drawbacks such as the requirement for special equipment. Time, material, and personal needed for preparation of a single metabolism study is higher than working with human liver preparations. In contrast to pS9, metabolizing enzyme content is higher in pHLM/pHLC, which leads to more abundant formation of metabolites but no qualitative differences could be observed. Therefore, the cheaper S9 fraction might also be used.

4. Conclusion

Incubations of the tested NPS with the human liver preparations and the HepaRG cell line provided comparable results. As expected, the incubations with HepaRG provided better results than those with HepG2 concerning total number and abundance of metabolites. Although HepaRG formed slightly more metabolites than pHLM/pHLC or pS9, the human liver preparations should be the best choice particularly for forensic laboratories without special equipment needed for cell handling. At least for the compounds investigated in this study, the cheap and easy to handle pS9 was sufficient enough to identify main excretion products for toxicological screening procedures. A further study should show the pros and cons of the much more expensive primary human hepatocytes in relation to the results described here.

Acknowledgements

The authors like to thank Heidi Löhr, Simon D. Brand, Pierce Kavanagh, Achim T. Caspar, Andreas G. Helfer, Julian A. Michely, Carsten Schröder, Gabriele Ulrich, Lea Wagmann, Armin A. Weber for support and/or helpful discussion.

This research did not receive any specific grant from funding agencies in the public, commercial, or not-for-profit sectors.

Appendix A. Supplementary data

Supplementary data associated with this article can be found, in the online version, at http://dx.doi.org/10.1016/j.jpba.2017.05.028.

References

[1] U.M. Stamer, F. Musshoff, M. Kobilay, B. Madea, A. Hoeft, F. Stuber, Concentrations of tramadol and O-desmethyltramadol enantiomers in different CYP2D6 genotypes, Clin. Pharmacol. Ther. 82 (2007) 41–47.

[2] A. Wohlfarth, M.S. Castaneto, M. Zhu, S. Pang, K.B. Scheidweiler, R. Kronstrand, M.A. Huestis, Pentylindole/pentylindazole synthetic cannabinoids and their 5-fluoro analogs produce different primary metabolites: metabolite profiling for AB-PINACA and 5F-AB-PINACA, AAPS J. 17 (2015) 660–677.

[3] F.T. Peters, M.R. Meyer, In vitro approaches to studying the metabolism of new psychoactive compounds [review], Drug Test. Anal. 3 (2011) 483–495.

[4] D.K. Wissenbach, M.R. Meyer, A.A. Weber, D. Remane, A.H. Ewald, F.T. Peters, H.H. Maurer, Towards a universal LC-MS screening procedure – can an LIT LC-MSn screening approach and reference library be used on a quadrupole-LIT hybrid instrument? J. Mass Spectrom. 47 (2012) 66–71.

[5] A.G. Helfer, J.A. Michely, A.A. Weber, M.R. Meyer, H.H. Maurer, Orbitrap technology for comprehensive metabolite-based liquid chromatographic-high resolution-tandem mass spectrometric urine drug screening – exemplified for cardiovascular drugs, Anal. Chim. Acta 891 (2015) 221–233.

[6] H. Maurer, K. Pfleger, Screening procedure for detection of phenothiazine and analogous neuroleptics and their metabolites in urine using a computerized gas chromatographic-mass spectrometric technique, J. Chromatogr. 306 (1984) 125–145.

[7] D.K. Wissenbach, M.R. Meyer, D. Remane, A.A. Philipp, A.A. Weber, H.H. Maurer, Drugs of abuse screening in urine as part of a metabolite-based LC-MS(n) screening concept, Anal. Bioanal. Chem. 400 (2011) 3481–3489.

[8] H.H. Maurer, K. Pfleger, A.A. Weber, Mass Spectral Data of Drugs, Poisons, Pesticides, Pollutants and Their Metabolites, Wiley-VCH, Weinheim (Germany), 2016.

[9] D. Dias-da-Silva, M.D. Arbo, M.J. Valente, M.L. Bastos, H. Carmo, Hepatotoxicity of piperazine designer drugs: comparison of different in vitro models, Toxicol. In Vitro 29 (2015) 987–996.

[10] K. Kittler, V. Fessard, R. Maul, D. Hurtaud-Pessel, CYP3A4 activity reduces the cytotoxic effects of okadaic acid in HepaRG cells, Arch. Toxicol. 88 (2014) 1519–1526.

[11] P. Adamowicz, J. Gieron, D. Gil, W. Lechowicz, A. Skulska, B. Tokarczyk, The prevalence of new psychoactive substances in biological material – a three-year review of casework in Poland, Drug Test. Anal. 8 (2016) 63–70.

[12] S.M. Khaled, E. Hughes, D. Bressington, M. Zolezzi, A. Radwan, A. Badnapurkar, R. Gray, The prevalence of novel psychoactive substances (NPS) use in non-clinical populations: a systematic review protocol, Syst. Rev. 5 (2016) 195.

[13] J. Welter, S.D. Brandt, P. Kavanagh, M.R. Meyer, H.H. Maurer, Metabolic fate mass spectral fragmentation, detectability, and differentiation in urine of the benzofuran designer drugs 6-APB and 6-MAPB in comparison to their 5-isomers using GC–MS and LC-(HR)-MS techniques, Anal Bioanal. Chem. 407 (2015) 3457–3470.

[14] J.A. Michely, A.G. Helfer, S.D. Brandt, M.R. Meyer, H.H. Maurer, Metabolism of the new psychoactive substances N,N-diallyltryptamine (DALT) and 5-methoxy-DALT and their detectability in urine by GC–MS, LC-MSn, and LC-HR-MS/MS, Anal. Bioanal. Chem. 407 (2015) 7831–7842.

[15] A.T. Caspar, A.G. Helfer, J.A. Michely, V. Auwaerter, S.D. Brandt, M.R. Meyer, H.H. Maurer, Studies on the metabolism and toxicological detection of the new psychoactive designer drug 2-(4-iodo-2,5-dimethoxyphenyl)-N-[(2-methoxyphenyl)methyl]ethanamine (25I-NBOMe) in human and rat urine using GC–MS, LC-MSn, and LC-HR-MS/MS, Anal. Bioanal. Chem. 407 (2015) 6697–6719.

[16] M.R. Meyer, H.H. Maurer, Enantioselectivity in the methylation of the catecholic phase I metabolites of methylenedioxy designer drugs and their capability to inhibit catechol-O-methyltransferase-catalyzed dopamine 3-methylation, Chem. Res. Toxicol. 22 (2009) 1205–1211.

[17] A.E. Schwaninger, M.R. Meyer, J. Zapp, H.H. Maurer, The role of human UDP-glucuronyltransferases on the formation of the methylenedioxymethamphetamine (ecstasy) phase II metabolites R- and S-3-methoxymethamphetamine 4-O-glucuronides, Drug Metab. Dispos. 37 (2009) 2212–2220.

[18] N. Negreira, C. Erratico, T. Kosjek, A.L. van Nuijs, E. Heath, H. Neels, A. Covaci, In vitro Phase I and Phase II metabolism of alpha-pyrrolidinovalerophenone (alpha-PVP), methylenedioxypyrovalerone (MDPV) and methedrone by human liver microsomes and human liver cytosol, Anal Bioanal. Chem. 407 (2015) 5803–5816.

[19] S. Strano-Rossi, A.B. Cadwallader, X. de la Torre, F. Botre, Toxicological determination and in vitro metabolism of the designer drug methylenedioxypyrovalerone (MDPV) by gas chromatography/mass spectrometry and liquid chromatography/quadrupole time-of-flight mass spectrometry, Rapid Commun. Mass Spectrom. 24 (2010) 2706–2714.

[20] H.H. Gerets, K. Tilmant, B. Gerin, H. Chanteux, B.O. Depelchin, S. Dhalluin, F.A. Atienzar, Characterization of primary human hepatocytes HepG2 cells, and HepaRG cells at the mRNA level and CYP activity in response to inducers and their predictivity for the detection of human hepatotoxins, Cell Biol. Toxicol. 28 (2012) 69–87.

[21] S. Antherieu, C. Chesne, R. Li, C. Guguen-Guillouzo, A. Guillouzo, Optimization of the HepaRG cell model for drug metabolism and toxicity studies, Toxicol. In Vitro 26 (2012) 1278–1285.

[22] A.P. Li, P. Maurel, M.J. Gomez-Lechon, L.C. Cheng, M. Jurima-Romet, Preclinical evaluation of drug-drug interaction potential: present status of the application of primary human hepatocytes in the evaluation of cytochrome P450 induction, Chem. Biol. Interact. 107 (1997) 5–16.

[23] K.P. Kanebratt, T.B. Andersson, HepaRG cells as an in vitro model for evaluation of cytochrome P450 induction in humans, Drug Metab. Dispos. 36 (2008) 137–145.

[24] S.N. Hart, Y. Li, K. Nakamoto, E.A. Subileau, D. Steen, X.B. Zhong, A comparison of whole genome gene expression profiles of HepaRG cells and HepG2 cells to primary human hepatocytes and human liver tissues, Drug Metab. Dispos. 38 (2010) 988–994.

[25] M. Lubberstedt, U. Muller-Vieira, M. Mayer, K.M. Biemel, F. Knospel, D. Knobeloch, A.K. Nussler, J.C. Gerlach, K. Zeilinger, HepaRG human hepatic cell line utility as a surrogate for primary human hepatocytes in drug metabolism assessment in vitro, J. Pharmacol. Toxicol. Methods 63 (2011) 59–68.

[26] M. Klein, M. Thomas, U. Hofmann, D. Seehofer, G. Damm, U.M. Zanger, A systematic comparison of the impact of inflammatory signaling on absorption distribution, metabolism, and excretion gene expression and activity in primary human hepatocytes and HepaRG cells, Drug Metab. Dispos. 43 (2015) 273–283.

[27] B. Berger, M. Donzelli, S. Maseneni, F. Boess, A. Roth, S. Krahenbuhl, M. Haschke, Comparison of liver cell models using the basel phenotyping cocktail, Front. Pharmacol. 7 (2016) 443.

[28] A.E. Schwaninger, M.R. Meyer, J. Zapp, H.H. Maurer, Sulfation of the 3,4-methylenedioxymethamphetamine (MDMA) metabolites 3,4-dihydroxymethamphetamine (DHMA) and 4-hydroxy-3-methoxymethamphetamine (HMMA) and their capability to inhibit human sulfotransferases, Toxicol. Lett. 202 (2011) 120–128.

[29] L. Estrada-Rodgers, G.N. Levy, W.W. Weber, Substrate selectivity of mouse N-acetyltransferases 1, 2, and 3 expressed in COS-1 cells, Drug Metab. Dispos. 26 (1998) 502–505.

[30] M.R. Meyer, C. Lindauer, J. Welter, H.H. Maurer, Dimethocaine, a synthetic cocaine derivative: studies on its in vivo metabolism and its detectability in urine by LC-HR-MS^n and GC–MS using a rat model, Anal. Bioanal. Chem. 406 (2014) 1845–1854.

[31] L. Wagmann, H.H. Maurer, M.R. Meyer, In vitro monoamine oxidase inhibition potential of alpha-methyltryptamine analog new psychoactive substances for assessing possible toxic risks, Toxicol. Lett. 272 (2017) 84–93.

[32] M.R. Meyer, L.H.R. Richter, H.H. Maurer, Methylenedioxy designer drugs: mass spectrometric characterization of their glutathione conjugates by means of liquid chromatography-high-resolution mass spectrometry/mass spectrometry and studies on their glutathionyl transferase inhibition potency, Anal. Chim. Acta 822 (2014) 37–50.

[33] L.H.R. Richter, Y.R. Kaminski, F. Noor, M.R. Meyer, H.H. Maurer, Metabolic fate of desomorphine elucidated using rat urine pooled human liver preparations, and human hepatocyte cultures as well as its detectability using standard urine screening approaches, Anal. Bioanal. Chem. 408 (2016) 6283–6294.

[34] D. Mueller, L. Kramer, E. Hoffmann, S. Klein, F. Noor, 3D organotypic HepaRG cultures as in vitro model for acute and repeated dose toxicity studies, Toxicol. In Vitro 28 (2014) 104–112.

[35] S. Klein, D. Mueller, V. Schevchenko, F. Noor, Long-term maintenance of HepaRG cells in serum-free conditions and application in a repeated dose study, J. Appl. Toxicol. 34 (2014) 1078–1086.

[36] F.L. Sauvage, F. Saint-Marcous, B. Duretz, D. Deporte, G. Lachatre, P. Marquet, Screening of drugs and toxic compounds with liquid chromatography-linear ion trap tandem mass spectrometry, Clin. Chem. 52 (2006) 1735–1742.

[37] J. Welter, P. Kavanagh, M.R. Meyer, H.H. Maurer, Benzofuran analogues of amphetamine and methamphetamine: studies on the metabolism and toxicological analysis of 5-APB and 5-MAPB in urine and plasma using GC–MS and LC-(HR)-MS^n techniques, Anal. Bioanal. Chem. 407 (2015) 1371–1388.

[38] M.R. Meyer, P. Du, F. Schuster, H.H. Maurer, Studies on the metabolism of the alpha-pyrrolidinophenone designer drug methylenedioxy-pyrovalerone (MDPV) in rat urine and human liver microsomes using GC–MS and LC-high-resolution-MS and its detectability in urine by GC–MS, J. Mass Spectrom. 45 (2010) 1426–1442.

[39] H.H. Maurer, M.R. Meyer, A.G. Helfer, A.A. Weber, Maurer/Meyer/Helfer/Weber MMHW LC-HR-MS/MS Library of Drugs, Poisons, and Their Metabolites, Wiley-VCH, Weinheim (Germany), 2017.

[40] D. Zhang, G. Luo, X. Ding, C. Lu, Preclinical experimental models of drug metabolism and disposition in drug discovery and development, Acta Pharm. Sin. B 2 (2012) 549–561.

[41] E.F. Brandon, C.D. Raap, I. Meijerman, J.H. Beijnen, J.H. Schellens, An update on in vitro test methods in human hepatic drug biotransformation research: pros and cons, Toxicol. Appl. Pharmacol. 189 (2003) 233–246.

[42] D. Springer, G. Fritschi, H.H. Maurer, Metabolism and toxicological detection of the new designer drug 3',4'-methylenedioxy-alpha-pyrrolidinopropiophenone studied in urine using gas chromatography-mass spectrometry, J. Chromatogr. B 793 (2003) 377–388.

[43] R.F. Staack, H.H. Maurer, New designer drug 1-(3,4-methylenedioxybenzyl) piperazine (MDBP): studies on its metabolism and toxicological detection in rat urine using gas chromatography/mass spectrometry, J. Mass Spectrom. 39 (2004) 255–261.

[44] K. Zaitsu, M. Katagi, H.T. Kamata, T. Kamata, N. Shima, A. Miki, H. Tsuchihashi, Y. Mori, Determination of the metabolites of the new designer drugs bk-MBDB and bk-MDEA in human urine, Forensic Sci. Int. 188 (2009) 131–139.

[45] M.R. Meyer, J. Wilhelm, F.T. Peters, H.H. Maurer, Beta-keto amphetamines: studies on the metabolism of the designer drug mephedrone and toxicological detection of mephedrone, butylone, and methylone in urine using gas chromatography-mass spectrometry, Anal. Bioanal. Chem. 397 (2010) 1225–1233.
[46] H.H. Maurer, J. Bickeboeller-Friedrich, T. Kraemer, F.T. Peters, Toxicokinetics and analytical toxicology of amphetamine-derived designer drugs (Ecstasy), Toxicol. Lett. 112 (2000) 133–142.
[47] H.H. Maurer, T. Kraemer, D. Springer, R.F. Staack, Chemistry, pharmacology, toxicology, and hepatic metabolism of designer drugs of the amphetamine (ecstasy), piperazine, and pyrrolidinophenone types, a synopsis [review], Ther. Drug Monit. 26 (2004) 127–131.
[48] M.R. Meyer, H.H. Maurer, Metabolism of designer drugs of abuse: an updated review [review], Curr. Drug Metab. 11 (2010) 468–482.
[49] A.E. Schwaninger, M.R. Meyer, A.J. Barnes, E.A. Kolbrich-Spargo, D.A. Gorelick, R.S. Goodwin, M.A. Huestis, H.H. Maurer, Human MDMA and phase I and phase II metabolite urinary excretion kinetics following controlled MDMA administration, Clin. Chem. 57 (2011) 1748–1756.
[50] M.R. Meyer, F.T. Peters, H.H. Maurer, The role of human hepatic cytochrome P450 isozymes in the metabolism of racemic 3,4-methylenedioxy-methamphetamine and its enantiomers, Drug Metab. Dispos. 36 (2008) 2345–2354.
[51] A.E. Schwaninger, M.R. Meyer, A.J. Barnes, E.A. Kolbrich-Spargo, D.A. Gorelick, R.S. Goodwin, M.A. Huestis, H.H. Maurer, Stereoselective urinary MDMA (ecstasy) and metabolites excretion kinetics following controlled MDMA administration to humans, Biochem. Pharmacol. 83 (2012) 131–138.
[52] M.R. Meyer, F.T. Peters, H.H. Maurer, The role of human hepatic cytochrome P450 isozymes in the metabolism of racemic 3,4-methylenedioxyethylamphetamine and its single enantiomers, Drug Metab. Dispos. 37 (2009) 1152–1156.
[53] D. Springer, L.D. Paul, R.F. Staack, T. Kraemer, H.H. Maurer, Identification of cytochrome P450 enzymes involved in the metabolism of 3',4'-methylenedioxy-α – pyrrolidinopropiophenone (MDPPP), a designer drug, in human liver microsomes, Xenobiotica 35 (2005) 227–237.
[54] T. Kanamori, K. Kanda, T. Yamamuro, K. Kuwayama, K. Tsujikawa, Y.T. Iwata, H. Inoue, Detection of main metabolites of XLR-11 and its thermal degradation product in human hepatoma HepaRG cells and human urine, Drug Test. Anal. 7 (2015) 341–345.
[55] A. Wohlfarth, S. Pang, M. Zhu, A.S. Gandhi, K.B. Scheidweiler, H.F. Liu, M.A. Huestis, First metabolic profile of XLR-11 a novel synthetic cannabinoid, obtained by using human hepatocytes and high-resolution mass spectrometry, Clin. Chem. 59 (2013) 1638–1648.
[56] N. Shima, M. Katagi, H. Kamata, K. Zaitsu, T. Kamata, M. Nishikawa, A. Miki, H. Tsuchihashi, T. Sakuma, N. Nemoto, Urinary excretion of the main metabolites of 3,4-methylenedioxymethamphetamine (MDMA), including the sulfate and glucuronide of 4-hydroxy-3-methoxymethamphetamine (HMMA), in humans and rats, Xenobiotica 38 (2008) 314–324.
[57] N. Shima, H.T. Kamata, M. Katagi, H. Tsuchihashi, Urinary excretion of the main metabolites of methamphetamine, including p-hydroxymethamphetamine-sulfate and p-hydroxymethamphetamine-glucuronide, in humans and rats, Xenobiotica 36 (2006) 259–267.
[58] J. Dinger, M.R. Meyer, H.H. Maurer, In vitro cytochrome P450 inhibition potential of methylenedioxy-derived designer drugs studied with a two cocktail approach, Arch. Toxicol. 90 (2016) 305–318.
[59] H.H. Maurer, On the metabolism and the toxicological analysis of methylenedioxyphenylalkylamine designer drugs by gas chromatography-mass spectrometry, Ther. Drug Monit. 18 (1996) 465–470.

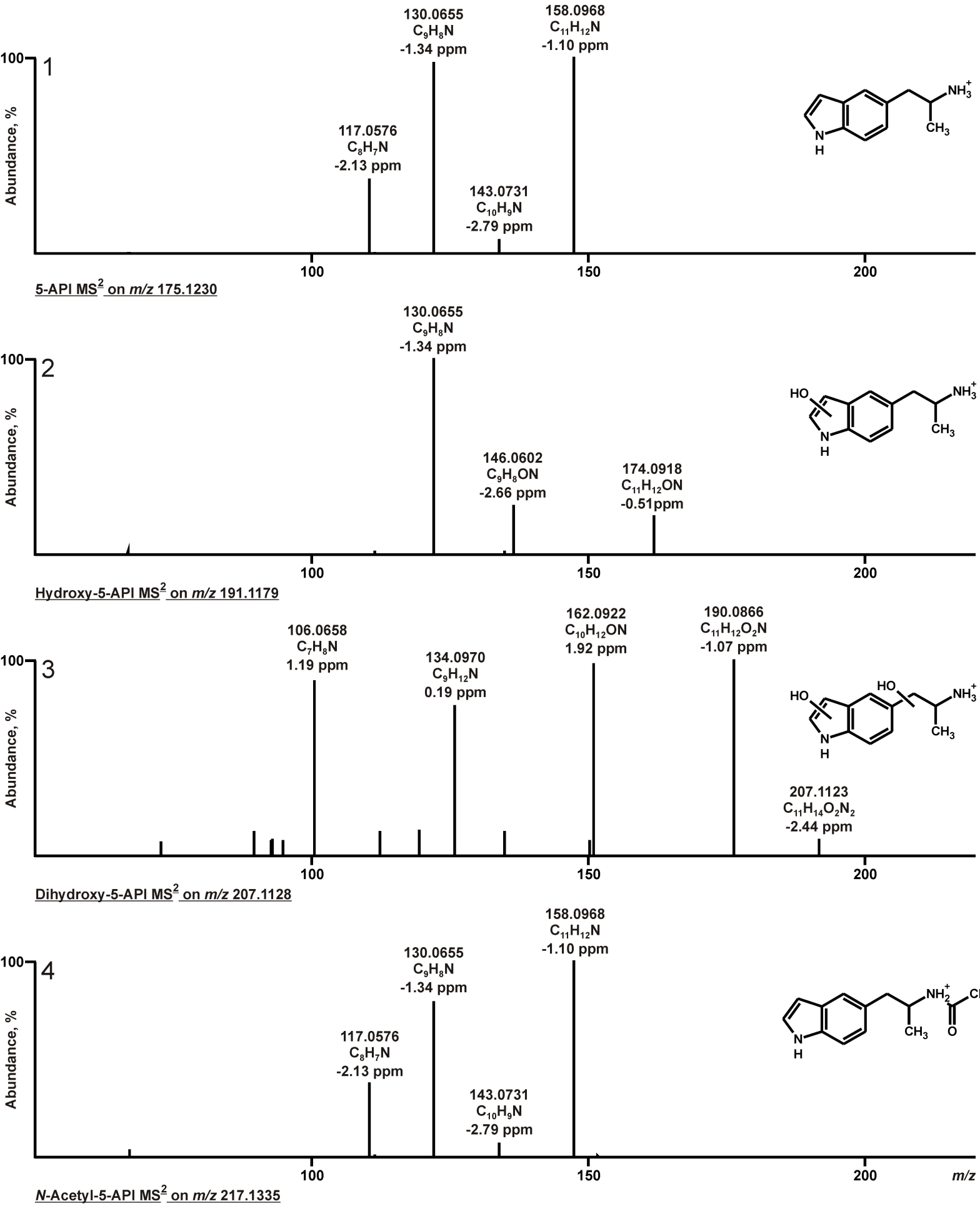

Figure S1 HR-MS/MS spectra, proposed structures, and predominant fragmentation patterns of 5-API and its metabolites arranged according to precursor mass

3.3. New Psychoactive Substances: Studies on the Metabolism of XLR-11, AB-PINACA, FUB-PB-22, 4-Methoxy-α-PVP, 25-I-NBOMe, and Meclonazepam Using Human Liver Preparations in Comparison to Primary Human Hepatocytes and Human Urine[12]

(DOI: 10.1016/j.toxlet.2017.07.90)

Toxicology Letters 280 (2017) 142–150

Contents lists available at ScienceDirect

Toxicology Letters

journal homepage: www.elsevier.com/locate/toxlet

New psychoactive substances: Studies on the metabolism of XLR-11, AB-PINACA, FUB-PB-22, 4-methoxy-α-PVP, 25-I-NBOMe, and meclonazepam using human liver preparations in comparison to primary human hepatocytes, and human urine

Lilian H.J. Richter, Hans H. Maurer, Markus R. Meyer*

Department of Experimental and Clinical Toxicology, Institute of Experimental and Clinical Pharmacology and Toxicology, Center for Molecular Signaling (PZMS), Saarland University, Homburg, Germany

ARTICLE INFO

Keywords:
New psychoactive substances (NPS)
Drugs of abuse
Metabolism
Human liver preparations
Primary human hepatocytes
LC-HR-MS/MS

ABSTRACT

New psychoactive substances (NPS) are an increasing problem in clinical and forensic toxicology. The knowledge of their metabolism is important for toxicological risk assessment and for developing toxicological urine screenings. Considering the huge numbers of NPS annually appearing on the market, metabolism studies should be realized in a fast, simple, cost efficient, and reliable way. Primary human hepatocytes (PHH) were recommended to be the gold standard for in vitro metabolism studies as they are expected to contain natural enzyme clusters, co-substrates, and drug transporters. In addition, they were already successfully used for metabolism studies of NPS. However, they also have disadvantages such as high costs and limited applicability without special equipment. The aims of the present study were therefore first to investigate exemplarily the phase I and phase II metabolism of six NPS (XLR-11, AB-PINACA, FUB-PB-22, 4-methoxy-α-PVP, 25-I-NBOMe, and meclonazepam) from different drug classes using pooled human S9 fraction (pS9) or pooled human liver microsomes combined with cytosol (pHLM/pHLC) after addition of the co-substrates for the main metabolic phase I and II reactions. Second to compare results to published data generated using primary human hepatocytes and human urine samples. Results of the incubations with pS9 or pHLM/pHLC were comparable in number and abundance of metabolites. Formation of metabolites, particularly after multi-step reactions needed a longer incubation time. However, incubations using human liver preparations resulted in a lower number of total detected metabolites compared to PHH, but they were still able to allow the identification of the main human urinary excretion products. Human liver preparations and particularly the pooled S9 fraction could be shown to be a sufficient and more cost-efficient alternative in context of metabolism studies also for developing toxicological urine screenings.

It might be recommended to use the slightly cheaper pS9 fraction instead of a pHLM/pHLC combination. As formation of some metabolites needed a long incubation time, two sampling points at 60 and 360 min should be recommended.

1. Introduction

New psychoactive substances (NPS) are a challenging task for toxicologists as the numbers of NPS on the drugs of abuse (DOAs) market continuously increased in recent years (Adamowicz et al., 2016; Khaled et al., 2016; UNODC, 2016). In contrast to traditional DOAs such as amphetamine, heroin, cocaine, and THC, their targets for toxicological urine screenings are most unknown. This is especially a problem for compounds that are extensively metabolized such as synthetic cannabinoids (Diao et al., 2016; Wohlfarth et al., 2013) or so-called NBOMe's (Caspar et al., 2017, 2015; Wohlfarth et al., 2017). In such cases, the parent compound itself is not a reliable target and metabolism or excretion studies need to be done.

As nowadays LC–MS approaches, which do not necessarily need cleavage of conjugates prior to analysis (Helfer et al., 2015; Wissenbach et al., 2011), are mainly used for screening, metabolism studies are expected to include phase II reactions. Due to species differences in metabolism (Dias-da-Silva et al., 2015; Kittler et al., 2014), human samples are still considered to be best suitable for such metabolism studies. However, in the case of NPS, human samples are often not (yet)

* Corresponding author.
E-mail address: markus.meyer@uks.eu (M.R. Meyer).

http://dx.doi.org/10.1016/j.toxlet.2017.07.901
Received 21 June 2017; Received in revised form 26 July 2017; Accepted 31 July 2017
Available online 04 August 2017
0378-4274/

available and controlled studies cannot be performed due to lack of preclinical safety data and thus ethical reasons (Richter et al., 2017). As long as in vivo data on their metabolism, toxicity, and analytical targets in body fluids are missing, their metabolism can systematically be studied using human in vitro or animal in vivo models mimicking human metabolism (Richter et al., 2017).

Primary human hepatocytes (PHH) were considered as gold standard in in vitro metabolism studies due to natural enzyme clusters, co-substrates, and drug transporters (Antherieu et al., 2012; Gerets et al., 2012; Li et al., 1997) and were expected to provide the most authentic spectrum of human metabolites (Wohlfarth et al., 2013) but they also have some disadvantages. Particularly high costs limit their applicability for high throughput metabolism studies although they were already successfully used for metabolism studies of NPS (Diao et al., 2016; Ellefsen et al., 2016; Vikingsson et al., 2017; Wohlfarth et al., 2015, 2013, 2017) but high costs, limited availability, and variability in the expression of metabolic enzymes may limit their applicability (Kanebratt and Andersson, 2008; Kittler et al., 2014; Maurer and Meyer, 2016; Peters and Meyer, 2011; Rodrigues et al., 2016). Previous studies have already shown that incubations using pooled human S9 fraction (pS9) or pooled human microsomes combined with human cytosol (pHLM/pHLC) might be a suitable alternative to cell-based approaches for identification of main urinary excretion products (Richter et al., 2017). However, no comparison of pS9 or pHLM/pHLC towards PHH for NPS metabolism was done so far.

Therefore, the aim of the present study was to investigate exemplarily the metabolism of six NPS from different drug classes (synthetic cannabinoids, cathinone, NBOMes, and benzodiazepine; structures shown in Fig. 1) using pS9 or pHLM/pHLC. Results should then be compared to published data using PHH or human urine for metabolism studies of NPS in the context of toxicological urine screenings.

2. Materials and methods

2.1. Chemicals and enzymes

[1-(5-Fluorpentyl)-1H-indol-3-yl]-(2,2,3,3-tetramethylcyclopropyl) methanone (XLR-11) and *N*-(1-amino-3-methyl-1-oxobutan-2-yl)-1-pentyl-1H-indazol-3-carboxamide (AB-PINACA) were obtained from Lipomed AG (Arlesheim, Switzerland), trimipramide-d_3, quinolin-8-yl 1-[(4-fluorphenyl)methyl]-1H-indol-3-carboxylate (FUB-PB-22), 4-methoxy-α-pyrrolidinovalerophenone HCl (4-methoxy-α-PVP), (2-(4-iodo-2,5-dimethoxyphenyl)-*N*-[(2-methoxyphenyl)methyl]ethan-1-amine) HCl (25-I-NBOMe), and meclonazepam were obtained from LGC Standards (Wesel, Germany), isocitrate, isocitrate dehydrogenase, superoxide dismutase, 3′-phosphoadenosine-5′-phosphosulfate (PAPS), S-(5′-Adenosyl)-L-methionine (SAM), dithiothreitol (DTT), reduced glutathione (GSH), acetylcarnitine transferase (AcT), acetylcarnitine, acetyl coenzyme A (AcCoA), from Sigma-Aldrich (Taufkirchen, Germany), and $NADP^+$ from Biomol (Hamburg, Germany), acetonitrile (LC–MS grade), ammonium formate (analytical grade), formic acid (LC–MS grade), methanol (LC–MS grade), and all other chemicals and reagents (analytical grade) from VWR (Darmstadt, Germany). Pooled human liver microsomes (pHLM, 20 mg microsomal protein/mL, 330 pmol total CYP/mg protein, from 34 individual donors), ultra-pooled human liver cytosol (pHLC, 20 mg cytosolic protein/mL, from 150 individual donors), pS9 (20 mg protein/mL, from 30 individual donors), UGT reaction mix solution A (25 mM UDP-glucuronic acid),

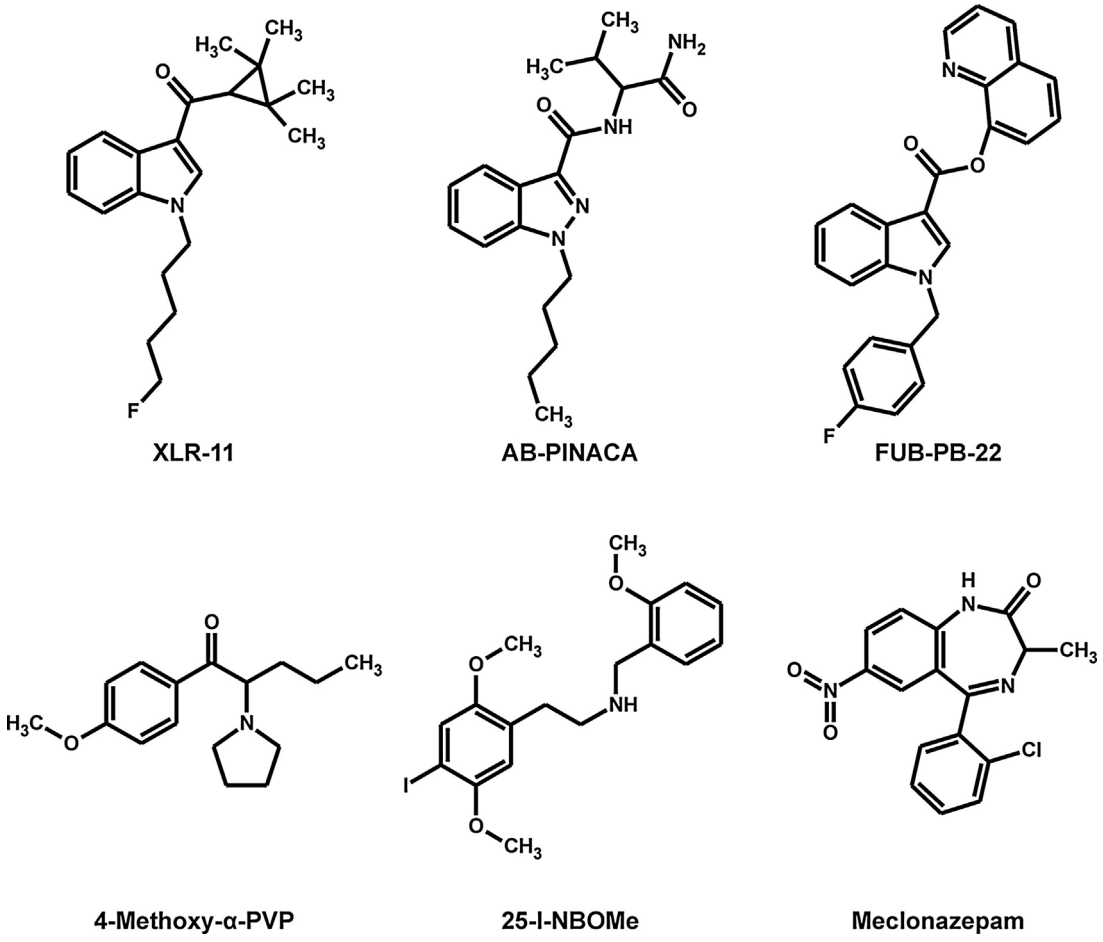

Fig. 1. Chemical structures of investigated compounds.

Table 1
Metabolites identified in pS9, pHLM/pHLC incubations or reported in literature for XLR-11 in PHH incubations or human urine (RT = retention time, – = no RT available, D = detected, ND = not detected, / = detection not possible, * = *m/z* and formula of the corresponding aglycone, which was detected due to potential in-source fragmentation of the glucuronide). The three most abundant metabolites detected in pHLM/pHLC, pS9, PHH samples after an incubation time of 180 min or human urine (HU) after unknown dose and time of consumptions are marked with an "M". Metabolites are listed according to increasing mass.

Metabolite ID	Metabolic Reaction	*m/z*	Formula	RT, min	pS9		pHLM/pHLC		PHH	HU after hydrolysis
					PC	TD	PC	TD		
	Parent compound (PC)	330.2227	$C_{21}H_{29}FNO$	13.4	D	D	D	D	D	ND
TD	XLR-11 thermal degradant (TD)	330.2227	$C_{21}H_{29}FNO$	13.1	/	D	/	D	/	ND
M1	Oxidative defluorination	328.2271	$C_{21}H_{30}NO_2$	12.2	D^M	D^M	D^M	D^M	D^M	D
TDM1	Oxidative defluorination	328.2271	$C_{21}H_{30}NO_2$	11.5	/	D^M	/	D^M	/	D^M
M2	Oxidative defluorination to carboxylic acid	340.1972	$C_{21}H_{26}NO_3$	–	ND	ND	ND	ND	D	ND
M3	Oxidative defluorination to carboxylic acid	342.2063	$C_{21}H_{28}NO_3$	11.9	D^M	D	D^M	D	D^M	D
TDM2	Oxidative defluorination to carboxylic acid	342.2063	$C_{21}H_{28}NO_3$	11.4	/	D^M	/	D^M	/	D^M
M4	Di-oxidation followed by internal dehydration	344.2020	$C_{21}H_{27}FNO_2$	12.6	D^M	D	D	D	D	D
TDM3	Oxidatioin	346.2176	$C_{21}H_{29}FNO_2$	9.4	/	D	/	ND	/	D
TDM4	Oxidatioin	346.2176	$C_{21}H_{29}FNO_2$	11.7	/	D	/	ND	/	D
M5	Oxidative defluorination to carboxylic acid + Di-oxidation followed by internal dehydration	356.1856	$C_{21}H_{26}NO_4$	10.3	D	ND	D	ND	D	ND
M6	Oxidative defluorination to carboxylic acid + oxidation	358.2012	$C_{21}H_{28}NO_4$	9.6	D	ND	D	ND	D	D
M7	Oxidative defluorination to carboxylic acid + oxidation	358.2012	$C_{21}H_{28}NO_4$	9.9	D	D	D	D	D	D
M8	Oxidative defluorination to carboxylic acid + oxidation + hemiketal formation	358.2012	$C_{21}H_{28}NO_4$	–	ND	ND	ND	ND	D	ND
TDM5	Oxidative defluorination to carboxylic acid + oxidation + hemiketal formation	358.2012	$C_{21}H_{28}NO_4$	–	/	ND	/	ND	/	D^M
TDM6	Oxidative defluorination to carboxylic acid + oxidation + hemiketal formation	358.2012	$C_{21}H_{28}NO_4$	–	/	ND	/	ND	/	D
M9	Oxidative defluorination + carboxylation	358.2016	$C_{21}H_{28}NO_4$	–	ND	ND	ND	ND	D	ND
M10	Carboxylation	360.1969	$C_{21}H_{27}FNO_3$	–	ND	ND	ND	ND	D^M	ND
M11	Oxidative defluorination to carboxylic acid + carboxylation	372.1805	$C_{21}H_{26}NO_5$	–	ND	ND	ND	ND	D	ND
M12	Oxidative defluorination to carboxylic acid oxidation aldehyde foramtion followed by hemiacetal formation	372.1805	$C_{21}H_{26}NO_5$	–	ND	ND	ND	ND	D	ND
M13	Carboxylation + oxidation	376.1918	$C_{21}H_{27}FNO_4$	–	ND	ND	ND	ND	D	ND
M14	Carboxylation + oxidation	376.1918	$C_{21}H_{27}FNO_4$	–	ND	ND	ND	ND	D	ND
M15	Oxidative defluorination + glucuronidation	504.2591	$C_{27}H_{38}NO_8$	10.8	D	D	D^M	D	D	ND
TDM7	Oxidative defluorination + glucuronidation	504.2591	$C_{27}H_{38}NO_8$	10.2	/	D	/	D	/	ND
M16	Oxidative defluorination to carboxylic acid + glucuronidation	518.2384	C27H36NO9	10.6	D	D	D	D	D	ND
M17	Oxidative defluorination + oxidation + glucuronidation	518.2384 342.2063*	$C_{27}H_{36}NO_9$ $C_{21}H_{28}NO_3$*	–	ND	ND	ND	ND	D	ND
M18	Oxidative defluorination + oxidation + glucuronidation	520.2541	$C_{27}H_{38}NO_9$	8.7	D	ND	D	ND	D	ND
M19	Oxidative defluorination + oxidation + glucuronidation	520.2541	$C_{27}H_{38}NO_9$	8.9	D	ND	D	ND	D	ND
M20	Oxidative defluorination + oxidation + glucuronidation	520.2541	$C_{27}H_{38}NO_9$	9.3	D	ND	D	ND	D	ND
M21	Oxidation + glucuronidation	522.2497	$C_{27}H_{37}FNO_8$	10.2	D	D	D	D	D	ND
M22	Oxidation + glucuronidation	522.2497	$C_{27}H_{37}FNO_8$	10.4	D	D	D	D	D	ND
M23	Oxidation + glucuronidation	522.2497	$C_{27}H_{37}FNO_8$	10.6	D	D	D	D	D	ND
TDM8	Oxidation + glucuronidation	522.2497	$C_{27}H_{37}FNO_8$	8.5	/	D	/	D	/	ND
TDM9	Oxidation + glucuronidation	522.2497	$C_{27}H_{37}FNO_8$	10.2	/	D	/	D	/	ND
M24	Oxidation + aldehyde foramtion followed by hemiacetal foramtion + glucuronidation	536.2290	$C_{27}H_{35}FNO_9$	–	ND	ND	ND	ND	D	ND
M25	Carboxylation + glucuronidation (diasteriomer 1)	536.2294 360.1969*	$C_{21}H_{27}FNO_3$ $C_{21}H_{27F}NO_3$*	11.6	ND	ND	D	ND	D	ND
M26	Carboxylation + glucuronidation (diasteriomer 2)	536.2294 360.1969*	$C_{21}H_{27}FNO_3$ $C_{21}H_{27F}NO_3$*	–	ND	ND	ND	ND	D	ND
M27	Di-oxidation + glucuronidation	538.2446	$C_{27}H_{37}FNO_9$	–	ND	ND	ND	ND	D	ND
M28	Oxidative defluorination to carboxylic acid + carboxylation + glucuronidation	548.2126 372.1805*	$C_{27}H_{34}NO_{11}$ $C_{21}H_{26}NO_5$*	–	ND	ND	ND	ND	D	ND
M29	Oxidative defluorination to carboxylic acid oxidation aldehyde foramtion followed by hemiacetal foramtion and glucuronidation	548.2126	$C_{27}H_{34}NO_{11}$	–	ND	ND	ND	ND	D	ND
M30	Tri-oxidation + glucuronidatoin	554.2396	$C_{27}H_{37}FNO_{10}$	–	ND	ND	ND	ND	D	ND
References									Wohlfarth et al. (2013)	Kanamori et al. (2015)

and UGT reaction mix solution B (250 mM Tris-HCl, 40 mM $MgCl_2$, and 0.125 mg/mL alamethicin) were obtained from Corning (Amsterdam, The Netherlands). After delivery, the enzyme preparations were thawed at 37 °C, aliquoted, snap-frozen in liquid nitrogen, and stored at −80 °C until use. Damiana leaves (Turnera diffusa Willd. ex Schult) were purchased from an online vendor (Krautrausch, Berlin, Germany). The pipe was bought at a local shop.

2.2. In vitro drug metabolism studies using pS9 or pHLM combined with pHLC

According to previous studies (Richter et al., 2017), incubations were performed using pS9 at a final protein concentration of 2 mg/mL or pHLM/pHLC both at a final protein concentration of 1 mg/mL. A 10 min preincubation at 37 °C with 25 µg/mL alamethicin (UGT reaction mix solution B), 90 mM phosphate buffer (pH 7.4), 2.5 mM Mg^{2+},

Table 2
Metabolites identified in pS9, pHLM/pHLC incubations or reported in literature for AB-PINACA in PHH incubations or human urine (RT = retention time, − = no RT available, D = detected, ND = not detected, * = *m/z* and formula of corresponding aglycone potential in-source fragmentation of the glucuronidated metabolite because only the mass of the aglycone was detected). The three most abundant metabolites detected in pHLM/pHLC, pS9, PHH samples after an incubation time of 180 min or in human urine after unknown dose and time of consumptions are marked with an M. Metabolites are listed according to increasing mass.

Metabolite ID	Metabolic Reaction	*m/z*	Formula	RT, min	pS9	pHLM/pHLC	PHH	HU
	Parent compound	331.2133	$C_{18}H_{27}N_4O_2$	11.2	D	D	D	D
M1	Internal amide hydrolysis	233.1285	$C_{13}H_{17}N_2O_2$	10.1	D	D	D	D
M2	Amide hydrolysis	332.1974	$C_{18}H_{26}N_3O_3$	12.0	D^M	D^M	D^M	D^M
M3	Ketone formation	345.1921	$C_{18}H_{25}N_4O_3$	8.6	D	D^M	D^M	D
M4	Amide hydrolysis + ketone formation	346.1761	$C_{18}H_{24}N_3O_4$	9.4	D	D	D	D^M
M5	Oxidation	347.2077	$C_{18}H_{27}N_4O_3$	8.4	D^M	D^M	D^M	D
M6	Oxidation	347.2077	$C_{18}H_{27}N_4O_3$	8.7	D	D	D	D
M7	Oxidation	347.2077	$C_{18}H_{27}N_4O_3$	–	ND	ND	D	D
M8	Oxidation	347.2077	$C_{18}H_{27}N_4O_3$	10.1	D	D	D	D
M9	Oxidation at butane moiety	347.2077	$C_{18}H_{27}N_4O_3$	–	ND	ND	D	D
M10	Oxidation at indazole	348.1917	$C_{18}H_{26}N_4O_3$	–	ND	ND	D	D
M11	Amide hydrolysis + oxidation	348.1917	$C_{18}H_{26}N_3O_4$	9.2	D	D	D	D^M
M12	Amide hydrolysis + oxidation	348.1917	$C_{18}H_{26}N_3O_4$	–	ND	ND	D	D
M13	Amide hydrolysis + oxidation	348.1917	$C_{18}H_{26}N_3O_4$	–	ND	ND	D	D
M14	Amide hydrolysis + oxidation at indazole	348.1917	$C_{18}H_{26}N_3O_4$	11.0	D	D	D	D
M15	Ketone formation + oxidation	361.1870	$C_{18}H_{25}N_4O_4$	–	ND	ND	D	D
M16	Carboxylation	361.1870	$C_{18}H_{25}N_4O_4$	–	ND	ND	D	D
M17	Amide hydrolysis + carboxylation	362.1716	$C_{18}H_{24}N3O_5$	–	ND	ND	D	D
M18	Dioxidation	363.2026	$C_{18}H_{27}N_4O_4$	–	ND	ND	D	D
M19	Epoxide foramtion with subsequent hydrolysis dihydrodiol	365.2183	$C_{18}H_{29}N_4O_4$	–	ND	ND	D	D
M20	Internal amide hydrolysis + glucuronidation	409.1605 233.1285*	$C_{19}H_{25}N_2O_8$ $C_{13}H_{17}N_2O_2$*	8.7	D	D	ND	ND
M21	Amide hydrolyse + glucuronidation	508.2286	$C_{24}H_{34}N_3O_9$	10.7	D	D	D	D
M22	Amide hydrolysis + glucuronidation (in-source fragmentation)	508.2286 332.1974*	$C_{24}H_{34}N_3O_9$ $C_{18}H_{26}N_3O_3$*	10.7	D^M	D	ND	ND
M23	Amide hydrolysis + ketone formation + glucuronidation	522.2082 346.1761*	$C_{24}H_{32}N_3O_{10}$ $C_{18}H_{24}N_3O_4$*	8.3	ND	D	ND	ND
M24	Oxidation + glucuonidation	523.2398	$C_{24}H_{35}N_4O_9$	7.9	D	D	D	D
M25	Amide hydrolysis + oxidation + glucuronidation	524.2239	$C_{24}H_{34}N_3O_{10}$	–	ND	ND	D	D
M26	Amide hydrolysis + oxidation + glucuronidation	524.2239	$C_{24}H_{34}N_3O_{10}$	–	ND	ND	D	D
References							Wohlfarth et al. (2015)	Wohlfarth et al. (2015)

Table 3
Metabolites identified in pS9, pHLM/pHLC incubations or reported in literature for FUB-PB-22 in PHH incubations or human urine (RT = retention time, − = no RT available, D = detected, ND = not detected, FIB-COOH = carboxylic acid after ester hydrolysis of FUB-PB-22, * = *m/z* and formula of corresponding aglycone potential in-source fragmentation of the glucuronidated metabolite because only the mass of the aglycone was detected). The two most abundant metabolites detected in pHLM/pHLC, pS9, PHH samples after an incubation time of 180 min or in human urine after unknown dose and time of consumptions are marked with an M. Metabolites are listed according to increasing mass.

Metabolite ID	Metabolic Reaction	*m/z*	Formula	RT, min	pS9	pHLM/pHLC	PHH	HU
	Parent compound	397.1346	$C_{25}H_{18}FN_2O_2$	12.6	D	D	D	ND
M1	Quinolinol	146.0600	C_9H_8NO	2.5	D^M	D^M	ND	ND
M2	Quinolinol + sulfation	226.0168	$C_9H_8NO_4S$	2.5	D	D	D	ND
M3	FIB-COOH	270.0924	$C_{16}H_{13}FNO_2$	10.4	D	D	D^M	D
M4	FIB-COOH + hydroxylation	286.2771	$C_{16}H_{13}FNO_3$	–	ND	ND	D	ND
M5	FIB-COOH + hydroxylation	286.2771	$C_{16}H_{13}FNO_3$	–	ND	ND	D	ND
M6	FIB-COOH + hydroxylation	286.2771	$C_{16}H_{13}FNO_3$	–	ND	ND	D	D
M7	FIB-COOH + glucuronidation	446.4018 270.0924*	$C_{22}H_{21}FNO_8$ $C_{16}H_{13}FNO_2$*	9.0	D^M	D^M	D^M	D^M
M8	FIB-COOH + hydroxylation + glucuronidation	462.1194	$C_{22}H_{21}FNO_9$	–	ND	ND	D	D^M
References							Diao et al. (2016)	Diao et al. (2016)

2.5 mM isocitrate, 0.6 mM $NADP^+$, 0.8 U/mL isocitrate dehydrogenase, 100 U/mL superoxide dismutase, 0.1 mM AcCoA, 2.3 mM acetyl carnitine, and 8 U/mL carnitine acetyltransferase was done. Thereafter, 2.5 mM UDP-glucuronic acid (UGT reaction mix solution A), 40 µM aqueous PAPS, 1.2 mM SAM, 1 mM DTT, 10 mM GSH, and 10 µM substrate in phosphate buffer were added (final volume, 300 µL). All given concentrations were final concentrations.

Reactions were initiated by addition of substrate and the mixtures were incubated for a maximum of 480 min. Single 30 µL aliquots of the mixtures were transferred into reaction tubes and reactions were terminated by addition of 10 µL ice-cold acetonitrile containing 1 µM trimipramine-d_3 as internal standard after 15, 30, 60, 120, 180, 240, 360, and 480 min as it was shown previously that microsomes and pS9 are active up to 480 min (Richter et al., 2017). The tubes were cooled for 30 min at −18 °C, centrifuged for 2 min at 10,000 × *g*, 30 µL of the supernatants were transferred into autosampler vials, and 1 µL injected onto the Orbitrap (OT)-based liquid chromatography-high resolution-tandem mass spectrometry (LC-HR-MS/MS) system as described below. Blank incubations without substrate and control samples with substrate, but without pS9 or pHLM/pHLC were prepared to confirm the absence of interfering compounds and to identify not metabolically formed compounds. All incubations were done in duplicates.

Table 4
Metabolites identified in pS9, pHLM/pHLC incubations or reported in literature for 4-methoxy-α-PVP in PHH incubations (RT = retention time, – = no RT available, D = detected, ND = not detected). The two most abundant metabolites detected in pHLM/pHLC, pS9, PHH samples after an incubation time of 180 min are marked with an M. Metabolites are listed according to increasing mass.

Metabolite ID	Metabolic Reaction	*m/z*	Formula	RT, min	pS9	pHLM/pHLC	PHH
	Parent compound	262.1801	$C_{16}H_{24}NO_2$	6.4	D	D	D
M1	*O*-Demethylation + *N*-dealkylation	194.1177	$C_{11}H_{16}NO_2$	–	ND	ND	D
M2	*O*-Demethylation	248.1645	$C_{15}H_{22}NO_2$	4.8	D^M	D^M	D^M
M3	Ketone reduction + *O*-demethylation	250.1801	$C_{15}H_{24}NO_2$	–	ND	ND	D
M4	Iminum ion formation	260.1645	$C_{16}H_{22}NO_2$	–	ND	ND	D
M5	Ketone reduction	264.1958	$C_{16}H_{26}NO_2$	–	ND	ND	D
M6	Carboxylation	276.1594	$C_{16}H_{22}NO_3$	9.9	D^M	D^M	D
M7	Hydroxylation	278.1749	$C_{16}H_{24}NO_3$	6.0	D	D	D
M8	Aliphatic *N*-oxidation	278.1749	$C_{16}H_{24}NO_3$	–	ND	ND	D
M9	Pyrolidine ring opening + hydroxylation	280.1906	$C_{16}H_{26}NO_3$	–	ND	ND	D
M10	Dihydroxylation	294.1699	$C_{16}H_{24}NO_4$	6.3	D	D	D^M
M11	*O*-Demethylation + sulfation	328.1213	$C_{15}H_{22}NO_5S$	4.4	D	D	ND
M12	*O*-Demethylation + glucuronidation	424.1965	$C_{21}H_{30}NO_8$	3.1	D	D	ND
References							Ellefsen et al. (2016)

Table 5
Metabolites identified in pS9, pHLM/pHLC incubations or reported in literature for 25-I-NBOMe in PHH incubations or human urine (RT = retention time, – = no RT available, D = detected, ND = not detected). The three most abundant metabolites detected in pHLM/pHLC, pS9, PHH samples after an incubation time of 180 min or in human urine after unknown dose and time of consumptions are marked with an M, if the data is available in the literature. Metabolites are listed according to increasing mass.

Metabolite ID	Metabolic Reaction	*m/z*	Formula	RT, min	pS9	pHLM/pHLC	PHH	HU	
	Parent compound	428.0717	$C_{18}H_{23}INO_3$	9.4	D	D	D	D	D
M1	*N*-Dealkylation	308.0141	$C_{10}H_{15}INO_2$	6.5	D^M	D^M	D	ND	D
M2	Demethylation (phenyl)	414.0560	$C_{17}H_{21}INO_3$	8.3	D	D	D	D^M	D
M3	Demethylation (phenyl)	414.0560	$C_{17}H_{21}INO_3$	8.4	D^M	D^M	D	D	D
M4	Demethylation (NBOMe)	414.0560	$C_{17}H_{21}INO_3$	8.7	D^M	D^M	D^M	ND	D
M5	Demethylation (NBOMe) + hydroxylation (NBOMe)	430.0509	$C_{17}H_{21}INO_4$	–	ND	ND	D	D	D
M6	Carboxylation	442.0509	$C_{18}H_{21}INO_4$	–	ND	ND	D	ND	ND
M7	Hydroxylation (NBOMe)	444.0666	$C_{18}H_{23}INO_4$	8.5	D	D	D	D	D
M8	Hydroylation (phenyl)	444.0666	$C_{18}H_{23}INO_4$	9.0	D	D	ND	ND	D
M9	*N*-Oxidation	444.0666	$C_{18}H_{23}INO_4$	–	ND	ND	D	ND	ND
M10	Demethylation (phenyl) + sulfation	494.0128	$C_{17}H_{21}INO_6S$	8.1	D	D	D	D^M	D
M11	Di-demethylation (phenyl/NBOMe) + glucuronidation	576.0727	$C_{22}H_{27}INO_9$	–	ND	ND	D	D	D
M12	Demethylation (phenyl) + glucuronidation	590.0881	$C_{23}H_{29}INO_9$	7.2	D	D	D^M	D^M	D
M13	Demethylation (phenyl) + glucuronidation	590.0881	$C_{23}H_{29}INO_9$	7.3	D	D	D	ND	D
M14	Demethylation (NBOMe) + glucuronidation	590.0881	$C_{23}H_{29}INO_9$	–	ND	ND	D^M	ND	D
M15	Demethylation (NBOMe) + hydroxylation (NBOMe) + glucuronidation	606.0830	$C_{23}H_{29}INO_{10}$	–	ND	ND	D	ND	D
M16	Hydroxylation (NBOMe) + glucuronidation	620.0987	$C_{24}H_{31}INO_{10}$	–	ND	ND	D	D	D
References							Wohlfarth et al. (2017)	Wohlfarth et al. (2017)	Caspar et al. (2015)

Table 6
Metabolites identified in pS9, pHLM/pHLC incubations or reported in literature for meclonazepam in PHH incubations or human urine (RT = retention time, D = detected, ND = not detected). The two most abundant metabolites detected in pHLM/pHLC, pS9, samples after an incubation time of 360 min or in PHH after an incubation time of 300 min or in human urine after unknown dose and time of consumptions are marked with an M. Metabolites are listed according to increasing mass.

Metabolite ID	Metabolic Reaction	*m/z*	Formula	RT, min	pS9	pHLM/pHLC	PHH	HU	
	Parent compound	330.0639	$C_{16}H_{13}ClN_3O_3$	9.6	D	D	D	D	D
M1	Reduction	300.0898	$C_{16}H_{15}ClN_3O$	6.0	D^M	D^M	D^M	D^M	D^M
M2	Reduction + acetylation	342.1003	$C_{18}H_{17}ClN_3O_2$	6.9	D^M	D^M	D^M	D^M	D^M
M3	Hydroxylation	346.0589	$C_{16}H_{13}ClN_3O_4$	3.5	D	D	D	ND	D
References							Vikingsson et al. (2017)	Meyer et al. (2016)	Vikingsson et al. (2017)

2.3. Smoke condensate for in vitro incubations

Based according to previous studies (Franz et al., 2017, 2016), Damania plant material (50 mg) was sprayed with 150 mL of a methanol solution of 3 mg/mL XLR-11. After drying overnight at room temperature, the fortified plant material was filled in a pipe and burned down twice in about 30 s using a tube connected to a 100 mL syringe filled with 1 mL methanol. Presence of XLR-11 and its thermal degradant were verified by LC-HR-MS/MS. Blank samples were collected to confirm the absence of interfering compounds. Obtained smoke condensate solutions were used for in vitro incubations as described above.

2.4. Apparatus for analysis of metabolites

The processed samples were analyzed using a ThermoFisher

Table 7
Metabolites detected in pS9, pHLM/pHLC, or reported in PHH, and/or human urine.

Compound	pS9		pHLM/pHLC		PHH		HU	
	Phase I	Phase II	Phase I	Phase II	Phase I	Phase II	Phase I	Phase II
XLR-11	6	8	6	9	14	16	11	0*
					Wohlfarth et al. (2013)			
XLR-11 degradant	7	8	5	8	–	–		
							Kanamori et al. (2015)	
AB-PINACA	9	4	9	5	19	4	19	4
					Wohlfarth et al. (2015)		Wohlfarth et al. (2015)	
FUB-PB-22	3	1	3	1	5	2	2	2
					Diao et al. (2016)		Diao et al. (2016)	
4-Methoxy-α-PVP	4	2	4	2	10	0	–	–
					Ellefsen et al. (2016)			
25-I-NBOMe	7	2	7	2	10	5	6	2
					Wohlfarth et al. (2017)		Wohlfarth et al. (2017)	
							9	5
							Caspar et al. (2015)	
Meclonazepam	2	1	2	1	2	1	2	1
					Vikingsson et al. (2017)		Vikingsson et al. (2017)	
							1	1
							Meyer et al. (2016)	

* = only data after urine hydrolysis available, – = data not available.

Scientific (TF, Dreieich, Germany) Dionex UltiMate 3000 RS pump consisting of a degasser, a quaternary pump and an UltiMate autosampler, coupled to a TF Q-Exactive Plus system equipped with a heated electrospray ionization (HESI)-II source (Helfer et al., 2015; Richter et al., 2016, 2017). Mass calibration was done prior to analysis according to the manufacturer's recommendations using external mass calibration.

Gradient elution was performed on a TF Accucore PhenylHexyl column (100 mm × 2.1 mm, 2.6 µm). The mobile phases consisted of 2 mM aqueous ammonium formate containing acetonitrile (1%, v/v) and formic acid (0.1%, v/v, pH 3, eluent A) and ammonium formate solution with acetonitrile:methanol (1:1, v/v) containing water (1%, v/v) and formic acid (0.1%, v/v, eluent B). The flow rate was set to 500 µL/min using the following gradient: 0–1.0 min 99% A, 1–18.5 min to 99% A, 18.5–19.5 min hold 1% A, 19.5–20.5 min hold 99% A. The HESI-II source conditions were as follows: ionization mode, positive; sheath gas, 53 AU; auxiliary gas, 14 AU; sweep gas, 3 AU; spray voltage, 3.50 kV; heater temperature, 438 °C; ion transfer capillary temperature, 320 °C; and S-lens RF level, 60.0. Mass spectrometry was performed using full scan data and a subsequent data-dependent acquisition (DDA) with priority to mass to charge ratios (m/z) of parent compounds and their expected metabolites.

The settings for FS data acquisition were as follows: resolution, 35,000; microscans, 1; automatic gain control (AGC) target, 1e6; maximum injection time, 120 ms; and scan range, m/z 50–750. The settings for the DDA mode with an inclusion list for substrates and the expected metabolites were as follows: option "pick others", enabled, dynamic exclusion, 1 s; resolution, 17,500; microscans, 1; loop count, 5; AGC target, 2e4; maximum injection time, 250 ms; isolation window, m/z 1.0; high collision dissociation (HCD) with stepped normalized collision energy (NCE), 17.5, 35, and 52.5%; spectrum data type, profile; and underfill ratio, 1%. The inclusion list contained m/z values of metabolites, which were already described in the literature and metabolites, which were likely to be formed such as hydroxy, oxo, carboxy, dihydro, and dealkyl metabolites (phase I) as well as sulfates, glucuronides, *N*-acetyl, and GSH-conjugated metabolites (phase II), and combinations of them. ChemSketch 2016 1.1 (ACD/Labs, Toronto, Canada) was used to draw structures of hypothetical metabolites and to calculate the exact masses. Xcalibur Qual Browser software version 3.0.63 was used for data handling. The obtained MS^2 spectra were compared to published LC-HR-MS/MS spectra (Caspar et al., 2015; Diao et al., 2016; Ellefsen et al., 2016; Kanamori et al., 2015; Vikingsson et al., 2017; Wohlfarth et al., 2015, 2013, 2017).

3. Results and discussion

Although PHH were expected to provide the most authentic spectrum of human metabolites (Wohlfarth et al., 2013), alternative in vitro systems such as pHLM, pHLC, or pS9 were already frequently used (Kittler et al., 2014) for identifying phase I (Caspar et al., 2015; Michely et al., 2015; Welter et al., 2015), but also phase II metabolites after addition of the corresponding co-substrates (Meyer and Maurer, 2009; Negreira et al., 2015; Richter et al., 2017; Schwaninger et al., 2009; Strano-Rossi et al., 2010).

Also for developing toxicological screening procedures, it is of outmost importance to identify the main urinary excretion products being the analytical targets. As already mentioned, LC–MS approaches without conjugate cleavage were used more and more (Helfer et al., 2015; Maurer et al., 2016; Wissenbach et al., 2011) and thus phase II metabolism has gained increasing attention in such in vitro metabolism studies (Richter et al., 2017).

In previous studies, incubations using pS9 or a combination of pHLM and pHLC after addition of co-substrates for main metabolic reactions were shown to be a more cost-efficient alternative to cell line based systems. So far, no comparison with PHH was done in the context of metabolism studies for toxicological screening procedures. Therefore, six NPS from different drug classes with published data on their metabolism in PHH using cryopreserved human hepatocytes from a 10 donor pool, except of the XLR-11 study (three donor pool), were selected and results compared to evaluate whether human liver preparations might be a suitable alternative for identification of main urinary excretion products. If possible, similar substrate concentrations, incubation times, sample preparations, and analytical strategies were chosen as in the studies using PHH. If incubations and authentic human urine samples in the already published data were investigated before and/or after hydrolysis, only results before hydrolysis were used for comparison.

3.1. XLR-11

Two different substrates were used. First, XLR-11 for comparison with previously published PHH data (Wohlfarth et al., 2013) and second XLR-11 thermal degradant as human urinary metabolites were described for this compound, too (Adamowicz et al., 2013; Grigoryev

et al., 2013; Kanamori et al., 2015). This is also of interest for developing toxicological urine screenings as synthetic cannabinoids are usually smoked (Kanamori et al., 2015; Wohlfarth et al., 2013). It is likely that thermal degradation products and/or their metabolites can be found in human urine.

Wohlfarth et al. (2013) identified 14 phase I and 16 phase II metabolites in PHH and Kanamori et al. (2015) described 11 phase I metabolites in human urine after hydrolysis. The three most abundant metabolites in human urine were originated from the thermal degradant of XLR-11. The parent compound XLR-11 and its thermal degradant were not detected in human urine.

The pS9 incubations allowed identification of six phase I and eight phase II metabolites of XLR-11 and two phase I and three phase II metabolites of thermal degradant. The pHLM/pHLC incubations formed six phase I and nine phase II metabolites and four phase I and three phase II metabolites, respectively (Table 1). Hence, pS9 and pHLM/pHLC were comparable in number and abundance of metabolites as shown in Supplementary Fig. 1 (Sup. Fig. 1). The oxidative defluorinated thermal degradant of XLR-11 (TDM1) and the oxidative defluorinated to carboxylic acid thermal degradant of XLR-11 (TDM2) were the most abundant metabolites, which is in accordance to human urine studies.

3.2. AB-PINACA

AB-PINCA is a synthetic cannabinoid, which is extensively metabolized and the predominate biotransformation in PHH was the terminal carboxamide hydrolysis to AB-PINACA carboxylic acid (M2) (Wohlfarth et al., 2015). Besides M2, carbonyl AB-PINACA (M3) and hydroxypentyl AB-PINACA (M5) were the most abundant metabolites in PHH after 60 and 180 min incubation time. Two hydroxylated AB-PINACA metabolites were detected only as glucuronides in human urine (Wohlfarth et al., 2015). Therefore, phase II metabolism in in vitro studies should be encouraged in the case of missing conjugate cleavage prior to analysis. In addition, AB-PINACA was detected only at low amounts or could not be detected in urine (Wohlfarth et al., 2015), which again underlined the importance of metabolism studies also for developing toxicological urine screenings.

M2, M3, and M5 were also the most abundant metabolites in pS9 and pHLM/pHLC after an incubation time of 30 min and after 360 min, M2 became more abundant then the parent compound (Sup. Fig. 2). The carbonyl AB-PINACA carboxylic acid glucuronide metabolite (M23) was detected in pHLM/pHLC but not in pS9. Overall peak area ratios increased faster in pHLM/pHLC incubations than in pS9, which is probably due to a generally higher enzyme activity in pHLM in contrast to pS9 fraction (Brandon et al., 2003; Richter et al., 2017; Zhang et al., 2012). Not all metabolites described for PHH were detected in pHLM/pHLC or pS9 incubations but all metabolites, most abundant in human urine (M2, M11, and M4) (Wohlfarth et al., 2015), were detected in both alternative in vitro models (Table 2).

3.3. FUB-PB-22

Seven metabolites were detected in PHH (Diao et al., 2016) and five metabolites in pS9 and pHLM/pHLC incubations (Table 3). The glucuronide of the carboxylic acid after ester hydrolysis of FUB-PB-22 (M7) and the hydroxylated glucuronide of the carboxylic acid after ester hydrolysis (M8) were the most abundant metabolites in human urine (Diao et al., 2016). M7 was one of the most abundant metabolites in all in vitro models, too (Sup. Fig. 3). M8 could not be detected in pS9 or pHLM/pHLC incubations but in the incubations with PHH most likely due to a too low formation rate in the liver preparations. Differences of in vitro and in vivo models such as reuptake, efflux transports, and excretion may influence the relative abundance of the metabolites, but this would only explain the difference between pS9, pHLM/pHLC, and human urine.

3.4. 4-Methoxy-α-PVP

The most abundant metabolite in PHH samples was 4-hydroxy-α-PVP (M2) (Ellefsen et al., 2016), which was the same in pS9 and pHLM/pHLC incubations (Table 4; Sup. Fig. 4). In addition, a sulfate (M11) and a glucuronide (M12) of M2 were detected in pS9 and pHLM/pHLC, for incubations using PHH one glucuronide was mentioned but not described of which phase I metabolite and no MS spectrum was obtained (Ellefsen et al., 2016). Further metabolites such as carboxy (M6), hydroxy (M7), and dihydroxy (M10) were detected in pS9, pHLM/pHLC, and PHH. The dihydro metabolite (M5) was not detected in pS9 and pHLM/pHLC incubations. Interestingly, previous studies on β-keto compounds showed that reduction of the β-keto group could also not be observed using pHLM (Richter et al., 2017; Takayama et al., 2014). Unfortunately, no metabolism studies using human urine samples were published so far.

3.5. 25-I-NBOMe

The dominant phase I biotransformation step observed in PHH and human urine was the *O*-demethylation at the NBOMe moiety (M4) (Caspar et al., 2015; Wohlfarth et al., 2017). Most phase I metabolites were conjugated with sulfate or glucuronic acid. Further metabolic steps were hydroxylation, *N*-dealkylation, and combinations thereof (Wohlfarth et al., 2017). Wohlfarth et al. (2017) and Caspar et al. (2015) found eight and 13 metabolites in human urine, respectively, which were the same as those in PHH.

Similar metabolic patterns were obtained after pS9 and pHLM/pHLC incubations (Table 5), but only nine metabolites could be detected in contrast to 15 observed in PHH (Table 5). However, the most abundant metabolites in human urine (M2, M3, and M12), which should be used as targets for toxicological urine screenings, were also detected in pS9 and pHLM/pHLC incubations.

3.6. Meclonazepam

Main human urinary excretion products of meclonazepam were described to be 7-amino-meclonazepam (M2) and 7-acetamino-meclonazepam (M3) (Meyer et al., 2016; Vikingsson et al., 2017). Both were detected in pS9 and pHLM/pHLC incubations in addition to a hydroxy metabolite (M1) already described for pHLM incubations (Huppertz et al., 2015) (Table 6). 7-Acetamino-meclonazepam (M3) was detected after an incubation time of 120 min and the peak area ratio increased until 480 min (Sup. Fig. 6). This supported again the recommendation for choosing two incubation time points, one for initial metabolic steps and one for late phase metabolites (Richter et al., 2017). In incubations with PHH, only M2 and M3 were detected (Vikingsson et al., 2017). Thus, PHH provided no benefit in the case of meclonazepam. In incubations using only pHLM, M3 was not detected (Huppertz et al., 2015; Vikingsson et al., 2017) as NAT1 and NAT2 are cytosolic enzymes (Jancova et al., 2010). Therefore, pS9 or a combination of pHLM and pHLC together with the co-substrates for *N*-acetylation were of benefit in this case.

3.7. Are pS9 or pHLM/pHLC incubations a sufficient alternative to PHH?

The aim of this study was to assess whether through incubations with pS9 or pHLM/pHLC might be a sufficient, easy to handle, and more cost-efficient alternative to PHH for metabolism studies of NPS. The knowledge about the main urinary excretion products in human urine are also important for developing toxicological urine screenings. Therefore, the way of consumption of the investigated compounds should also be considered, as exemplified for XLR-11. Comparison of the identified metabolites of six selected NPS using either PHH, human urine, pS9, or pHLM/pHLC showed that results using pS9 or pHLM/pHLC were comparable. Therefore, it might be recommended to use the

slightly cheaper pS9 fraction instead of a pHLM/pHLC combination. As expected, formation of some metabolites, particularly those after multi-step reactions needed a longer incubation time than the initial metabolites (Sup. Figs. 1–6). Therefore, two sampling points at 60 and 360 min should be recommended. However, incubations using human liver preparations resulted in a lower number of total detected metabolites compared to PHH. An overview of the detected metabolites in the different models is given in Table 7. Although less metabolites were detected in human liver preparations they were still able to allow the identification of the main human urinary excretion products. Thus, human liver preparations can be used as more cost-efficient alternative to PHH for NPS, despite the described limitations of in vitro models.

4. Conclusion

The metabolism of six NPS was re-investigated using human liver preparations after addition of co-substrates for the main metabolic phase I and II reactions. Results were compared to studies using PHH or to human urine. The pS9 fraction was identified as most cost-efficient but still sufficient in vitro alternative to PHH for developing toxicological urine screenings for NPS. The setting allowed the identification of an appropriate number of phase I and phase II metabolites.

Conflict of interest

The authors declare that they have no conflict of interest.

Acknowledgements

The authors like to thank Achim T. Caspar, Sascha K. Manier, Julian A. Michely, Lea Wagmann, and Armin A. Weber for their support and fruitful discussion.

Appendix A. Supplementary data

Supplementary data associated with this article can be found, in the online version, at http://dx.doi.org/10.1016/j.toxlet.2017.07.901.

References

Adamowicz, P., Zuba, D., Sekula, K., 2013. Analysis of UR-144 and its pyrolysis product in blood and their metabolites in urine. Forensic Sci. Int. 233, 320–327.
Adamowicz, P., Gieron, J., Gil, D., Lechowicz, W., Skulska, A., Tokarczyk, B., 2016. The prevalence of new psychoactive substances in biological material—a three-year review of casework in Poland. Drug Test Anal. 8, 63–70.
Antherieu, S., Chesne, C., Li, R., Guguen-Guillouzo, C., Guillouzo, A., 2012. Optimization of the HepaRG cell model for drug metabolism and toxicity studies. Toxicol. In Vitro 26, 1278–1285.
Brandon, E.F., Raap, C.D., Meijerman, I., Beijnen, J.H., Schellens, J.H., 2003. An update on in vitro test methods in human hepatic drug biotransformation research: pros and cons. Toxicol. Appl. Pharmacol. 189, 233–246.
Caspar, A.T., Helfer, A.G., Michely, J.A., Auwarter, V., Brandt, S.D., Meyer, M.R., Maurer, H.H., 2015. Studies on the metabolism and toxicological detection of the new psychoactive designer drug 2-(4-iodo-2,5-dimethoxyphenyl)-N-[(2-methoxyphenyl)methyl]ethanamine (25I-NBOMe) in human and rat urine using GC–MS, LC-MS(n), and LC-HR-MS/MS. Anal. Bioanal. Chem. 407, 6697–6719.
Caspar, A.T., Brandt, S.D., Stoever, A.E., Meyer, M.R., Maurer, H.H., 2017. Metabolic fate and detectability of the new psychoactive substances 2-(4-bromo-2,5-dimethoxyphenyl)-N-[(2-methoxyphenyl)methyl]ethanamine (25B-NBOMe) and 2-(4-chloro-2,5-dimethoxyphenyl)-N-[(2-methoxyphenyl)methyl]ethanamine (25C-NBOMe) in human and rat urine by GC–MS, LC-MSn, and LC-HR-MS/MS approaches. J. Pharm. Biomed. Anal. 134, 158–169.
Diao, X., Scheidweiler, K.B., Wohlfarth, A., Pang, S., Kronstrand, R., Huestis, M.A., 2016. In vitro and in vivo human metabolism of synthetic cannabinoids FDU-PB-22 and FUB-PB-22. AAPS J. 18, 455–464.
Dias-da-Silva, D., Arbo, M.D., Valente, M.J., Bastos, M.L., Carmo, H., 2015. Hepatotoxicity of piperazine designer drugs: comparison of different in vitro models. Toxicol. In Vitro 29, 987–996.
Ellefsen, K.N., Wohlfarth, A., Swortwood, M.J., Diao, X., Concheiro, M., Huestis, M.A., 2016. 4-Methoxy-alpha-PVP: in silico prediction, metabolic stability, and metabolite identification by human hepatocyte incubation and high-resolution mass spectrometry. Forensic Toxicol. 34, 61–75.
Franz, F., Angerer, V., Hermanns-Clausen, M., Auwarter, V., Moosmann, B., 2016. Metabolites of synthetic cannabinoids in hair-proof of consumption or false friends for interpretation? Anal. Bioanal. Chem. 408, 3445–3452.
Franz, F., Angerer, V., Brandt, S.D., McLaughlin, G., Kavanagh, P.V., Moosmann, B., Auwarter, V., 2017. In vitro metabolism of the synthetic cannabinoid 3,5-AB-CHMFUPPYCA and its 5,3-regioisomer and investigation of their thermal stability. Drug Test Anal. 9, 311–316.
Gerets, H.H., Tilmant, K., Gerin, B., Chanteux, H., Depelchin, B.O., Dhalluin, S., Atienzar, F.A., 2012. Characterization of primary human hepatocytes, HepG2 cells, and HepaRG cells at the mRNA level and CYP activity in response to inducers and their predictivity for the detection of human hepatotoxins. Cell Biol. Toxicol. 28, 69–87.
Grigoryev, A., Kavanagh, P., Melnik, A., Savchuk, S., Simonov, A., 2013. Gas and liquid chromatography-mass spectrometry detection of the urinary metabolites of UR-144 and its major pyrolysis product. J. Anal. Toxicol. 37, 265–276.
Helfer, A.G., Michely, J.A., Weber, A.A., Meyer, M.R., Maurer, H.H., 2015. Orbitrap technology for comprehensive metabolite-based liquid chromatographic-high resolution-tandem mass spectrometric urine drug screening – exemplified for cardiovascular drugs. Anal. Chim. Acta 891, 221–233.
Huppertz, L.M., Bisel, P., Westphal, F., Franz, F., Auwarter, V., Moosmann, B., 2015. Characterization of the four designer benzodiazepines clonazolam, deschloroetizolam, flubromazolam, and meclonazepam, and identification of their in vitro metabolites. Forensic Toxicol. 33, 388–395.
Jancova, P., Anzenbacher, P., Anzenbacherova, E., 2010. Phase II drug metabolizing enzymes. Biomed. Pap. Med. Fac. Univ. Palacky Olomouc Czech Repub. 154, 103–116.
Kanamori, T., Kanda, K., Yamamuro, T., Kuwayama, K., Tsujikawa, K., Iwata, Y.T., Inoue, H., 2015. Detection of main metabolites of XLR-11 and its thermal degradation product in human hepatoma HepaRG cells and human urine. Drug Test Anal. 7, 341–345.
Kanebratt, K.P., Andersson, T.B., 2008. HepaRG cells as an in vitro model for evaluation of cytochrome P450 induction in humans. Drug Metab. Dispos. 36, 137–145.
Khaled, S.M., Hughes, E., Bressington, D., Zolezzi, M., Radwan, A., Badnapurkar, A., Gray, R., 2016. The prevalence of novel psychoactive substances (NPS) use in non-clinical populations: a systematic review protocol. Syst. Rev. 5, 195.
Kittler, K., Fessard, V., Maul, R., Hurtaud-Pessel, D., 2014. CYP3A4 activity reduces the cytotoxic effects of okadaic acid in HepaRG cells. Arch. Toxicol. 88, 1519–1526.
Li, A.P., Maurel, P., Gomez-Lechon, M.J., Cheng, L.C., Jurima-Romet, M., 1997. Preclinical evaluation of drug–drug interaction potential: present status of the application of primary human hepatocytes in the evaluation of cytochrome P450 induction. Chem. Biol. Interact. 107, 5–16.
Maurer, H.H., Meyer, M.R., 2016. High-resolution mass spectrometry in toxicology: current status and future perspectives. Arch. Toxicol. 90, 2161–2172.
Maurer, H.H., Pfleger, K., Weber, A.A., 2016. Mass Spectral Data of Drugs, Poisons, Pesticides, Pollutants and Their Metabolites. Wiley-VCH, Weinheim.
Meyer, M.R., Maurer, H.H., 2009. Enantioselectivity in the methylation of the catecholic phase I metabolites of methylenedioxy designer drugs and their capability to inhibit catechol-O-methyltransferase-catalyzed dopamine 3-methylation. Chem. Res. Toxicol. 22, 1205–1211.
Meyer, M.R., Bergstrand, M.P., Helander, A., Beck, O., 2016. Identification of main human urinary metabolites of the designer nitrobenzodiazepines clonazolam, meclonazepam, and nifoxipam by nano-liquid chromatography-high-resolution mass spectrometry for drug testing purposes. Anal. Bioanal. Chem. 408, 3571–3591.
Michely, J.A., Helfer, A.G., Brandt, S.D., Meyer, M.R., Maurer, H.H., 2015. Metabolism of the new psychoactive substances N,N-diallyltryptamine (DALT) and 5-methoxy-DALT and their detectability in urine by GC–MS, LC-MSn, and LC-HR-MS-MS. Anal. Bioanal. Chem. 407, 7831–7842.
Negreira, N., Erratico, C., Kosjek, T., van Nuijs, A.L., Heath, E., Neels, H., Covaci, A., 2015. In vitro Phase I and Phase II metabolism of alpha-pyrrolidinovalerophenone (alpha-PVP), methylenedioxypyrovalerone (MDPV) and methedrone by human liver microsomes and human liver cytosol. Anal. Bioanal. Chem. 407, 5803–5816.
Peters, F.T., Meyer, M.R., 2011. In vitro approaches to studying the metabolism of new psychoactive compounds. Drug Test Anal. 3, 483–495.
Richter, L.H., Kaminski, Y.R., Noor, F., Meyer, M.R., Maurer, H.H., 2016. Metabolic fate of desomorphine elucidated using rat urine, pooled human liver preparations, and human hepatocyte cultures as well as its detectability using standard urine screening approaches. Anal. Bioanal. Chem. 408, 6283–6294.
Richter, L.H.J., Flockerzi, V., Maurer, H.H., Meyer, M.R., 2017. Pooled human liver preparations, HepaRG, or HepG2 cell lines for metabolism studies of new psychoactive substances? A study using MDMA, MDBD, butylone, MDPPP, MDPV, MDPB, 5-MAPB, and 5-API as examples. J. Pharm. Biomed. Anal. 143, 32–42.
Rodrigues, R.M., Heymans, A., De Boe, V., Sachinidis, A., Chaudhari, U., Govaere, O., Roskams, T., Vanhaecke, T., Rogiers, V., De Kock, J., 2016. Toxicogenomics-based prediction of acetaminophen-induced liver injury using human hepatic cell systems. Toxicol. Lett. 240, 50–59.
Schwaninger, A.E., Meyer, M.R., Zapp, J., Maurer, H.H., 2009. The role of human UDP-glucuronyltransferases on the formation of the methylenedioxymethamphetamine (ecstasy) phase II metabolites R- and S-3-methoxymethamphetamine 4-O-glucuronides. Drug Metab. Dispos. 37, 2212–2220.
Strano-Rossi, S., Cadwallader, A.B., de la Torre, X., Botre, F., 2010. Toxicological determination and in vitro metabolism of the designer drug methylenedioxypyrovalerone (MDPV) by gas chromatography/mass spectrometry and liquid chromatography/quadrupole time-of-flight mass spectrometry. Rapid Commun. Mass Spectrom. 24, 2706–2714.
Takayama, T., Suzuki, M., Todoroki, K., Inoue, K., Min, J.Z., Kikura-Hanajiri, R., Goda, Y., Toyo'oka, T., 2014. UPLC/ESI–MS/MS-based determination of metabolism of several new illicit drugs, ADB-FUBINACA, AB-FUBINACA, AB-PINACA, QUPIC, 5F-QUPIC and alpha-PVT, by human liver microsome. Biomed. Chromatogr. 28, 831–838.

UNODC, 2016. World Drug Report 2016. United Nations publication Sales No. E.16. XI.7.
Vikingsson, S., Wohlfarth, A., Andersson, M., Green, H., Roman, M., Josefsson, M., Kugelberg, F.C., Kronstrand, R., 2017. Identifying metabolites of meclonazepam by high-resolution mass spectrometry using human liver microsomes, hepatocytes, a mouse model, and authentic urine samples. AAPS J. 19, 736–742.
Welter, J., Kavanagh, P., Meyer, M.R., Maurer, H.H., 2015. Benzofuran analogues of amphetamine and methamphetamine: studies on the metabolism and toxicological analysis of 5-APB and 5-MAPB in urine and plasma using GC–MS and LC-(HR)-MS(n) techniques. Anal. Bioanal. Chem. 407, 1371–1388.
Wissenbach, D.K., Meyer, M.R., Remane, D., Philipp, A.A., Weber, A.A., Maurer, H.H., 2011. Drugs of abuse screening in urine as part of a metabolite-based LC-MSn screening concept. Anal. Bioanal. Chem. 400, 3481–3489.
Wohlfarth, A., Pang, S., Zhu, M., Gandhi, A.S., Scheidweiler, K.B., Liu, H.F., Huestis, M.A., 2013. First metabolic profile of XLR-11, a novel synthetic cannabinoid, obtained by using human hepatocytes and high-resolution mass spectrometry. Clin. Chem. 59, 1638–1648.
Wohlfarth, A., Castaneto, M.S., Zhu, M., Pang, S., Scheidweiler, K.B., Kronstrand, R., Huestis, M.A., 2015. Pentylindole/pentylindazole synthetic cannabinoids and their 5-fluoro analogs produce different primary metabolites: metabolite profiling for AB-PINACA and 5F-AB-PINACA. AAPS J. 17, 660–677.
Wohlfarth, A., Roman, M., Andersson, M., Kugelberg, F.C., Diao, X., Carlier, J., Eriksson, C., Wu, X., Konradsson, P., Josefsson, M., Huestis, M.A., Kronstrand, R., 2017. 25C-NBOMe and 25I-NBOMe metabolite studies in human hepatocytes, in vivo mouse and human urine with high-resolution mass spectrometry. Drug Test Anal. 9, 680–698.
Zhang, D., Luo, G., Ding, X., Lu, C., 2012. Preclinical experimental models of drug metabolism and disposition in drug discovery and development. Acta Pharm. Sin. B 2, 549–561.

4. DISCUSSION AND CONCLUSION

4.1 BEST SUITED IN VITRO MODEL FOR IDENTIFYING MAIN URINARY EXCRETION PRODUCTS AS TARGETS FOR TOXICOLOGICAL URINE SCREENING PROCEDURES

Metabolic fate of desomorphine was investigated using rat urine, pHLM in combination with pHLC adding co-substrates for oxidation, glucuronidation, and sulfation, and the human hepatic cell lines HepG2 and HepaRG. Nordesomorphine, desomorphine-*N*-oxide, hydroxydesomorphine (isomer 1-5), desomorphine sulfate, nordesomorphine glucuronide, desomorphine glucuronide, and desomorphine-*N*-oxide glucuronide could be identified by LC-HR-MS/MS. A sufficient separation of desomorphine-*N*-oxide and hydroxydesomorphine isomer 1-5 was achieved by hydrophilic interaction liquid chromatography (HILIC). All phase I metabolic steps were exclusively catalyzed by CYP3A4. For the glucuronidation of the parent compound, UGT1A1, UGT1A8, UGT1A9, UGT1A10, UGT2B4, UGT2B7, UGT2B15, and UGT2B17 were responsible. Differences could be observed between the different in vivo and in vitro models for the formation of hydroxydesomorphine isomers 1-5 and metabolites formed by multiple metabolic steps. However, all investigated models were able to identify desomorphine glucuronide as the relatively most abundant metabolite. Desomorphine and desomorphine glucuronide were identified as sufficient targets for standard urine screening approaches (SUSAs). All investigated in vitro models provided results, which indicated that they were able to replace rat in vivo studies for identifying main targets for SUSAs; of course with the limitations of in vitro models such as lack of reabsorption, entero-hepatic circulation,

or renal elimination. Due to peak area ratios and number of formed metabolites, HepaRG seemed to be the most promising cell line, but further studies are needed for testing compounds, which are metabolized more extensively and for comparing those data with human in vivo data. To verify the best suited in vitro model, comparative studies were performed. First of all, the assays using human liver preparations were optimized to cover all main metabolic phase I and II steps, namely oxidation, reduction, glucuronidation, sulfation, *O*-methylation, *N*-acetylation, and glutathione conjugation. There were two possibilities to include phase I and II metabolism, either using pS9 or using pHLM in combination with pHLC (pHLM/pHLC). For both, the addition of all co-substrates for the main metabolic reactions was necessary. The applicability was tested by using model substrates and showed convincing evidence. Afterwards six methylenedioxy derivatives and two bioisosteric analogs (MDMA, MBDB, butylone, MDPPP, MDPV, MDPB, 5-MAPB, and 5-API) were chosen for an exemplified comparison of human liver preparations with the human hepatic cell lines HepG2 and HepaRG. To test the correlation of the in vitro to in vivo data, human urine was also included if available. Methylenedioxy derivatives were chosen for two reasons. First, they are extensively metabolized by various metabolic reactions and second, CYP2D6 is often mainly involved in phase I metabolism. As CYP2D6 showed low gene expression in HepaRG cells, this can limit their applicability. For all compounds, the metabolism was re-investigated, except for 5-API, where no data existed, yet, and thus its metabolism was investigated for the first time. Outcomes for human liver preparations and HepaRG were comparable. As expected, due to the low gene expression for phase I metabolizing enzymes in HepG2 cells, these cell line provided worse results compared to HepaRG considering total number and total abundance of metabolites. Known main human urinary

excretion products were detected in human liver preparations and HepaRG incubations. HepaRG formed slightly more metabolites than pS9 or pHLM/pHLC. Therefore, human liver preparations should be the best choice particularly for laboratories without special equipment needed for cell handling. Hence, human liver preparations were identified as best alternative in vitro model, a comparison with PHH, which are considered as gold standard for in vitro metabolism studies, was performed. As already mentioned, PHH have some disadvantages such as high costs, limited availability, differences in cell viability, and variability in the expression and activity of metabolizing enzymes.[20,21,32] A cost-efficient, easy to handle, and reliable alternative would be desirable. Therefore, six NPS from different drug classes with existing data from metabolism studies using PHH were selected,[30,42-46] the three synthetic cannabinoids XLR-11, AB-PINACA, and FUB-PB-22, the pyrrolidinophenone 4-methoxy-α-PVP, the NBOMe derivative 25I-NBOMe, and the designer benzodiazepine meclonazepam. For all NPS except for 4-methoxy-α-PVP, human urine samples were already investigated.[42,44-49] Therefore, the main urinary excretion products used as targets for toxicological urine screenings were already known and considered for assessment of results. Metabolism of the six NPS was re-investigated using pS9 and pHLM/pHLC after addition of co-substrates for the main metabolic phase I and II reactions. Same substrate concentrations, incubation times, sample preparations, and analytical strategies were chosen as in the studies using PHH,[30,42-46] if possible. For synthetic cannabinoids, thermal degradation products should be considered as well, as these substances are usually smoked. These thermal degradation products and/or their metabolites could be found in human urine and are probably the main targets for toxicological urine screening procedures as described for XLR-11.[47] Thus, XLR-11 thermal degradant was also included in the

study, in contrast to the study using PHH, which investigated only XLR-11 itself. It is important to choose a sufficient in vitro model for metabolism studies and in addition to consider the way of consumption. All in all, 38 phase I and 26 phase II metabolites were identified using pS9, 36 phase I and 28 phase II using pHLM/pHLC, and 60 phase I and 28 phase II metabolites using PHH. Human liver preparations formed less metabolites than PHH, but main human urinary excretion products were always detected. The pS9 fraction was identified as most cost-efficient, easy to handle, but still sufficient in vitro model for developing toxicological urine screenings for NPS.

5. SUMMARY

Different in vitro models were investigated and compared as surrogate for human in vivo metabolism studies to identify main urinary excretion products for developing toxicological urine screenings for new psychoactive substances (NPS). Assays using human liver preparations, which covered all main metabolic phase I and II steps were developed. Human hepatic cell lines HepG2 and HepaRG were tested as an alternative in vitro model. As expected, metabolic competence of HepG2 cells was not sufficient enough. In contrast, HepaRG cells showed slightly better results than the assay using human liver preparations. However, cell lines have the disadvantage of requiring special equipment for cell culture handling. Therefore, pS9 fraction was identified as most cost-efficient and easiest to handle in vitro model, still sufficient enough for developing toxicological urine screenings for NPS, even in comparison to PHH, the known gold standard for in vitro metabolism studies.

6. REFERENCES

1. Staack RF, Maurer HH. Metabolism of designer drugs of abuse. *Curr Drug Metab.* 2005;6(3):259-274.
2. Maurer H, Kraemer T, Springer D, Staack R. Chemistry, pharmacology, toxicology, and hepatic metabolism of designer drugs of the amphetamine (ecstasy), piperazine, and pyrrolidinophenone types - A synopsis. *Therapeutic Drug Monitoring.* 2004;26(2):127-131.
3. UN. United Nations - Single Convention on Narcotic Drugs. 1961.
4. EMCDDA. Reviewing legal aspects of substitution treatment at international level. 2000.
   HTTP://ELDD.EMCDDA.ORG/DATABASES/ELDD_COMPARATIVE_ANALYSES.CFM.
5. UNODC. World Drug Report. *United Nations publication.* 2016;Sales No. E.16.XI.7.
6. UNODC. World Drug Report. In: UNODC, ed: United Nations publication; 2017.
   HTTP://WWW.UNODC.ORG/WDR2017/
7. EMCDDA. European Drug Report 2017: Trends and Developments. *Publications of of the European Union.* 2017.
   HTTP://WWW.EMCDDA.EUROPA.EU/SYSTEM/FILES/PUBLICATIONS/4541/TDAT17001ENN.PDF.
8. Meyer MR. New psychoactive substances: an overview on recent publications on their toxicodynamics and toxicokinetics. *Arch Toxicol.* 2016;90(10):2421-2444.

9. Meyer MR, Maurer HH. Metabolism of designer drugs of abuse: an updated review. *Curr Drug Metab.* 2010;11(5):468-482.

10. EMCDDA. Germany - Country Drug Report 2017. In: Publications Office of the European Union; 2017. HTTP://WWW.EMCDDA.EUROPA.EU/SYSTEM/FILES/PUBLICATIONS/4541/TDAT17001ENN.PDF

11. Richter LHJ, Flockerzi V, Maurer HH, Meyer MR. Pooled human liver preparations, HepaRG, or HepG2 cell lines for metabolism studies of new psychoactive substances? A study using MDMA, MDBD, butylone, MDPPP, MDPV, MDPB, 5-MAPB, and 5-API as examples. *J Pharm Biomed Anal.* 2017;143:32-42.

12. Richter LHJ, Maurer HH, Meyer MR. New psychoactive substances: Studies on the metabolism of XLR-11, AB-PINACA, FUB-PB-22, 4-methoxy-alpha-PVP, 25-I-NBOMe, and meclonazepam using human liver preparations in comparison to primary human hepatocytes, and human urine. *Toxicol Lett.* 2017;280:142-150.

13. Wissenbach DK, Meyer MR, Remane D, Philipp AA, Weber AA, Maurer HH. Drugs of abuse screening in urine as part of a metabolite-based LC-MSn screening concept. *Anal Bioanal Chem.* 2011;400(10):3481-3489.

14. Wissenbach DK, Meyer MR, Remane D, Weber AA, Maurer HH. Development of the first metabolite-based LC-MS(n) urine drug screening procedure-exemplified for antidepressants. *Anal Bioanal Chem.* 2011;400(1):79-88.

15. Helfer AG, Michely JA, Weber AA, Meyer MR, Maurer HH. Orbitrap technology for comprehensive metabolite-based liquid chromatographic-high resolution-

tandem mass spectrometric urine drug screening - exemplified for cardiovascular drugs. *Anal Chim Acta.* 2015;891:221-233.

16. Meyer MR, Maurer HH. Review: LC coupled to low- and high-resolution mass spectrometry for new psychoactive substance screening in biological matrices - Where do we stand today? *Anal Chim Acta.* 2016;927:13-20.
17. Maurer HH, Meyer MR. High-resolution mass spectrometry in toxicology: current status and future perspectives. *Arch Toxicol.* 2016;90(9):2161-2172.
18. Diao X, Huestis MA. Approaches, Challenges, and Advances in Metabolism of New Synthetic Cannabinoids and Identification of Optimal Urinary Marker Metabolites. *Clin Pharmacol Ther.* 2017;101(2):239-253.
19. Dias-da-Silva D, Arbo MD, Valente MJ, Bastos ML, Carmo H. Hepatotoxicity of piperazine designer drugs: Comparison of different in vitro models. *Toxicol In Vitro.* 2015;29(5):987-996.
20. Kittler K, Fessard V, Maul R, Hurtaud-Pessel D. CYP3A4 activity reduces the cytotoxic effects of okadaic acid in HepaRG cells. *Arch Toxicol.* 2014;88(8):1519-1526.
21. Peters FT, Meyer MR. In vitro approaches to studying the metabolism of new psychoactive compounds. *Drug Test Anal.* 2011;3(7-8):483-495.
22. Zhang D, Luo G, Ding X, Lu C. Preclinical experimental models of drug metabolism and disposition in drug discovery and development. *Acta Pharmaceutica Sinica B.* 2012;2(6):549-561.
23. Wagmann L, Meyer MR, Maurer HH. What is the contribution of human FMO3 in the N-oxygenation of selected therapeutic drugs and drugs of abuse? *Toxicol Lett.* 2016;258:55-70.

24. Jancova P, Anzenbacher P, Anzenbacherova E. Phase II drug metabolizing enzymes. *Biomed Pap Med Fac Univ Palacky Olomouc Czech Repub.* 2010;154(2):103-116.

25. Meyer MR, Richter LH, Maurer HH. Methylenedioxy designer drugs: mass spectrometric characterization of their glutathione conjugates by means of liquid chromatography-high-resolution mass spectrometry/mass spectrometry and studies on their glutathionyl transferase inhibition potency. *Anal Chim Acta.* 2014;822:37-50.

26. Godoy P, Hewitt NJ, Albrecht U, et al. Recent advances in 2D and 3D in vitro systems using primary hepatocytes, alternative hepatocyte sources and non-parenchymal liver cells and their use in investigating mechanisms of hepatotoxicity, cell signaling and ADME. *Arch Toxicol.* 2013;87(8):1315-1530.

27. Antherieu S, Chesne C, Li R, Guguen-Guillouzo C, Guillouzo A. Optimization of the HepaRG cell model for drug metabolism and toxicity studies. *Toxicol In Vitro.* 2012;26(8):1278-1285.

28. Gerets HH, Tilmant K, Gerin B, et al. Characterization of primary human hepatocytes, HepG2 cells, and HepaRG cells at the mRNA level and CYP activity in response to inducers and their predictivity for the detection of human hepatotoxins. *Cell Biol Toxicol.* 2012;28(2):69-87.

29. Li AP, Maurel P, Gomez-Lechon MJ, Cheng LC, Jurima-Romet M. Preclinical evaluation of drug-drug interaction potential: present status of the application of primary human hepatocytes in the evaluation of cytochrome P450 induction. *Chem Biol Interact.* 1997;107(1-2):5-16.

30. Wohlfarth A, Pang S, Zhu M, et al. First metabolic profile of XLR-11, a novel synthetic cannabinoid, obtained by using human hepatocytes and high-resolution mass spectrometry. *Clin Chem.* 2013;59(11):1638-1648.

31. Castell JV, Jover R, Martinez-Jimenez CP, Gomez-Lechon MJ. Hepatocyte cell lines: their use, scope and limitations in drug metabolism studies. *Expert Opin Drug Metab Toxicol.* 2006;2(2):183-212.

32. Kanebratt KP, Andersson TB. HepaRG cells as an in vitro model for evaluation of cytochrome P450 induction in humans. *Drug Metab Dispos.* 2008;36(1):137-145.

33. Hart SN, Li Y, Nakamoto K, Subileau EA, Steen D, Zhong XB. A comparison of whole genome gene expression profiles of HepaRG cells and HepG2 cells to primary human hepatocytes and human liver tissues. *Drug Metab Dispos.* 2010;38(6):988-994.

34. Parent R, Marion MJ, Furio L, Trepo C, Petit MA. Origin and characterization of a human bipotent liver progenitor cell line. *Gastroenterology.* 2004;126(4):1147-1156.

35. Westerink WM, Schoonen WG. Phase II enzyme levels in HepG2 cells and cryopreserved primary human hepatocytes and their induction in HepG2 cells. *Toxicol In Vitro.* 2007;21(8):1592-1602.

36. Gripon P, Rumin S, Urban S, et al. Infection of a human hepatoma cell line by hepatitis B virus. *Proc Natl Acad Sci U S A.* 2002;99(24):15655-15660.

37. Maurer HH, Pfleger K, Weber AA. *Mass spectral data of drugs, poisons, pesticides, pollutants and their metabolites.* Weinheim: Wiley-VCH; 2016.

38. Maurer HH, Pfleger K, Weber AA. *Mass spectral library of drugs, poisons, pesticides, pollutants and their metabolites.* Weinheim, Germany: Wiley-VCH; 2016.

39. Maurer HH, Wissenbach DK, Weber AA. *Maurer/Wissenbach/Weber MWW LC-MSn library of drugs, poisons, and their metabolites.* Weinheim, Germany: Wiley-VCH; 2014.

40. Maurer HH, Meyer MR, Helfer AG, Weber AA. *Maurer/Meyer/Helfer/Weber MMHW LC-HR-MS/MS library of drugs, poisons, and their metabolites.* Weinheim, Germany: Wiley-VCH; 2017.

41. Richter LH, Kaminski YR, Noor F, Meyer MR, Maurer HH. Metabolic fate of desomorphine elucidated using rat urine, pooled human liver preparations, and human hepatocyte cultures as well as its detectability using standard urine screening approaches. *Anal Bioanal Chem.* 2016;408(23):6283-6294.

42. Diao X, Scheidweiler KB, Wohlfarth A, Pang S, Kronstrand R, Huestis MA. In Vitro and In Vivo Human Metabolism of Synthetic Cannabinoids FDU-PB-22 and FUB-PB-22. *AAPS J.* 2016;18(2):455-464.

43. Ellefsen KN, Wohlfarth A, Swortwood MJ, Diao X, Concheiro M, Huestis MA. 4-Methoxy-alpha-PVP: in silico prediction, metabolic stability, and metabolite identification by human hepatocyte incubation and high-resolution mass spectrometry. *Forensic Toxicol.* 2016;34:61-75.

44. Vikingsson S, Wohlfarth A, Andersson M, et al. Identifying Metabolites of Meclonazepam by High-Resolution Mass Spectrometry Using Human Liver Microsomes, Hepatocytes, a Mouse Model, and Authentic Urine Samples. *AAPS J.* 2017;19(3):736-742.

45. Wohlfarth A, Castaneto MS, Zhu M, et al. Pentylindole/Pentylindazole Synthetic Cannabinoids and Their 5-Fluoro Analogs Produce Different Primary Metabolites: Metabolite Profiling for AB-PINACA and 5F-AB-PINACA. *AAPS J.* 2015;17(3):660-677.

46. Wohlfarth A, Roman M, Andersson M, et al. 25C-NBOMe and 25I-NBOMe metabolite studies in human hepatocytes, in vivo mouse and human urine with high-resolution mass spectrometry. *Drug Test Anal.* 2017;9(5):680-698.

47. Kanamori T, Kanda K, Yamamuro T, et al. Detection of main metabolites of XLR-11 and its thermal degradation product in human hepatoma HepaRG cells and human urine. *Drug Test Anal.* 2015;7(4):341-345.

48. Caspar AT, Helfer AG, Michely JA, et al. Studies on the metabolism and toxicological detection of the new psychoactive designer drug 2-(4-iodo-2,5-dimethoxyphenyl)-N-[(2-methoxyphenyl)methyl]ethanamine (25I-NBOMe) in human and rat urine using GC-MS, LC-MS(n), and LC-HR-MS/MS. *Anal Bioanal Chem.* 2015;407(22):6697-6719.

49. Meyer MR, Bergstrand MP, Helander A, Beck O. Identification of main human urinary metabolites of the designer nitrobenzodiazepines clonazolam, meclonazepam, and nifoxipam by nano-liquid chromatography-high-resolution mass spectrometry for drug testing purposes. *Anal Bioanal Chem.* 2016;408(13):3571-3591.

7. ABBREVIATIONS

5-API	5-(2-aminopropyl)indole
5-MAPB	(benzofuran-5-yl)-*N*-methylpropan-2-amine
25I-NBOMe	2-(4-iodo-2,5-dimethoxyphenyl)-*N*-[(2-methoxyphenyl)methyl]-ethanamine
4-Methoxy-α-PVP	4-methoxy-α-pyrrolidinovalerophenone
AB-PINACA	*N*-(1-amino-3-methyl-1-oxobutan-2-yl)-1-pentyl-1*H*-indazol-3-carboxamide
AC	acetylcarnitine
C_{max}	maximum drug concentration
COMT	catechol-*O*-methyltransferase
CYP	cytochrome P450 monooxygenase
DOA	drugs of abuse
EMA	European Medicines Agency
EMCDDA	European Monitoring Centre for Drugs and Drug Addiction
FDA	US Food and Drug Administration
FMO	flavin-containing monooxygenase
FUB-PB-22	quinolin-8-yl1-[(4-fluorphenyl)methyl]-1*H*-indol-3-carboxylate
GC	gas chromatography
GSH	reduced glutathione

GST	glutathione-*S*-transferase
HILIC	hydrophilic interaction liquid chromatography
HR	high resolution
LC	liquid chromatography
LSD	lysergic acid diethylamide
MBDB	*R,S*-2-methylamino-1-(3,4-methyledioxyphenyl)butane
MDMA	*R,S*-3,4-ethylendioxy-*N*-methylamphetamine
MDPB	1-(3,4-methylenedioxybenzyl)piperazine
MDPPP	*R,S*-3',4'-methylenedioxy-α-pyrrolidinopropiophenone
MDPV	*R,S*-methylenedioxypyrovalerone
MS	mass spectrometry
MS/MS	tandem mass spectrometry
MS^n	multi stage mass spectrometry
NADPH	nicotinamide adenine dinucleotide phosphate
NAT	*N*-acetyltransferase
NBOMe	*N*-2-methoxybenzyl phenethylamine
NPS	new psychoactive substances
PAPS	3′-phosphoadenosine-5′-phosphosulfate
PHH	primary human hepatocytes
pHLC	pooled human liver cytosol
pHLM	pooled human liver microsomes

pS9	pooled S9 fraction
SAM	S-(5′-adenosyl)-L-methionine
SULT	sulfotransferase
SUSA	standard urine screening approach
UGT	diphosphate glucuronyltransferase
UNODC	United Nation Organization on Drugs and Crime
XLR-11	[1-(5-fluorpentyl)-1*H*-indol-3-yl]-(2,2,3,3-tetramethylcyclopropyl)

8. ZUSAMMENFASSUNG

Für Verschiedene in vitro Modelle wurden als Surrogat für menschliche in vivo Metabolismusstudien untersucht. Dabei stand die Identifizierung der Hauptausscheidungsprodukte im Urin zur Entwicklung eines toxikologischen Urinscreenings für neue psychoaktive Substanzen (NPS) im Vordergrund. Ein in vitro Modell mit humanen Leberpräparationen wurde entwickelt, welches sowohl metabolische Phase I als auch Phase II Schritte abdeckt. Des Weiteren wurden die humanen Leberzelllinien HepG2 und HepaRG getestet. Wie erwartet, zeigten die HepG2 Zellen keine ausreichende Metabolisierungsfähigkeit, anders als die HepaRG Zellen, welche minimal bessere Ergebnisse als die Leberzellpräparationen erbrachten. Jedoch haben Zelllinien allgemein den Nachteil, dass eine besondere Ausstattung für den Umgang mit Zellkulturen notwendig ist. Das pS9 Modell ist das kosteneffizienteste und am einfachsten zu handhabende in vitro Modell. Trotz Einschränkungen kann es zur Entwicklung eines toxikologischen Urinscreenings genutzt werden. Aus den eben genannten Gründen ist es daher das beste Model, auch im direkten Vergleich mit primären humanen Hepatocyten.